

NASA CONTRACTOR
REPORT

T 75996
N69-15744
NASA CR-61251

December 1968

**CASE FILE
COPY**

NASA CR-61251

RESEARCH AND DEVELOPMENT ON CRYOGENIC STRETCH-FORMED
HELIUM BOTTLES, SATURN IV-B (Final Report)

Prepared under Contract No. NAS 8-20713 by

R. Alper
ARDE, INCORPORATED

For

NASA-GEORGE C. MARSHALL SPACE FLIGHT CENTER

December 1968

NASA CR-61251

RESEARCH AND DEVELOPMENT ON
CRYOGENIC STRETCH-FORMED HELIUM BOTTLES
SATURN IV-B
(Final Report)

By

R. Alper

Prepared under Contract No. NAS 8-20713 by
ARDE, INCORPORATED
580 Winters Avenue
Paramus, New Jersey

For

Manufacturing Engineering Laboratory

Distribution of this report is provided in the interest of
information exchange. Responsibility for the contents
reside in the author or organization that prepared it.

NASA-GEORGE C. MARSHALL SPACE FLIGHT CENTER

TABLE OF CONTENTS

<u>SECTION</u>	<u>TITLE</u>	<u>PAGE NO.</u>
I	ABSTRACT	1
II	INTRODUCTION	2
III	SUMMARY.	5
IV	PREFORM DESIGN	
	A. Design Philosophy for Stretch Formed Spheres	10
	B. Spherical Shell Design.	14
	C. Boss Analyses	16
	D. Completed Vessel Design	18
V	MATERIAL ACCEPTANCE AND EVALUATION	
	A. Material Acceptance Procedures.	20
	B. Evaluation of Material	22
VI	FABRICATION TECHNIQUES	
	A. Processing Sequence	30
	B. Hydroforming and Machining of Hemispheres . .	30
	1. Starting Material Thickness	32
	2. Final Thickness Variation	32
	C. Forging and Machining of Bosses	36
	D. Welding of the Helium Vessel Assembly	37
	E. Annealing	41
	F. Cryogenic Forming of Helium Vessels	42
	G. Final Processing.	46
	1. Aging	46
	2. Final Testing, Processing & Acceptance. .	49
	H. Fabrication Results	51

TABLE OF CONTENTS (cont'd)

<u>SECTION</u>	<u>TITLE</u>	<u>PAGE NO.</u>
VII	EFFECT OF INCLUSIONS ON STRETCHING OF PREFORMS	
	A. Background	52
	B. Analysis of Burst Vessel S/N 2	52
	C. Analysis of Sphere S/N 1 Burst Tested @ -320°F	60
	D. Method for Detection of Slag Inclusions.	66
	E. Inspection of Deliverable Vessels.	67
	F. Metallographic Examination of X-Ray Detected . Weld Defects	68
VIII	MATERIAL PROPERTIES	
	A. Mechanical Test Procedures	70
	B. Tensile Testing.	73
	C. Notch Testing.	99
	D. Mechanical Testing of Welds.	112
	E. Stress Corrosion Testing of Welds.	113
IX	RECOMMENDED QUALIFICATION TEST PROCEDURES.	120
X	CONCLUSIONS.	126
XI	APPENDIX	127
	Appendix A - Uniaxial Biaxial Correlation	
	Appendix B - Boss Analysis	
	Appendix C - AES 256	
	Appendix D - AES 454	
	Appendix E - Ogden Lab Test Report	
	Appendix F - Mechanical Properties - Heat 50793	

LIST OF ILLUSTRATIONS

<u>FIGURE NO.</u>	<u>TITLE</u>	<u>PAGE NO.</u>
III-1	Uniaxial Tensile and K_{Ic} Test Data	7
IV-1	Sphere Design Chart - Heat 97107	13
IV-2	Saturn S-IVB Helium Storage Vessel Drawing . . .	19
VI-1	Manufacturing Flow Chart	31
VI-2	Wall Thickness of Hemisphere	34
VI-3	Helium Storage Vessel Details.	35
VI-4	Helium Storage Vessel Welded Subassembly	40
VI-5	Stretch Facility	44
VI-6	Vessel After Cryogenic Stretch Forming	47
VI-7	Grit Scrubbing Set-up.	48
VI-8	Finished Vessel.	50
VI-9	S/N 5 Cryogenic Stretch Pit Failure.	52
VII-1	Laminar Slag Inclusions.	56
VII-2	Microphotos, Inclusions.	57
VII-3	" "	59
VII-4	" "	62
VII-5	" "	63
VII-6	" "	64
VII-7	" "	69
VIII-1	Tensile Specimen Drawing	72
VIII-2	Tensile Test Equipment	74
VIII-3	True Stress vs. True Strain @ -320°F Heat 97056	78
VIII-4	" " " " " Heat 97057	79
VIII-5	" " " " " Heat 97058	80
VIII-6	" " " " " Heat 97106	81
VIII-7	" " " " " Heat 97107	82

LIST OF ILLUSTRATIONS (cont'd)

<u>FIGURE NO.</u>	<u>TITLE</u>	<u>PAGE NO.</u>
VIII-8	Room Temperature Strength - Heat 97056	89
VIII-9	" " " - Heat 97057	90
VIII-10	" " " - Heat 97058	91
VIII-11	" " " - Heat 97106	92
VIII-12	" " " - Heat 97107	93
VIII-13	Strength at -320°F - Heat 97056	94
VIII-14	" " - Heat 97057	95
VIII-15	" " - Heat 97058	96
VIII-16	" " - Heat 97106	97
VIII-17	" " - Heat 97107	98
VIII-18	Notch Specimen Drawing	100
VIII-19	Specimen Undergoing Fatigue Cracking	102
VIII-20	Surface Fatigue Crack.	103
VIII-21	Specimen Failure Away from Notch	105
VIII-22	K_{Ic} at Various Temperatures.	109
VIII-23	Notch Ratio at Various Temperatures	110
VIII-24	Notch Tensile Strength at Various Temperatures	111
VIII-25	Weld Tensile Specimen Drawing	114
IX-1	Saturn S-IVB Helium Storage Vessel Drawing. . .	123
IX-2	Boss Drawing.	124

LIST OF TABLES

<u>TABLE NO.</u>	<u>TITLE</u>	<u>PAGE NO.</u>
V-1	Certified & Check Chemical Analyses of Heats	24
V-2	Inclusion Content of Heats	28
VI-1	Postform Dimensions of Vessels	45
VIII-1	Mechanical Properties of Low Silicon Ardeform Material Heat 97056	84
VIII-2	Mechanical Properties of Low Silicon Ardeform Material Heat 97057	85
VIII-3	Mechanical Properties of Low Silicon Ardeform Material Heat 97058	86
VIII-4	Mechanical Properties of Low Silicon Ardeform Material Heat 97106	87
VIII-5	Mechanical Properties of Low Silicon Ardeform Material Heat 97107	88
VIII-6	Notched Specimen Test Results.	108
VIII-7	Mechanical Properties of Welded Specimens. . .	115
VIII-8	Weld Notched Tensile Properties.	116
VIII-9	Corrosion Specimen Preparation	118

Acknowledgment

Arde, Inc. gratefully acknowledges the efforts expended by

Mr. L. A. Hein R-P&VE-PMF

Mr. J. H. Hess R-P&VE-MM

Mr. C. N. Irvine R-ME-MMD

Mr. W. A. Wilson R-ME-MM

of NASA who were responsible for the technical administration of the program and through whose cooperation the technical goals of the program were realized.

I. ABSTRACT

A program was conducted to establish the manufacturing technology required to produce 22" diameter spherical helium pressure vessels for service at -423F. The vessels incorporated several attachment bosses and a fill port. The material used was a low silicon chromium-nickel stainless steel alloy. The vessels were manufactured by means of the ARDEFORM or cryogenic stretch forming process. Six (6) vessels of the desired configuration were produced for delivery. In addition, mechanical property tests were performed with several heats of this alloy.

II. INTRODUCTION

The requirements for high strength materials suitable for service at cryogenic temperature has, in recent years, focused considerable attention upon cold worked austenitic alloys. The ARDEFORM* process offers a means of cold working pressure vessels made from austenitic chrome-nickel stainless steels. In this process an undersize preform is first constructed from annealed material by welding or other means of producing a closed pressure vessel. The preform is immersed in liquid nitrogen to reduce its temperature to -320F and then pressurized internally with pumped, liquid nitrogen. The preform stretches, as a result of the pressurization, to the desired size and shape. During this deformation at -320F, the material transforms from austenite to martensite. High strength levels are achieved as a result of both the transformation and the cold working of the material. After the cryogenic deformation, additional strength may be obtained by aging the material at 800F for 20 hours. The cryogenically deformed material, in addition to high strength, exhibits a K_{Ic} value of approx. 80 at -423F and is compatible with a large variety of liquid rocket propellants and other corrosive fluids.

Several austenitic alloy compositions have been developed by Arde. By selecting the proper alloy the most favorable properties for each application can be obtained. A previous

* Subject of U.S. Patent #3197851

program, successfully conducted by Arde for NASA (Contract NAS - 11977) resulted in the fabrication of cylindrical pressure vessels suitable for the storage of gaseous helium while the vessels are submerged in an environment of liquid oxygen. Arde utilized a 17% chromium - 7% nickel austenitic stainless steel alloy containing over .4% silicon for these cylinders. This alloy is useful at operating temperatures down to -320F in the unaged condition.

For applications which require high strength and fracture toughness at cryogenic temperatures down to -423F, an 18% chromium - 7% nickel stainless steel alloy, with very low silicon (less than .1%) is used. This low silicon alloy is normally used in the aged condition for optimum strength and toughness characteristics.

The ARDEFORMed low silicon stainless steel alloy was evaluated, by means of tensile specimen tests, for -423F strength and fracture toughness characteristics by NASA-Lewis Laboratories. This investigation showed good performance at -423F as well as very impressive properties of the welded material at this same low temperature. ⁽¹⁾

- (1) NASA TN D3445 - "Evaluation of Special 301 - Type Stainless Steel for Improved Low-Temperature Notch Toughness of Cryoformed Pressure Vessels" by Thomas W. Orange, Lewis Research Center, Cleveland, Ohio May 1966

NASA initiated the present ARDEFORM manufacturing technology program because of a potential need in the Saturn IV B. The Saturn IV B requirement manifested itself when consideration was given to possible fire hazards in the use of titanium pressure vessels. This possibility was considered even though titanium vessels were to be stored in the oxygen atmosphere as unpressurized containers. The use of stainless steel, which is known to be far superior to titanium in this respect, was therefore considered. Specifically, the low silicon alloy, in the ARDEFORMed and aged condition, with its high strength at -423F, was selected for this application.

The objective of the program, therefore, was to develop the manufacturing technology necessary to produce the configuration required for the Saturn IV B helium storage bottles using the low silicon material. The design techniques utilized in adapting the ARDEFORM process to the configurational requirements; the manufacturing methods used in fabricating the vessels; an investigation of characteristics of several heats of low silicon material procured for this program; and some of the problems with inclusion in the material are discussed in this report.

III. SUMMARY

The program resulted in the fabrication of six (6) deliverable spheres which passed Arde's quality requirements and are suitable for -423F service. A high scrap rate was encountered in the program due to slag inclusions in a heat of material which was eventually rejected. The deliverable vessels, therefore, were fabricated from a different heat of material and carefully inspected to assure that they were free from any defects which could impair their operation at -423F.

The effort on this program was divided into three phases:

1. The selection and testing of low silicon chromium-nickel austenitic stainless steel heats suitable for the fabrication of the pressure vessels.

2. The design of a sphere preform with mounting provisions and an inlet boss.

3. The application of the aforementioned ARDEFORM fabrication techniques to the production of cryogenically stretch formed vessels for helium gas storage.

A. Selection and Testing of Material Suitable for Use at -423F

This phase consisted of the procurement of material to specified chemical composition and cleanliness in order to obtain good mechanical properties after cryogenic (-320F) stretching.

A total of five (5) heats were poured for this program. Each of these heats were evaluated for its behavior during plastic deformation at liquid nitrogen temperatures (-320F) and for its properties at -320F and room temperature. In addition, selected heats were evaluated for notch toughness and strength level at temperatures as low as -423F. Both welded and unwelded

specimens were evaluated. The stress corrosion resistance of cryogenically prestrained ARDEFORM material was also determined during this phase of the program. Testing was performed with tensile specimens both by Arde and NASA with samples from the heats procured for this program. The results indicated that uniformly good fracture toughness and strength was exhibited by all heats which met specification chemistry. A summary of the material properties for four (4) of the five (5) heats of the low silicon material specifically procured for this program is presented in Figure III-1. Note from Figure III-1 that the -423°F K_{1C} values obtained for the heats tested ranged from 75 to 80 ksi $\sqrt{\text{in}}$. The data for Heat 50793 which became available during the course of the program and which was subsequently used to fabricate several vessels is also presented in Appendix "F".

B. Design of the Sphere Preform

Design of the spherical vessel preform was based on uniaxial test results which were used in a computerized design program to establish the preform dimensions. The yield strength of the material, as determined from uniaxial tests, dictated the final minimum thickness of the vessel. Conventional elastic stress analysis was utilized in the evaluation of the structural integrity of the vessel and its ports and bosses under combined internal pressure and external "g" loads.

Arde provided four clevis bosses for tie-down purposes as an alternative to the original design, which used straps to mount the vessel. Straps create crevices which tend to lead to crevice corrosion problems.

UNIAXIAL TENSILE AND K_{IC} TEST DATA
ARDEFORMED & AGED LOW SILICON MATERIAL

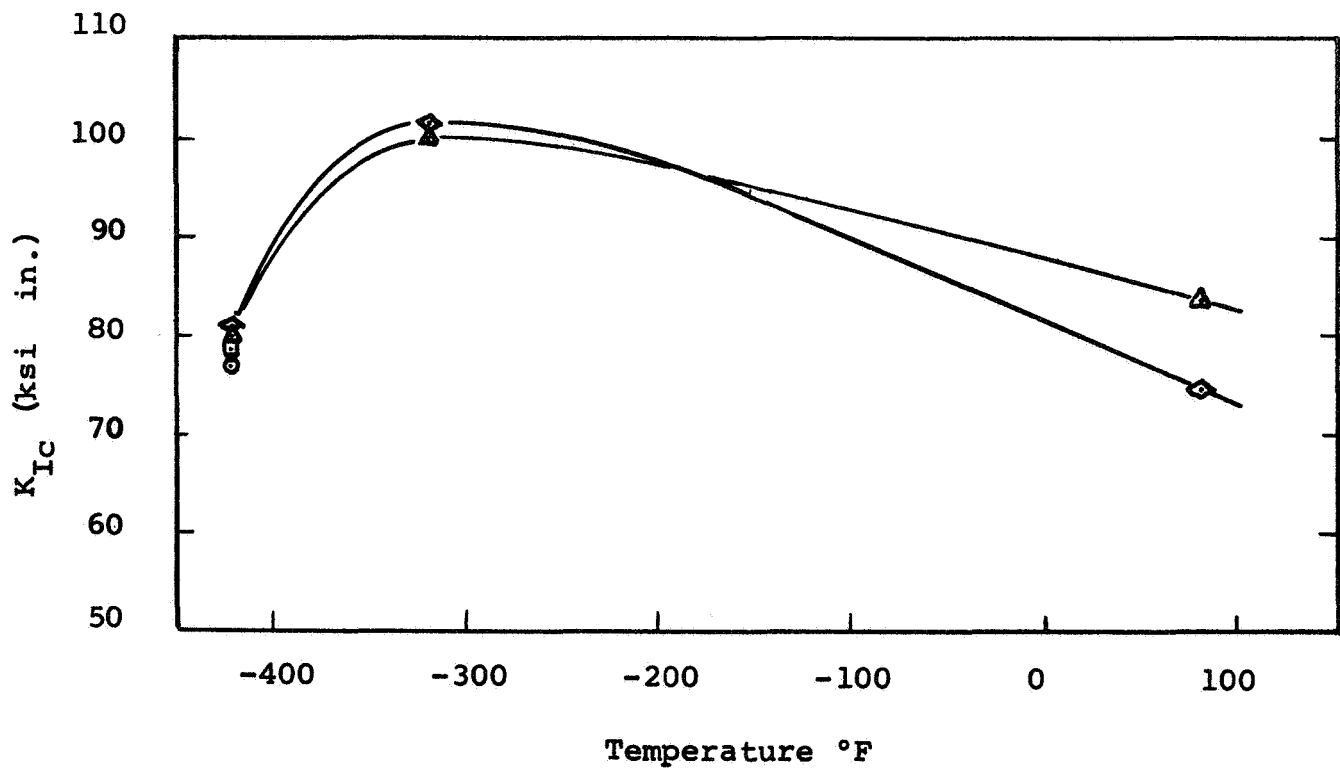
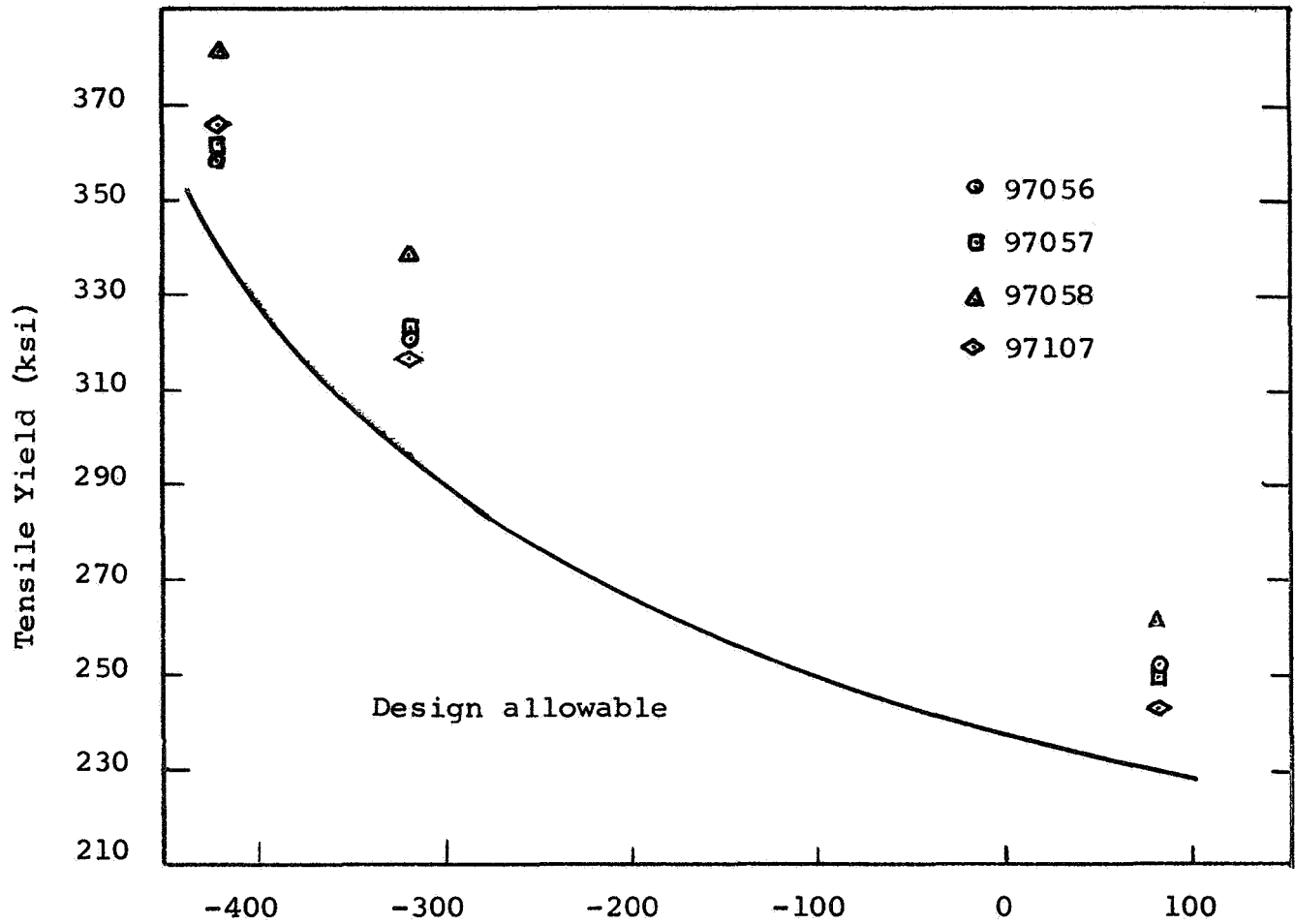


Figure III-1

A primary consideration in the production of the spheres was the incorporation of the inlet boss and clevis supports using the ARDEFORM process. Arde's previous experience with similar configurations indicated that the design decided upon could be fabricated. The results of the program bear out this contention. No major difficulty was encountered which related to the sphere configuration designed.

C. Vessel Fabrication

The hemispherical heads for the vessels were hydroformed and then machined in order to produce a uniform thickness. The details for the preform vessels were tungsten-inert gas (TIG) welded. The vessels were solution annealed, cryogenically stretched formed and aged. One vessel was cryogenically (-320F) burst tested by Arde. Two other vessels failed during the stretch forming operation and two were rejected after stretching, as a result of radiographic inspection. A total of six vessels were delivered to NASA.

The only problem of consequence which was encountered was the result of exogenous inclusions in the material. The failure of one vessel during stretch forming could be definitely traced to the inclusions. It was determined that welding large inclusions of this type resulted in the burst of preforms during stretch forming. In the course of the program, Arde worked out, in cooperation with Magnaflux Corporation, an ultrasonic inspection technique which can reduce the scrap rate due to the occurrence of such inclusions. Furthermore, it should be noted

that the heats procured for this program were single induction vacuum melted. Arde, in conjunction with a subsequent program, procured a double vacuum melted heat of material on the premise that the material would not contain these exogenous inclusions. The basis for this assumption is the fact that consumable electrode remelting tends to agitate and disperse inclusions of this nature. Two (2) vessels utilizing material from this heat were subsequently fabricated and delivered to NASA in performance of this program.

In addition to ultrasonic inspection of either the sheet stock or the head details, all vessels were radiographically inspected after stretching. Any cracks developing during the stretching operation can be detected by this method, whatever the cause of the cracks. All vessels delivered in performance of this program were shown to be free from detectable defects.

IV. PREFORM DESIGN

A. Design Philosophy for Stretch Formed Spheres

The high strength of Ardeform low silicon stainless steel is obtained through deformation at -320F. As has previously been described, the deformation is accomplished during the Ardeform process, by pressurizing a preform fabricated from annealed material. The preform is made smaller in size than the required final vessel in order to allow for sufficient expansion to achieve the strength required. The design of all components of the preform, then, must take into consideration the amount of stretching that will take place, for two reasons:

- 1) After stretching, the vessel must meet the dimensional requirements of the finished product.
- 2) After stretching, the vessel must have been cold worked sufficiently to produce the desired strength level.

Obviously, if the preform is too small, then it may burst during stretching before it achieves the desired size. If the preform is too large, then it will reach the desired size readily, but will not achieve a satisfactory strength level. In addition, the wall thickness must be sized so that the weight and burst pressure of the finished vessel will be as required, and make full use of the resulting material

strength level. In the preform design, therefore, mill and manufacturing thickness tolerances of the material must be carefully considered.

The design of preforms for cryogenic stretch forming, may be based on biaxially stretched vessel behavior predicted from uniaxial tensile specimen data. The derivation of equations predicting the stresses and strains in a plastically deformed sphere from uniaxial specimens is outlined in Appendix A. From simplified total deformation theory it can be shown that the following relationships hold for stretching spheres:

$$(1) \quad \epsilon_i = \frac{1}{2} \bar{\epsilon}$$

$$(2) \quad \sigma_i = \bar{\sigma}$$

where ϵ_i is the true hoop strain of a sphere at true hoop stress σ_i

$\bar{\epsilon}$ is the true strain of a uniaxial specimen at a true stress $\bar{\sigma}$

An empirical factor based on experience, however, indicates that the plastic strain component from equation (1) is more nearly:

$$1 \text{ (a) } \epsilon_i = .45 \bar{\epsilon}$$

Using equations (1a) and (2), a cryogenic biaxial stress-strain curve for spheres may be constructed from a cryogenic uniaxial stress-strain curve. Such biaxial curves are prepared for each heat of material and are used to predict the amount of stretching which spheres will undergo when they are pressurized during the stretch forming process. Modifications to these

relationships have been made at Arde to include the effects of the elastic components of the strain.

An additional design requirement is to predict the strength which results when spheres are stretched a specified amount. It has been shown, at Arde, that the strength of such spheres is equal to the strength of uniaxial specimens which have been prestressed to the same true stress levels.

A biaxial design chart for heat 97107 derived from uniaxial data, is presented in Figure IV-1. The true strains, ϵ , have been corrected for elastic rebound and converted to more familiar engineering strains in the chart.* Therefore, strains are

presented as -- $\frac{D_p}{D_o}$ i.e., $1 + \text{engineering strain}$, where:

D_p = the final diameter of stretched sphere
after elastic rebound

D_o = the initial diameter of the sphere
preform

* engineering strain = $e^{\epsilon} - 1$

The chart shows several curves of interest to the sphere designer. The curve labeled σ_T indicates the true stress achieved at -320F during the cryogenic stretching process, and is derived from the uniaxial data using equations (1a) and (2) and includes corrections for elastic strain. The curve labeled S_2 is more useful for the designer since it predicts the nominal cryogenic stretching stress required to stretch a sphere preform

SPHERE DESIGN CHART

Heat 97107

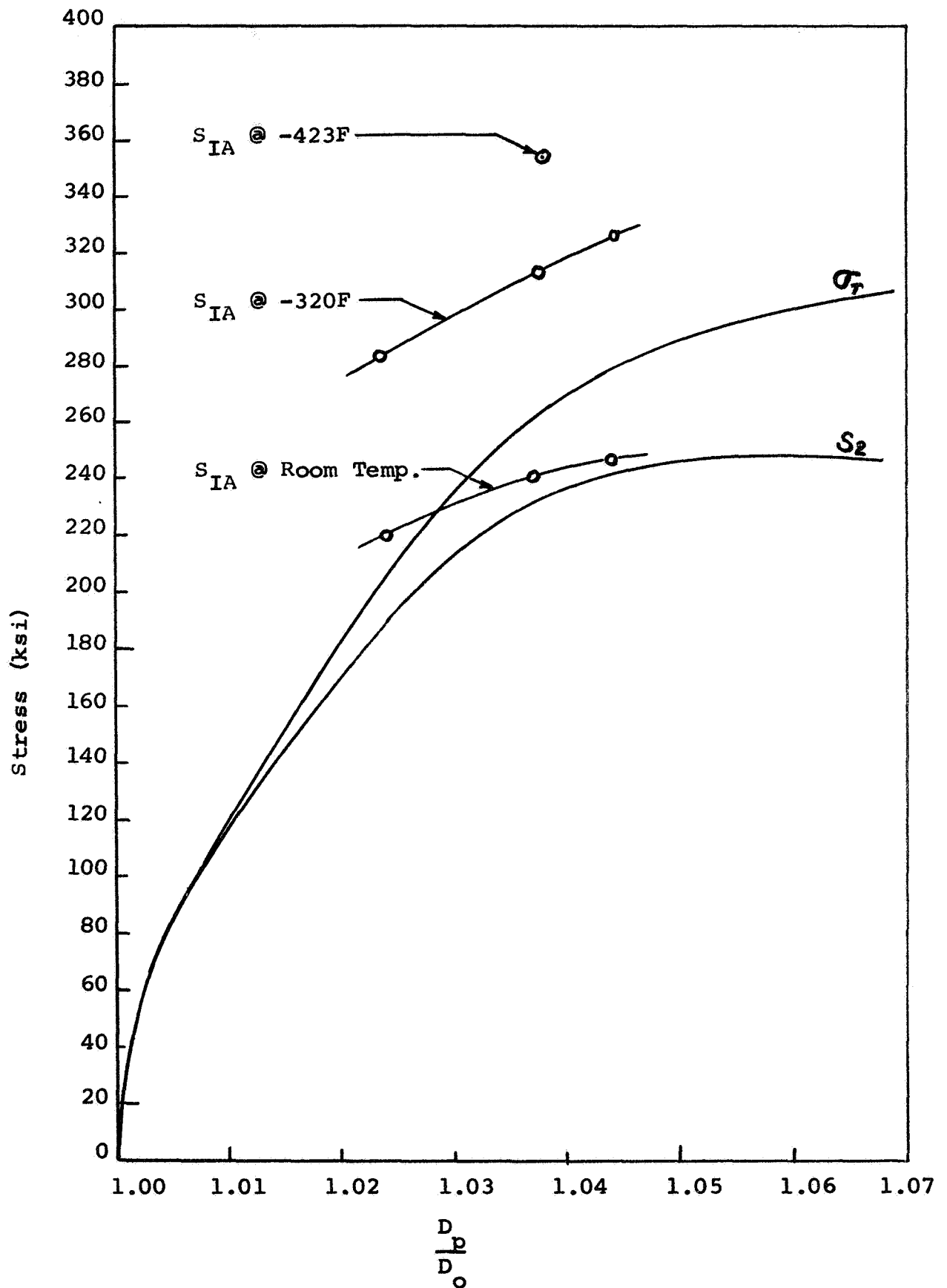


Figure IV-1

a given amount. Note that the S_2 curve exhibits a maximum. This maximum represents the limiting nominal stress and strain of spheres made from this material during the cryogenic stretching process. Exceeding the stress or strain at the maximum will cause the sphere to burst during the stretch. The S_{1A} curve shows the burst strengths at different operating temperatures for spheres which have been stretched to a diameter ratio, $\frac{D_p}{D_o}$ and which have then been aged.

B. Spherical Shell Design

To design a preform which will result in a high strength sphere, the following procedure is used:

A safe value of S_2 is chosen to the left of the maximum on the S_2 curve. This procedure prevents the strain of the sphere from exceeding its limit, and thereby avoids bursting during the stretch forming process. At the same time the value of the stretched and aged sphere burst strength must exceed a desired value. For example, from Figure IV-1, a nominal stretching stress of 240 ksi is selected from S_2 at a $\frac{D_p}{D_o}$ value of 1.042. This design point indicates that a sphere will stretch 4.2% in diameter if pressurized to a nominal stress of 240 ksi. At $\frac{D_p}{D_o} = 1.042$, the predicted burst strength at any operating temperature after stretching and aging is then determined from the suitable S_{1A} curve. Only one S_{1A} point at a -423F operating temperature is available for this heat. However, the desired -423F strength level is only 340,000 psi. This is less than the 354 ksi obtainable with only a 3.8% strain. Therefore, a 4.2% strain would assure a burst stress of 340,000 psi at -423F.

From the design chart then, the nominal cryogenic stretch forming stress of 240,000 ksi, and the strain of 4.2% have been determined. In addition, the desired -423F strength of 340 ksi has been shown to be achievable under these stretch conditions.

The minimum final vessel wall thickness is next determined from the design burst stress at -423F as follows:

$$(3) \quad t_f = \frac{P_B \times D_p}{4 \times S_{IA}}$$

where P_B is the design burst pressure of 7100 psi
 D_p is the design I.D. of 22.6 inches
 S_{IA} is the design stress of 340,000 psi at operating conditions

From equation (3), the final minimum wall thickness is .118 in.

At this point the dimension of the preform may be determined. The preform I.D. is determined from the 4.2% strain obtained from the design chart and the desired final I.D. of 22.6 inches.

$$(4) \quad D_o = D_p / \frac{D_p}{D_o} = \frac{22.6}{1.042} = 21.69 \text{ inches}$$

In order to determine the preform wall thickness, it is necessary to know the relationship between the preform wall thickness and the final vessel wall thickness for a known stretch percentage. This relationship may be shown to be:

$$t_o = t_f \frac{D_p}{D_o}^2 = .118 \times (1.042)^2 = .128 \text{ min. pre-form thickness}$$

where t_o is the preform thickness

Thus, the preform design of the spherical shell is accomplished except for manufacturing tolerances. A discussion of manufacturing tolerances is given in Section VI-B

C. Boss Analyses

The helium bottle contains four (4) small strap attachment bosses and one large boss which serves as a port as well as a support point for the bottle. The vibration and acceleration forces acting on the bottle are transmitted through these support points. An analysis was made to determine the stresses in the bosses and the bottle due to these loads superimposed on the pressure stresses. This analysis is presented in Appendix (B) of this report. The results indicate that the stresses imposed by these loads can be adequately carried by the shell structure designed in accordance with Section B above.

The method of analysis used in the boss stress determination followed these steps:

1. Determine the tank acceleration and vibration loads based on equivalent static vibration loads and flight acceleration loads in the radial and axial directions.
2. Apply a design yield factor of 1.25 to these loads and determine the tank support point reactions.

3. Determine the stresses in the large boss due to superposition of the radial support load and internal pressure. These stresses are found by a "discontinuity" analysis which consists of reducing the structure to component parts such as rings, cylinders, cones and spherical segments. Unknown edge shears and moments are applied to each component; and deflection and rotation expressions are written for each segment in terms of these unknown forces. Equating the deflections and rotations at adjacent points results in a series of simultaneous equations. The solution of these equations gives the magnitudes of the forces. Internal stresses are then computed.
4. Stresses due to the lateral support load on the large boss are then computed using the method of analysis presented in the Welding Research Council Bulletin No. 107 "Local Stresses in Spherical and Cylindrical Shells due to External Loadings". Pressure stresses are then added to determine the maximum combined stress.
5. The small boss is analyzed for the maximum strap load. This load is converted to a tangential and radial component and stresses in the shell are determined again using the above referenced Bulletin. Pressure stresses are added to these to determine the maximum combined stress.

D. Completed Vessel Design

The vessel is defined, after stretching the preform assembly and final machining, in the Arde Drawing SKE 10392 which is included in this Section. (Figure IV-2)

V. MATERIAL ACCEPTANCE AND EVALUATION

A. Material Acceptance Procedures

The material used for applications at cryogenic temperatures is an austenitic stainless steel with very low silicon, manganese and carbon levels. The Arde specification which sets forth the required tolerances on heat chemistry and other characteristics is AES 256. This specification is included in Appendix (C). The specification calls for the material to be vacuum induction melted from high purity charging materials. Of special significance are the high standards of material cleanliness included in the specification.

The tests performed to determine conformance to Specification AES 256 consist of independent check analyses of heat chemistry, metallographic examination for inclusion distribution and size, metallographic examination for grain size, and intergranular carbides. In addition, visual examination of sheet surface condition and dimensional inspection of the mill product is made. Finally, in accordance with the Arde specification, samples from each lot of material are radiographically inspected to establish that the material is free from sub-surface gross defects. All these requirements were established at Arde as a result of experience with materials used in cryogenic stretch forming.

Material cleanliness has been definitely established as a requirement for the production of reliable welds in pre-forms for the ARDEFORM process. Specifically note that the maximum size of globular oxides is limited to 25 microns in the Arde specification. The purpose of this limitation is to eliminate weld porosity which has been traced to this type of inclusion. The radiographic inspection procedure serves as a further check on the occurrence of non-metallic inclusions in the material. In the past, exogenous inclusions of rather large size were detected by the radiographic inspection of sheet. This type of inclusion is generally highly refractory in nature and can cause vessel failures during the cryogenic stretching operation.

Material chemistry has been shown to be the primary factor in establishing the mechanical properties which can be obtained from a given heat of material. As a result, close tolerances have been established for the constituents of this material. Unusual in terms of stainless steel specifications is the oxygen and hydrogen requirement in the Arde specification. This requirement was established because of evidence which showed that high oxygen levels over 140 ppm were responsible for increasing the heat cracking susceptibility of austenitic stainless steels of this general composition range. High levels of both oxygen and hydrogen were also noted to be detrimental to the fracture toughness of cryogenically stretch formed material particularly at cryogenic temperatures.

In addition to the aforementioned specification, which establishes the procurement requirements for the material, other evaluation procedures are performed with each heat of material. Thus, the heats procured for this program were evaluated for weldability by means of a specimen devised by Arde. Finally, a thorough investigation of the mechanical properties of the material was performed. The results of the evaluation and acceptance testing of the materials is discussed below. The mechanical property testing and results are presented in Section VIII.

B. Evaluation of Material

1. Check Analysis of the Material

Check analysis was made on a sample from the ingot of each heat. The analysis was performed for Arde by an independent laboratory. Wet chemical analytic methods were used for all elements except hydrogen and oxygen. Oxygen was determined using vacuum fusion gas analysis of the ingot sample. Nitrogen was determined by the Kjeldahl method. Hydrogen which is also determined by vacuum fusion gas analysis is variable throughout the processing of the ingot and reaches its final level only after conversion of the ingot to slab or sheet bar. Samples for the hydrogen check analysis, therefore, consisted of pieces cut from sheet bar made from each heat. The results of the check analyses along with the steel vendor's certified analysis for each heat are shown and compared with the specified composition from Arde Specification AES 256 in Table V-1.

The analysis of heat 97106 which was one of the five (5) heats initially procured was outwardly rejected due to non-conformance with chemistry requirements and hence has been omitted from the table.

The data for heat 50793 has been included in the table even though the material was not specifically procured for use in this program. This material was procured in conjunction with another program and a portion diverted to fulfill the requirements for two of the delivered vessels on this program.

TABLE V-1

CERTIFIED AND CHECK CHEMICAL ANALYSES OF HEATS

	C	Mn	Si	Cr	Ni	Mo	P and S	N	O	H
	%	%	%	%	%	%	%	%	PPM	PPM
Arde Specification	.025	.10	.10	18.30	7.10	.15	Total .015	.02	60	2 max
AES 256	.045	max	max	18.70	7.50	.35	max	.04	max	
Heat 97056 Cert.	.054	Nil	.03	18.40	7.35	.22	.015	Not Reported		
97056 Check	.052	.02	.01	18.41	7.14	.19	-	.024	22	.4
Heat 97057 Cert.	.054	Nil	Nil	18.50	7.34	-	.013	Not Reported		
97057 Check	.042	Nil	.045	18.42	7.51	-	.025	.041	120	3.0
Heat 97058 Cert.	.040	Nil	Nil	18.53	7.46	.22	.018	Not Reported		
97058 Check	.029	.02	.03	18.72	7.29	.27	.0113	.027	37	2.0
Heat 97107 Cert.	.043	Nil	.06	18.32	7.22	.22	.014	Not Reported		
97107 Check	.027	.02	.06	18.46	7.36	.28	.0035	.025	34	.5
Heat 50793 Cert.	.03	.01	.07	18.16	7.57	.27	.015	.04	37	2
50793 Check	.028	nil	.044	18.56	7.24	.16	.011	.034	11	21

Heat 97056 may be seen from Table V-1 to meet all of the composition requirements except for a somewhat higher carbon than specified. Because of the schedule requirements of the program at its initiation it was felt that if all other properties such as strength fracture toughness, cleanliness, weldability and general fabricability were acceptable then the slightly higher carbon level would not be sufficient reason for rejection. It was, therefore, decided to continue evaluation of the material for these other characteristics and if these proved satisfactory to accept the material.

Heat 97057 was shown to be too high in oxygen and hydrogen and was therefore rejected. The vendor indicated that the high oxygen level in this heat was traced to the use of a charging material of insufficient purity. Unfortunately, charging materials with a satisfactory purity was not available at the time the heat was poured. Subsequent heats were poured with the correct charging material.

Heat 97058 was acceptable in all respects except that the vendor reported a combined sulphur and phosphorous level of .018% which was high compared to the specification requirement of .015% maximum. The steel vendor informed Arde that this value resulted from the addition of the results of separate analyses for phosphorous and sulphur. This procedure often results in a value that is higher than that which would

be obtained if the two elements were analyzed in combination. The check analysis shows the results of analyzing the two elements in combination. The .0113% value reported is within the specification. Therefore, heat 97058 was accepted.

Heat 97107 was accepted inasmuch as it met all the specification composition requirements without deviation.

In summary, then, of the five (5) heats initially procured, one heat 97057 was rejected for high oxygen levels; heat 97106 was rejected for non-conformance to chemistry requirements, heat 97056 was conditionally accepted because of the high carbon level; and the two remaining heats, 97058 and 97107, were deemed to have acceptable heat chemistries.

Heat 50973, which became available in conjunction with another program and subsequently used in performance of this program, was found completely acceptable in accordance with Arde Specifications.

2. Metallographic Examination of the Material

All metallographic examinations were conducted using samples from the sheet rolled for the program. Intergranular carbides were found to be very lightly scattered throughout all of the sheet samples tested. This was not felt to be serious inasmuch as the manufacturing process called for a solution anneal after welding and prior to stretch forming. The specified restriction on inter-granular carbides on incoming sheet material was based on Arde experience which indicated that embrittlement at cryogenic temperatures occurs if heavy inter-granular carbide precipitation is present. Inasmuch as a complete solution anneal was part of the processing sequence in the fabrication of the spheres for this program, re-solution

of the light carbides noted would definitely take place at the time the parts were annealed. Therefore, all of the sheets were deemed acceptable in terms of the carbides noted.

The cleanliness of the heats were evaluated and the results are shown in Table V-2. All of the cleanliness ratings fell within the cleanliness specifications except that a slight deviation in Type D thins was noted in Heat 97058. The deviation was not felt to be serious enough for rejection. The primary reason for the control of this type of inclusion is avoidance of weld porosity and since no heavy globular oxides were found, it was felt that the additional small quantity of thin inclusions noticed would not significantly affect the weldability. The heat was, therefore, not rejected.

In summary, then, the general cleanliness of these heats was very good and no large inclusions were noted in any of the samples examined metallographically. It should be noted at this point, however, that as a result of premature bursting of preforms during stretch forming, some large defects were found and identified as the cause of the stretch pit bursts. These particular defects were very widely distributed and were not encountered during microscopic examination probably because of their low frequency of occurrence. More is said about these inclusions in Section VII.

Grain size was determined from the sheet samples and in all cases was smaller than the maximum size specified.

TABLE V-2

INCLUSION CONTENT OF HEATS

<u>Specified Characteristics</u>		<u>Heat 97056</u>	<u>Heat 97058</u>	<u>Heat 97107</u>
<u>Type</u>	<u>Rating</u>	<u>Rating</u>	<u>Rating</u>	<u>Rating</u>
A Thin	1	0	0	0
A Heavy	0	0	0	0
B Thin	1	0	0	0
B Heavy	0	0	0	0
C Thin	1	1	0	1
C Heavy	0	0	0	0
D Thin	1	0	1 1/2	1
D Heavy	1	0	0	0

3. Weldability Sample

As a check on the weldability of the heats, two cylindrical pieces 5 1/2 inches in diameter are fabricated, and these are welded together using a single pass girth weld. The cylinders were then cut in half along the longitudinal axis and the exterior and interior of the weld and heat affected zone dye checked. Examination for dye check indications was performed with 30X magnification. No cracks were found in samples from any of the heats.

4. Radiographic Inspection

Radiographic inspection of the sheet from the heats used on this program showed no defects. Because of the scheduled requirements on this program, one of the heats was shipped to a hydroform vendor prior to examination of the sheet by radiographic methods. However, radiographic inspection was performed after the heads were formed and these tests showed no defects. Again it should be noted that although fabrication and stretching brought to light large slag inclusions in the material, these were at no time detected by the radiographic inspection technique as was previously noted. More is said concerning these deleterious slag inclusions in Section VII.

VI FABRICATION TECHNIQUES

A. Processing Sequence

The fabrication of the helium spheres follows, essentially, the procedure of first building a spherical preform, stretching the preform at -320F, final machining and aging.

The spherical shells were constructed from hydroformed hemispheres which were machined to improve thickness tolerances. Bosses and ports were machined from forgings and all details were assembled by welding to produce the preform.

A flow chart, shown in Figure VI-1, lists the detailed processing and inspection steps in the fabrication of the vessels. Some of the more important fabrication steps are discussed in greater detail below.

B. Hydroforming and Machining of Hemispheres

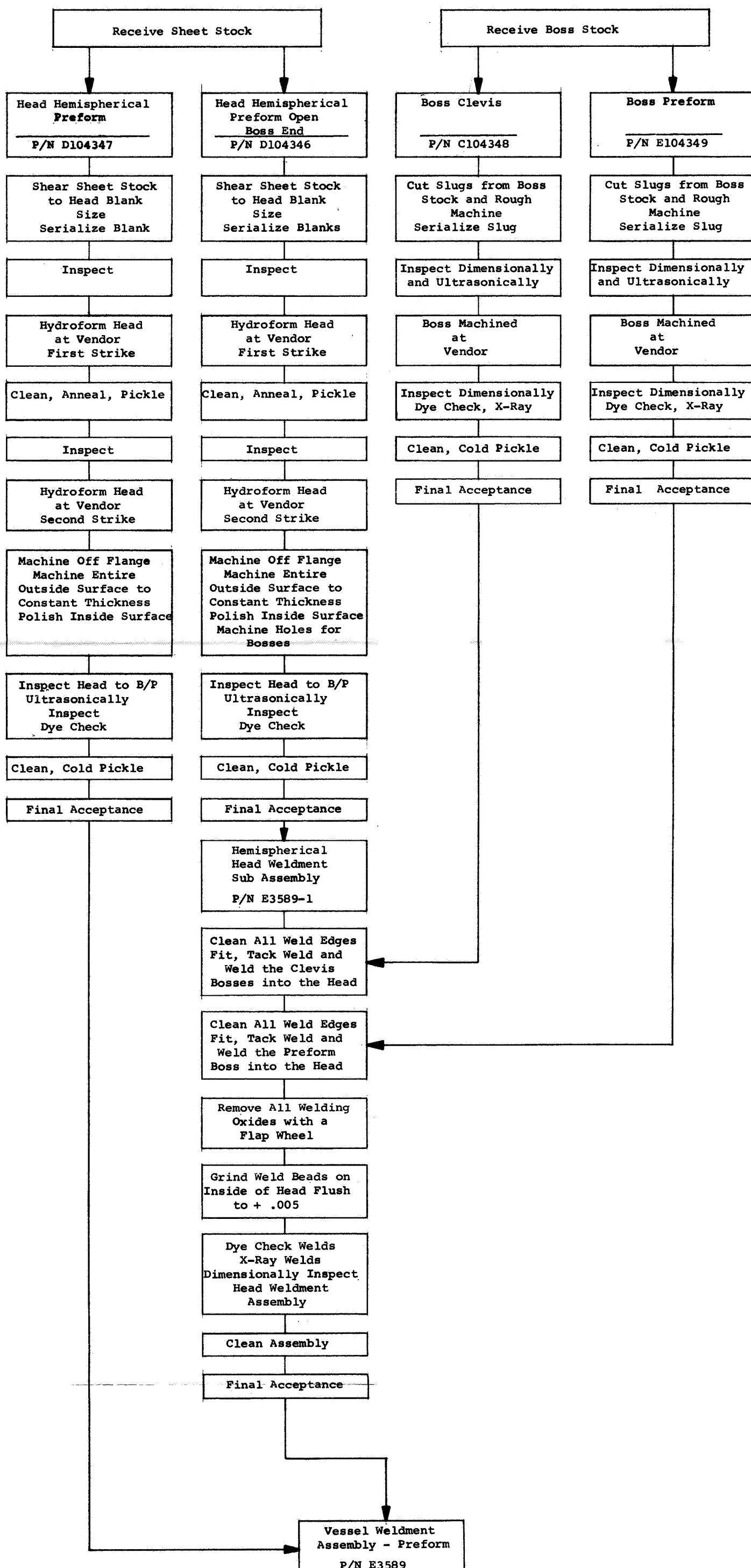
The hydroforming process was selected to produce the hemispherical heads for the spheres. Hydroforming requires relatively inexpensive initial tooling and is a reliable means of producing hemispheres from sheet stock.

For the thickness of heads utilized in this program, the hydroforming was done in two strikes. During the first strike the head was drawn to about 95% of its full depth. The head was then cleaned, solution annealed and restruck. The second strike was used to shape up the head and achieve closer dimensional control. All handling of material, cleaning and annealing was performed by the hydroform vendor in accordance with applicable Arde specifications.

ARDEFORM MANUFACTURING FLOW CHART

for

NASA HELIUM BOTTLE



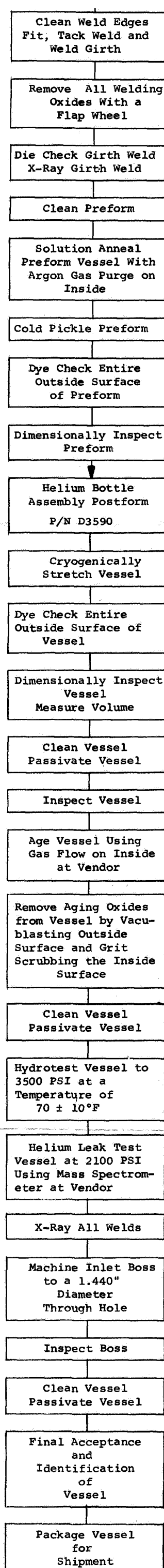


Figure VI-1

1. Starting Material Thickness

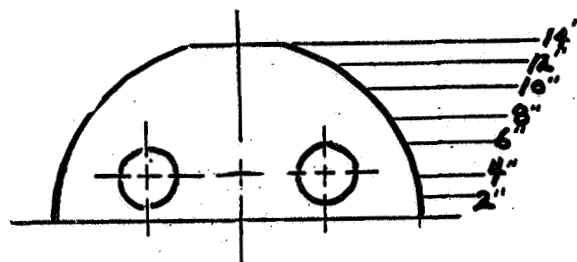
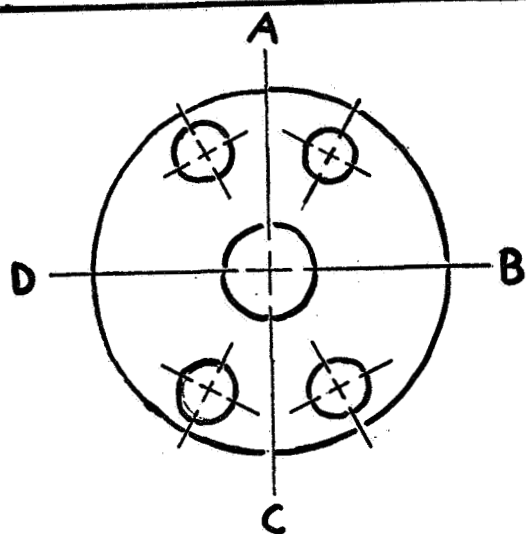
It has been Arde's experience that hydroforming of hemispheres generally results in about a 15% total variation in the wall thickness of the hemisphere. In order to reduce the weight of the vessels, the entire outside surface of each hemisphere was machined to a reasonably constant thickness. To provide enough material for machining, the as-formed head thickness was set at a minimum of .009 thicker than the minimum preform wall thickness. The minimum wall thickness of the preform vessel is .128" (See Section IV). Thus, the minimum head thickness after hydroforming must be .137. Since a thickness variation of 15% must be anticipated during the hydroforming, the minimum flat sheet stock thickness ordered was 15% greater than the minimum hydroformed head thickness. The minimum sheet stock thickness ordered, therefore, was .158 inches.

The specification to which sheet stock for this program was ordered, AES 256, allows a thickness variation of $\pm .007$ " for the nominal thickness required. The sheet thickness ordered, therefore, was $.165 \pm .007$ inches.

2. Final Thickness Variation

Based on discussions with head vendors prior to the inception of the program, it was felt that a tolerance of $\pm .003$ inches could be maintained during the machining of the surface of the hemispheres. Thus, the blueprint thickness of the head was set at .128" minimum and .134" maximum.

The heads used for the helium bottles were hydroformed and machined by a vendor. Two finished heads, one with the boss cut-outs and one without the boss cut-outs were submitted by the vendor prior to the production run of all heads. Arde carefully inspected these heads for thickness variations and sphericity. The heads were inspected for thickness variations, along four meridians 90° apart, arbitrarily drawn from apex to girth. Thickness readings were taken at two inch intervals along each meridional line. See Figure VI-2 for the dimension obtained. These thickness measurements revealed that the original assumption concerning thickness variation was unrealistic. The vendor, in spite of his best effort and the use of special tooling, could not obtain a thickness tolerance of $\pm .003$ inches. A tolerance of $\pm .007$ inches is more realistic. Thus, in order to retain a minimum preform wall thickness of .128, the head thickness was set at $.135 \pm .007$ inches. It should be noted that this head thickness specification represents a range of approximately 11%. Thus, by machining the heads, the thickness variation was reduced from the 15% tolerance that has been experienced with hydroforming, to 11%. The machining process thus represents a weight saving of 4% over hydroforming alone, although it did not result in the weight saving anticipated. All heads were hydroformed and machined to the above tolerances. The incoming inspection of each head included a thickness measurement procedure similar to that used on the first two heads and described above. The photograph of the two hemisphere details comprising each sphere is shown in Figure VI-3.



Wall Thickness of Hemisphere
Part No. D104346, Serial No. 1

Position	A-BAND	B-BAND	C-BAND	D-BAND
2"	.133	.134	.133	.134
4"	.132	.131	.130	.131
6"	.131	.130	.131	.130
8"	.128	.128	.128	.128
10"	.126	.124	.125	.125
12"	.124	.124	.123	.123
14"	.123	.123	.123	.123

Figure VI-2



Saturn S IV B Helium Storage Vessel
Details Ready for Welding

Figure VI-3

C. Forging and Machining of Bosses

Bosses and attachments welded into the shell must be machined from heavy sections of material. These heavier sections originate from the same ingot as the sheet material. The material from which the bosses are fabricated, therefore, has undergone considerably less reduction than the sheet material. For this reason some attention must be paid to the orientation of inclusions in the material. At Arde, experience has shown that when welding bosses to the sheet which forms the vessel shell, the most favorable condition occurs if the direction of boss inclusions lies more or less parallel to the shell surface where the weld is being made. Forged bars and pancakes were made which, upon machining, would result in approximately this weld orientation.

All bosses used on the final production type bottles were fabricated from heat 97102. For this purpose approximately 1500 pounds of the ingot from heat 97107 was forged into two bars each 2 5/8" square by 51" long, and 17 pancake forgings each approximately 7 inches in diameter and 3 inches thick. The bars and pancake forgings were annealed. The bars were then cut into 3 inch lengths. Each piece was then cut into two slices 3" x 2 5/8 x 1 5/16 and the clevis bosses machined from the slices. In this manner the proper orientation of the inclusions with respect to the weld could be maintained. The inlet bosses were machined from the seven inch diameter pancake forgings.

In the case of heat 50793, the clevis bosses were cut from 1.25 thick sheet bar whereas the inlet bosses were fabricated from pancake forgings as were the bosses from Heat 97107

The finished bosses were dimensionally inspected, dye penetrant checked, x-rayed, cleaned and cold pickled prior to final acceptance.

D. Welding of the Helium Vessel Assembly

The cryogenic stretching process requires a weld which will undergo plastic deformation at -320F and will exhibit a strength equivalent to that of the parent material. Investigations have been made to determine weld parameters that are reasonably independent of small changes in parent material composition, and that result in uniform reliable welds. Welds produced in a single pass, rather than multiple passes, have been found advantageous for several reasons. The single pass technique prevents carbide precipitation immediately adjacent to a weld bead. When a single pass weld is made, carbides precipitate some distance from the fusion zone. These carbides can be readily dissolved upon subsequent annealing. When multiple passes are made, the second pass can cause precipitation of carbides close to the weld pass below it. The grain boundaries of the material in which these carbides precipitate have been affected by the first pass. Carbides in these grain boundaries have been found very difficult to dissolve. Such grain boundary carbides tend to reduce the toughness of the material at cryogenic temperatures.

A single pass weld also eliminates the occurrence of lack of fusion between passes which is frequently experienced in multi-pass welds. Also, a single pass weld reduces the amount of filler material introduced into the joint.

An additional factor in welding of the Ardeform material is the avoidance of small micro cracks which will open during stretching. By removing all restraints during welding, such as back-up fixtures, a crack free weld can be made. Thus, for the Ardeform

process, a single pass gas-backed weld is used. Unless special techniques are used, in thicknesses over .125 inches, the weld bead may drop through if it is not supported.

Arde has developed an approach which produces a horizontal single pass weld made with a vertical torch. This is accomplished by means of a closely controlled pressurized gas back-up to support the weld. Thicknesses up to 3/8" have been welded in this manner using the tungsten inert gas (TIG) welding process. The filler wire used is type 308L stainless steel. For these vessels helium torch gas, and argon gas back-up was used. No special weld preparation or "V" joints are machined into the components prior to welding. Arde's experience has shown that a simple butt joint results in 100% fusion and requires a minimum of weld wire filler. However, great care is required in the pre-weld fitting and alignment of parts. Closely spaced tack welds are required to prevent the misalignment of parts during welding. All weld surfaces are carefully cleaned to prevent foreign particles from contaminating the welds.

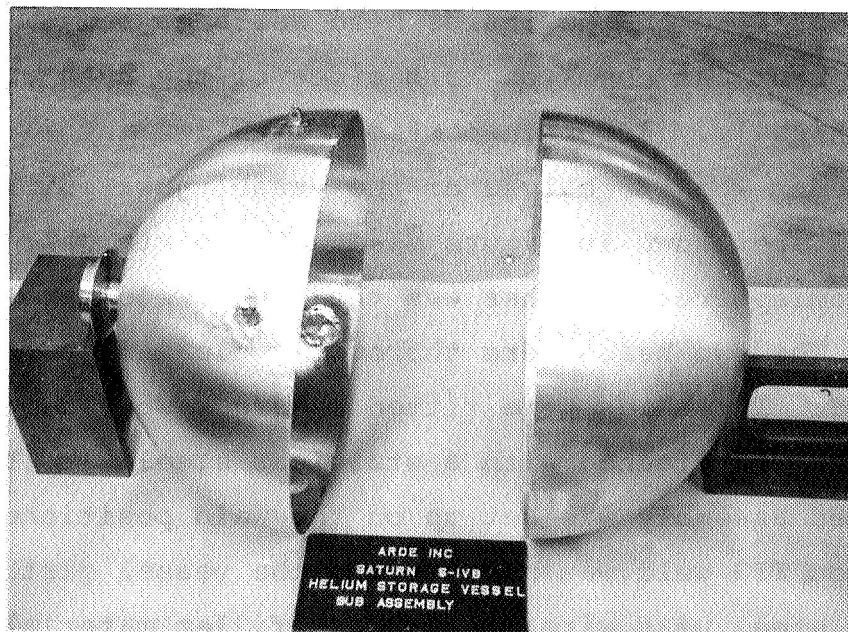
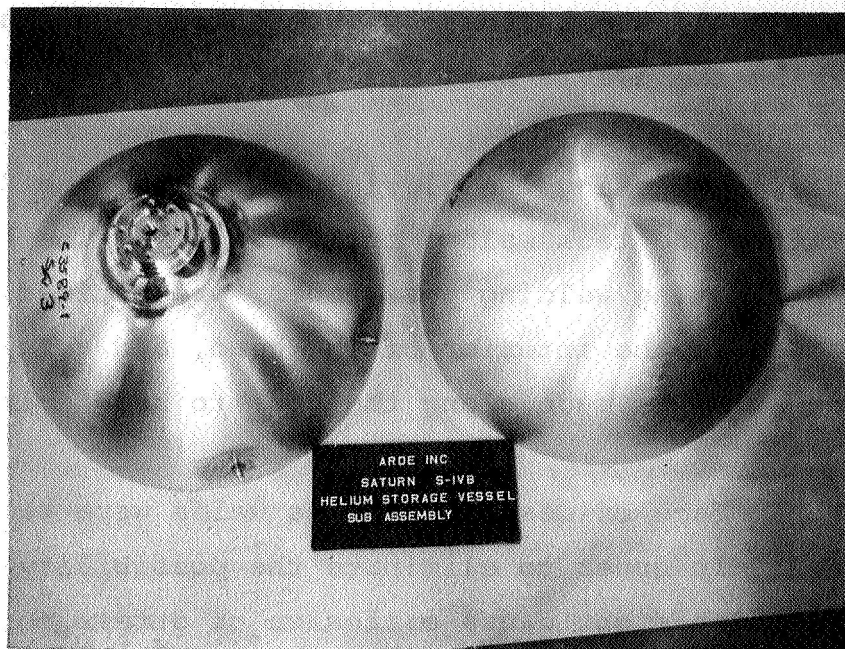
The welding of the helium vessels was done in three distinct steps...

First, the small clevis bosses were tack welded into place. The inlet boss opening and the bottom of the hemisphere were taped over and argon was passed through the inside of the hemisphere while a full penetration TIG weld was made around each of the clevis boss to head joint. The locations at which the clevis bosses are mounted on the head makes necessary elaborate

fixtures if machine welds of the clevis bosses were to be made. Instead, a simple holding fixture was made and a hand weld was used for the small clevis bosses. Pressurized gas back-up was used in making the clevis boss welds.

After completing the clevis boss welds, the large inlet boss was fitted and tack welded into position. The head was set up on a rotating welding positioner, pressurized argon gas was maintained in the interior of the head, and a full penetration TIG machine weld was made along the boss to head joint.

The surface oxides on the boss welds were removed with a flap wheel. In order to eliminate the possibility of notches or crevices which might cause corrosion or stress concentrations, the boss welds were ground flush to the parent material. This grinding was done on the inside head surfaces only. The welds were die penetrant check on both sides of the head and inspected radiographically. After inspection the alignment of the bosses was checked. The two halves of the vessel just prior to the final weld are shown in Figure VI-4. The girth weld which joins the two hemispheres together was the final weld made on the helium bottles. The two heads were thoroughly cleaned just prior to this final weld. The heads were fitted and tack welded together. The tack welds were cleaned with a stainless steel wire brush. The tack welded assembly was set up on the weld positioner and a full penetration TIG weld was made around the vessel girth. Type 308 stainless steel weld wire was used as filler material. After welding, oxides were removed from the exterior surfaces with a flap wheel. Oxidation of the interior of the vessel was prevented by the pressurized argon gas back-up. The weld was dye checked and X-rayed; and the preform was then checked dimensionally.



Saturn S-IVB Helium Storage Vessel
Welded Subassembly

Figure VI-4

E. Annealing

In order to eliminate welding carbides, and to remove any thermal stress which may have been created in the vessel during welding, each vessel was solution annealed after welding. Solution annealing is carried out at 1950F. Control of the oxidation of the vessel surfaces is therefore required. Inasmuch as a rapid quench in cold water is required to maintain carbides in solution with this material, inert gas or reducing gas protection is not very feasible. This is because the vessel would have to be removed from any protective atmosphere anyway for access to the quenching tanks. By scrupulously cleaning the vessel surfaces, it is possible to obtain a uniform scale which is readily removable by pickling for short times when vessels are annealed in air. Vessel interiors, however, may be protected from oxidation.

Each vessel was carefully cleaned in hot alkaline detergent solution and thoroughly rinsed in demineralized water prior to annealing. Stainless steel tubes were then connected to the vessel interior in such a way as to permit the flow of argon into and out of the vessel. Lengths of flexible tubing were incorporated between the stainless steel tubes and the argon source. The flexible lines allowed the vessel to be maneuvered into and out of the furnace while argon flow was maintained. A minimum of seven vessel volumes of argon was flowed through the vessel before it was placed in the furnace. The vessel, in a stainless steel cradle, was placed in the 1950F furnace. After forty minutes, the vessel was removed from the furnace and immediately plunged into a water bath and covered with a water

spray. As was stated previously, the rapid quench prevents the formation of carbides by quickly cooling the vessel through the carbide precipitation temperature range. Argon gas purge was maintained throughout the annealing cycle. The exterior of the vessel was cold pickled to remove annealing oxides. As a final step each vessel was dye penetrant inspected over its entire exterior surface, and dimensionally inspected.

F. Cryogenic Forming of the Helium Vessels

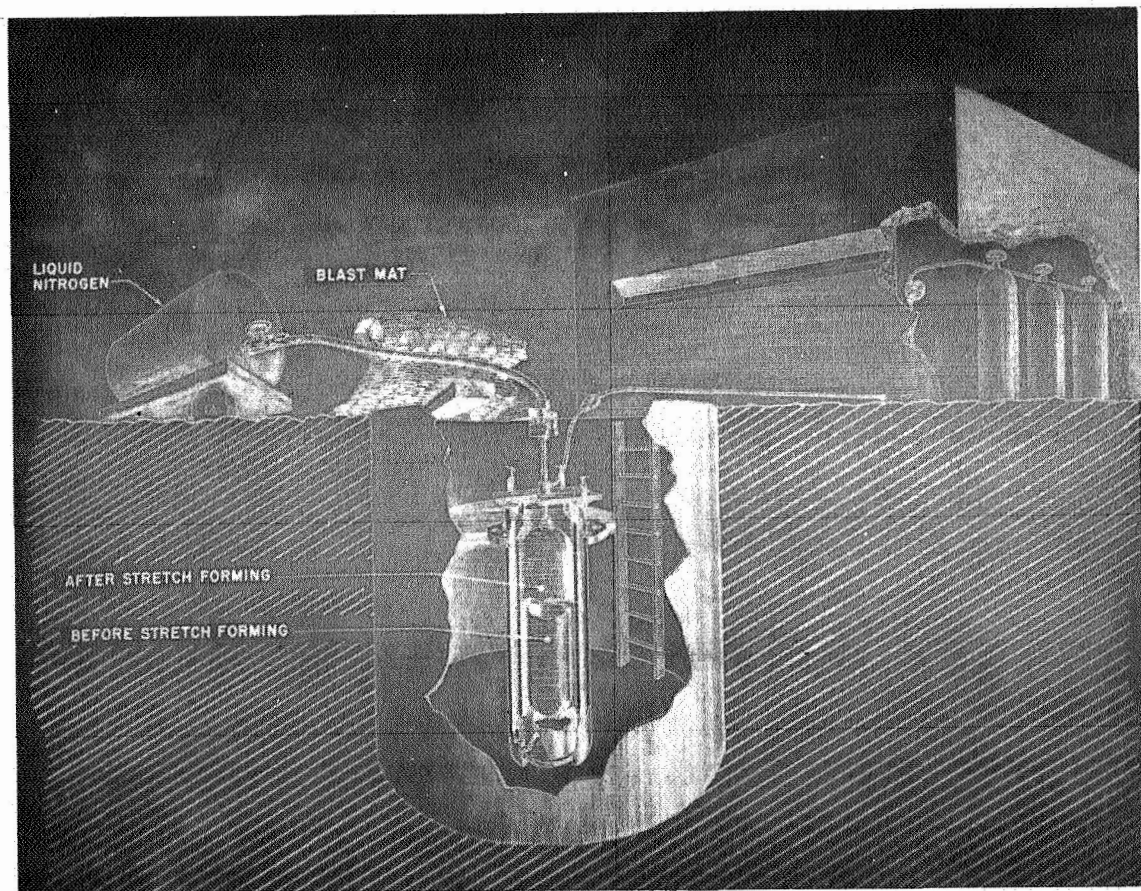
The stretch forming facility consists of the stretch pit, a control room and a liquid nitrogen storage and pumping system. The pit is approximately 18 feet deep by 8 feet in diameter and accepts forming tanks of various sizes which are filled with liquid nitrogen for the stretch forming operation. The size of the forming tank which is used is dictated by the vessel size. Often, for cylindrical vessels, the vessel is stretched into a forming die. The die limits the total amount of plastic deformation and controls the final diameter of the vessel. Since the middle of cylindrical vessels stretch more readily than the ends, a barrel shape results. The die permits the forming of cylinders of uniform diameters. Close dimensional control is achieved through the use of such dies. Spherical dies may also be used in the cryogenic stretch forming of vessels. Stretching into a spherical die could ensure closer dimensional control of the final vessels.

The vessels fabricated for this program, however, were subjected to a "free form" stretch. Dimensional control of a free

form vessel is achieved through close inspection of the preform vessel geometry, and thorough knowledge of the cryogenic behavior of the material from which the vessel is fabricated. Cryogenic behavior is determined by conversion of uniaxial tensile data into biaxial, sphere cryogenic behavior. A stretch forming operation proceeds as follows:

A forming tank is filled with liquid nitrogen to the level which covers the preform to be stretched. The preform is filled with liquid nitrogen. When the preform is full, it is lowered to the bottom of the forming tank. At this time the forming tank is topped off with liquid nitrogen so that the liquid level is maintained above the vessel. This is done to insure that boil-off of liquid nitrogen in the forming tank will not reduce the liquid level during stretching and cause a failure due to inadequate refrigeration. The preform is then connected to the pressurization source from the control room. A heavy steel blast mat is placed over the entire pit as a precautionary measure.

The final phase of the operation is the actual pressurization of the preform. Liquid nitrogen is pumped into the refrigerated preform until the predetermined pressure is achieved. When this occurs a vent valve is opened and the system is rapidly bled down to atmospheric pressure, ending the stretch. The pressurization process is controlled from the control room. The expanded preform is then removed from the forming tank. Figure VI-5 shows a cryostretch facility schematic.



STRETCH FACILITY

Figure VI-5

TABLE VI-1

NASA Helium Bottles

P/N D 3590

Postform Dimensions of Production Type Vessels

<u>S/N</u>	<u>Dia. Inches</u>	<u>Height Inches</u>	<u>Volume Measure in³</u>
3	22.875	24.730	6008.0
4	22.812	24.678	5994.8
6	22.825	24.698	5972.0
7	22.829	24.768	5974.1
8	22.887	24.742	5973.8
9	22.855	24.729	5973.2
10	23.046	25.196	6161.0
11	23.040	25.188	6168.0

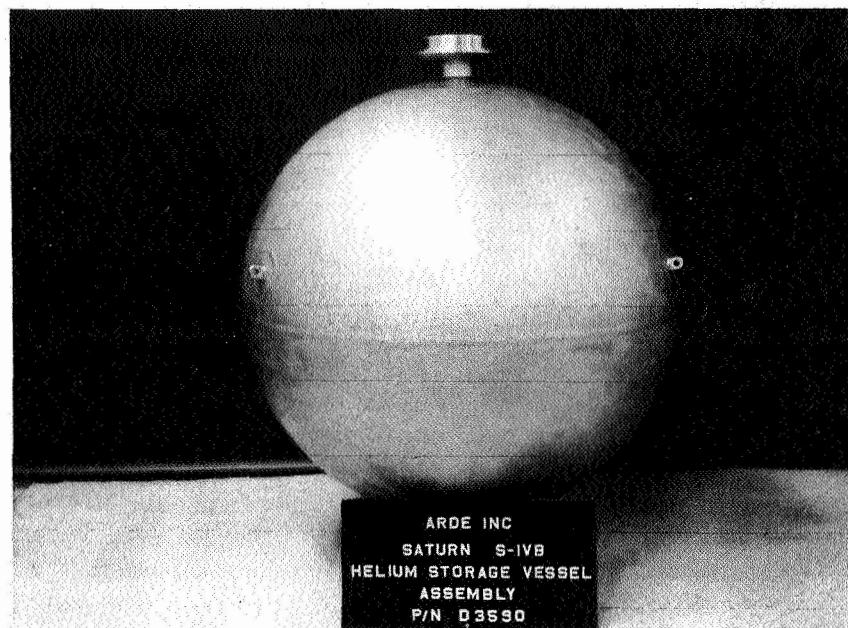
After each vessel was cryogenically stretched it was dye penetrant inspected over its entire outside surface. Each vessel was then dimensionally inspected, including volume measurement. Figure VI-6 shows a vessel after stretching, while Table VI-1 gives the dimensions of the stretched vessels. The vessels were cleaned and dried after the inspection was complete.

G. Final Processing

1. Aging

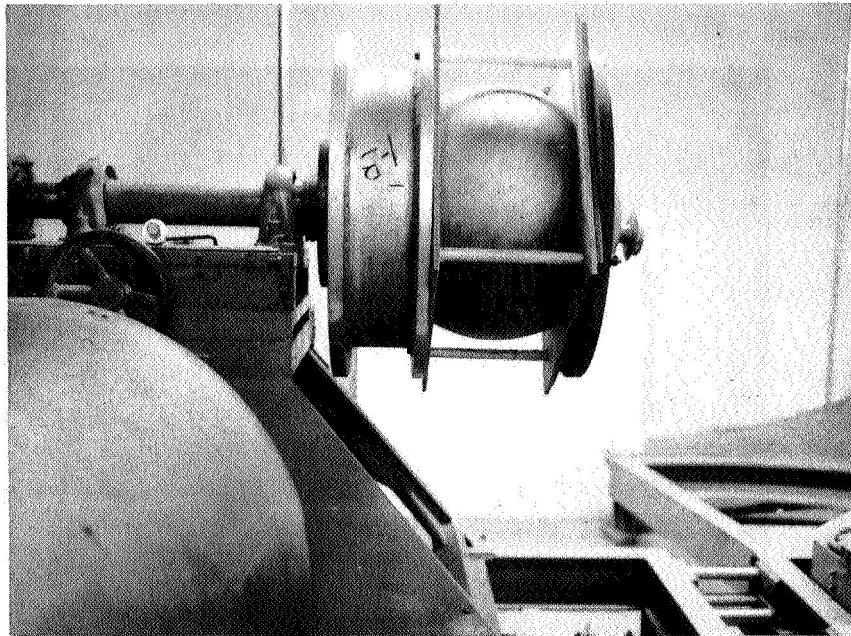
After each vessel had been cryogenically stretch formed, inspected and cleaned, the vessels were aged in air at 790F for twenty (20) hours. In the air atmosphere of the furnace at 790F, the stainless steel oxidizes and becomes covered with a light golden brown film. In order to minimize the oxidation on the inside of the vessel, argon gas is kept flowing through the vessels during aging.

After aging was complete, aging oxides were removed from the outside surface of the vessel by vacu-blasting. In order to remove any oxides which may have accumulated on the inside of the vessel during aging, the vessel was partially filled with a silicon carbide grit, set up on a rotating spindle, and slowly rotated. A fixture, used to hold the vessel for this purpose, allowed the vessel to be rotated at various angles and thus polish the entire interior surface with the silicon carbide grit. The vessel boss was not used as a support during grit scrubbing. Figure VI-7 shows a vessel during the grit scrub operation. After all aging oxides were removed each vessel was thoroughly cleaned on the inside and outside and passivated.



Saturn S IV B Helium Storage Vessel
After Cryogenic Stretch Forming

Figure VI-6



Saturn S IV B Helium Storage Vessel
During Grit Scrub

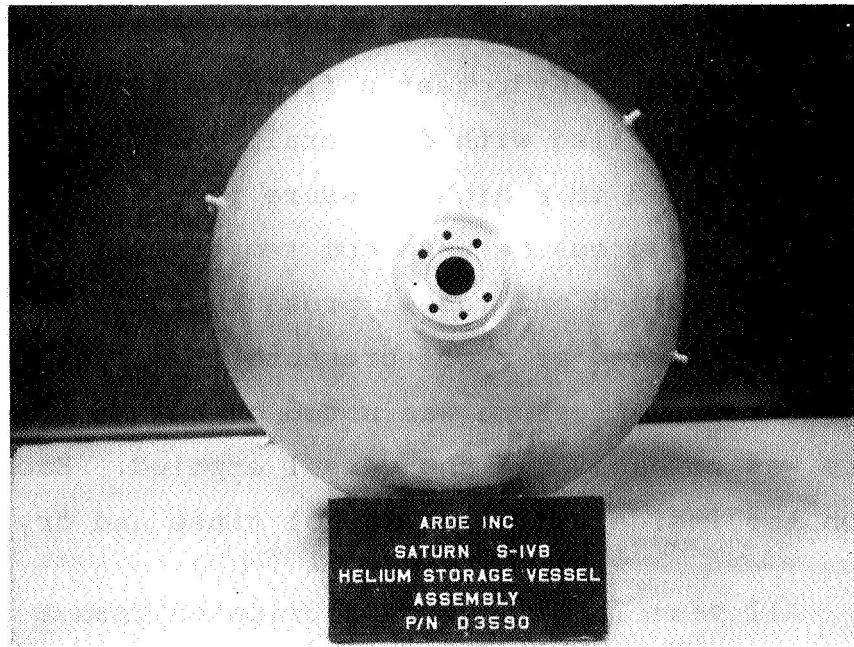
Figure VI-7

2. Final Testing, Processing and Acceptance

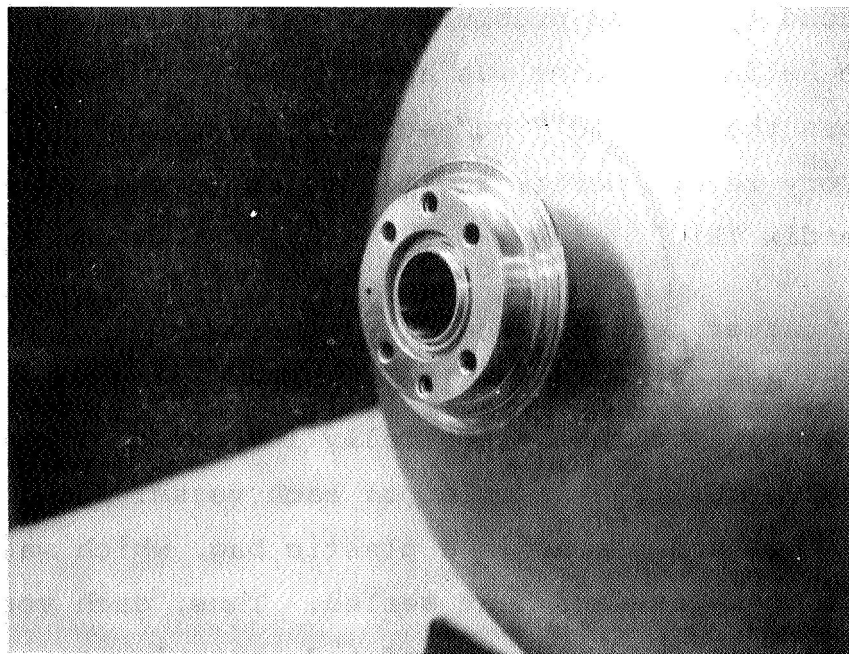
In order to hydrotest a finished vessel, it was placed in a cradle and filled with demineralized water. The vessel was then connected to a high pressure pump and pressurized to 3500 psig (proof pressure) at room temperature. At 3500 psig the pump was stopped and vessel pressure was held for one minute. If the vessel leaked at proof pressure, the pressure gage would drop. No drop in pressure was noted on any of the vessels. The pressure was released and the vessel emptied. Each vessel was dried on the inside using an alcohol rinse and dry nitrogen gas.

All vessels which were fabricated from Heat 97107 were shipped to Ogden Test Laboratory on Long Island, N.Y. for helium leak detection. The helium leak test was conducted per Arde Specification AES 454, Method II (App. D). Each vessel was pressurized with helium gas to 2100 psig at room temperature during leak testing. The vessels were cycled twice to 2100 psig. On the second cycle the pressure was held at 2100 psig for two minutes and the helium detector was applied. All vessels showed a leakage rate less than 1×10^{-6} cc/second. A copy of Ogden Test Laboratory report pertaining to the above testing will be found in Appendix (E).

After testing, the inlet boss was final machined to blueprint dimensions. Finally, each vessel produced, was dimensionally and radiographically inspected, weighed, cleaned and passivated. The interior of each vessel was purged with dry nitrogen gas and placed in a plastic bag, which was also purged with nitrogen gas, and heat sealed. Thus, each vessel was protected from the moisture and and contaminants of the atmosphere. Figure VI-8 shows a vessel ready for bagging.



Saturn S IV B Helium Storage Vessel
Ready for Delivery



Saturn S IV B Helium Storage Vessel
Close up View of Final Machined Boss

Figure VI-8

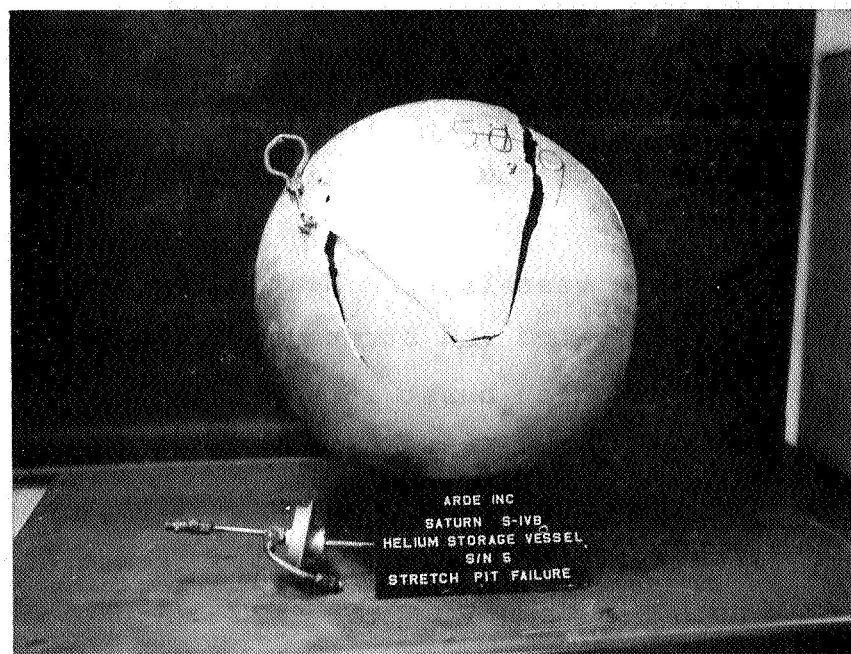
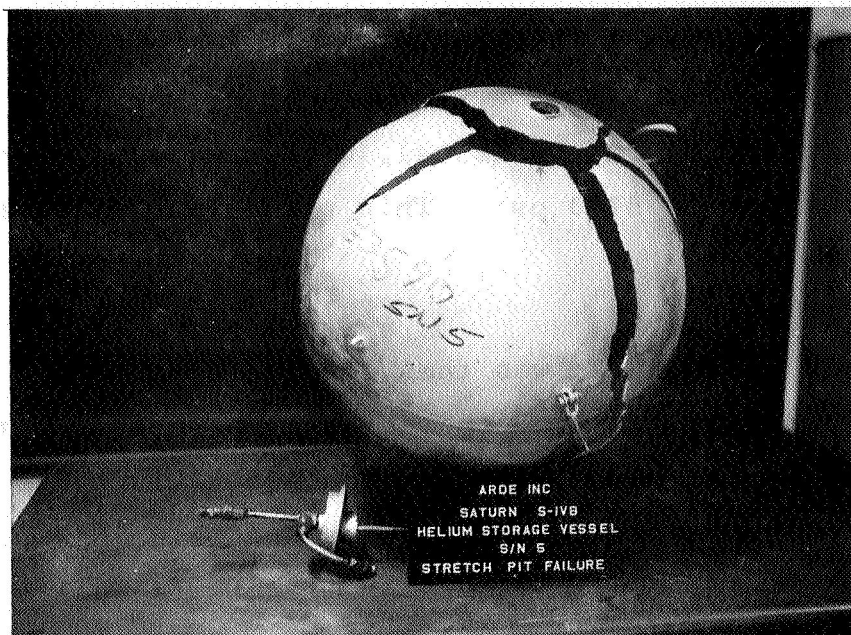
H. Fabrication Results

A total of twelve (12) preforms were fabricated and assigned serial numbers from 1 through 12.

The first preform, Serial #1, was successfully stretched in the stretch pit to 5100 psi. This vessel was fabricated from Heat 97058.

Vessel, Serial #2, was then stretched and burst in the pit during the stretch forming operation at a pressure of 5150 psi. Failure analysis showed that stretch pit failure resulted from presence of exogenous laminar inclusions which had been passed over by the weld. Further details of failure analysis may be found in Section VII. Because of the failure of Serial #2, vessel Serial #1 was aged at 800F and tested at -320F to burst. The burst test of Serial #1 indicated satisfactory strength at -320F. Nevertheless, because of the failure of vessel Serial #2 due to presence of large slag inclusions, Heat 97058 was rejected.

All the remaining vessels, from Heat 97107 Serial # 3 through #9 were fabricated and stretched successfully except for Serial #5 which burst at a stretch pressure of 5800 psi. Serial #5 showed, upon examination, a thin region in the vicinity of the boss which had apparently been excessively machined. The stretch pit failure of this vessel, then, was not due to the same cause as that noted in Vessel Serial #2. (A photograph of Vessel Serial #5 is shown in Figure VI-9. The arrow in the upper photo pin points failure origin). The remaining six (6) vessels were then radiographically inspected after the stretch forming operation. The X-Rays from two of these vessels showed the presence of hair line cracks in the welds. Vessel S/N 3 had a single crack indication



Saturn S IV B Helium Storage Vessel S/N 5

Cryogenic Stretch Pit Failure

Figure VI-9

and vessel S/N 7 had two such indications. As a result, these two vessels were rejected. The four remaining vessels, S/N 4, 6, 8 and 9 passed radiographic inspection and are considered acceptable for service at -423F.

The nature of the crack-like indications on the two rejected vessels, which were not shipped to NASA, was the subject of a subsequent investigation described in detail elsewhere in this report.

Three (3) preforms S/N 10 through 12 from Heat 50793 were processed of which two (2) S/N 10 and 11 were subsequently delivered to NASA. The S/N-12 unit was processed up to the point of cryogenic stretching and then terminated since only two (2) of three (3) vessels processed were required.

In summary, six vessels, free from slag inclusions detectable by the ultrasonic inspection technique and free from cracks detectable by radiographic inspection have been shipped to NASA.

VII EFFECT OF INCLUSIONS ON STRETCHING OF PREFORMS

A. Background

During the hydroforming of hemispheres using sheet rolled from heat 97058, several defects were noted on the surface of the parts. These were initially diagnosed as laps caused by improper sheet rolling. In order to prepare satisfactory heads, the I.D. surfaces were ground where these laps occurred. In addition, all finished hemispheres were ultrasonically checked, using a 1/2" diameter transducer, and a gain level based on a standard 3/64" diameter flat bottom hole. No defects were found by this technique. Two sphere preforms, S/N 1 and S/N 2 were then fabricated from heat 97058. The first vessel, S/N 1, was successfully stretched at -320F to a stretch pressure of 5100 psi. The second vessel S/N 2 failed, however, during stretch at a pressure of 5150 psi. Detailed examination of this vessel indicated that inclusions were the cause of the failure. As a result of this examination, heat 97058 was rejected and the vessels deliverable under this contract were fabricated instead from a second heat, 97107. Arde's inspection techniques established that four vessels fabricated from heat 97107 and delivered to NASA, were free from defects which would be detrimental to their performance at -423F. A detailed discussion of the failure analysis of the vessels from the rejected heat and a description of Arde's inspection steps for insuring the reliability of the delivered vessels, follows.

B. Analysis of Burst Vessel

The fracture path on vessel S/N 2 followed around the girth weld near the weld base metal interface. The fracture origin was located by means of the fracture appearance. At the origin, a

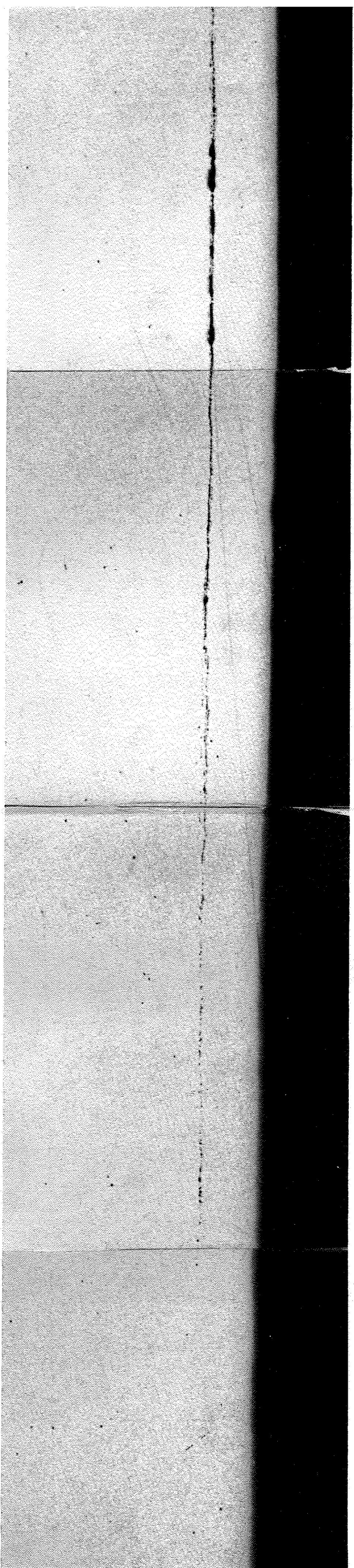
crescent shaped area could be distinguished on the fracture face. Examination of this area at 30X showed three suspicious features:

1. An apparent "split", laminar in nature which seemed to penetrate into the base metal.
2. A greenish colored protrusion which matched a hole of the same color on the mating fracture face.
3. Grainy area which showed black under one direction of illumination, and sparkled with apparent facets under other directions of illumination.

Microsection revealed that the cause of failure was a laminar slag inclusion which extended for at least .180 inches in length from the fracture edge into the base metal. This was shown by sectioning through the laminar split seen on the fracture face. Sections near the green protrusion demonstrated a considerable amount of non-metallic material and crack-like voids in the weld itself.

No additional information was elicited from sectioning the faceted areas and this section was therefore not pursued further than a few polishes which revealed nothing. It is concluded that the "facets" were probably burnished metal caused by rubbing of the mating fracture faces at that location.

A series of overlapping micro photographs were made to show the extent of the laminar inclusion (see Figure VII-1). The region in the weld adjacent to the green protrusion is shown in Figure VII-2a. Figure VII-2b shows the laminar inclusion in relation to the weld metal and in relation to the base metal surfaces. The laminar inclusion was located approximately .006



1

2

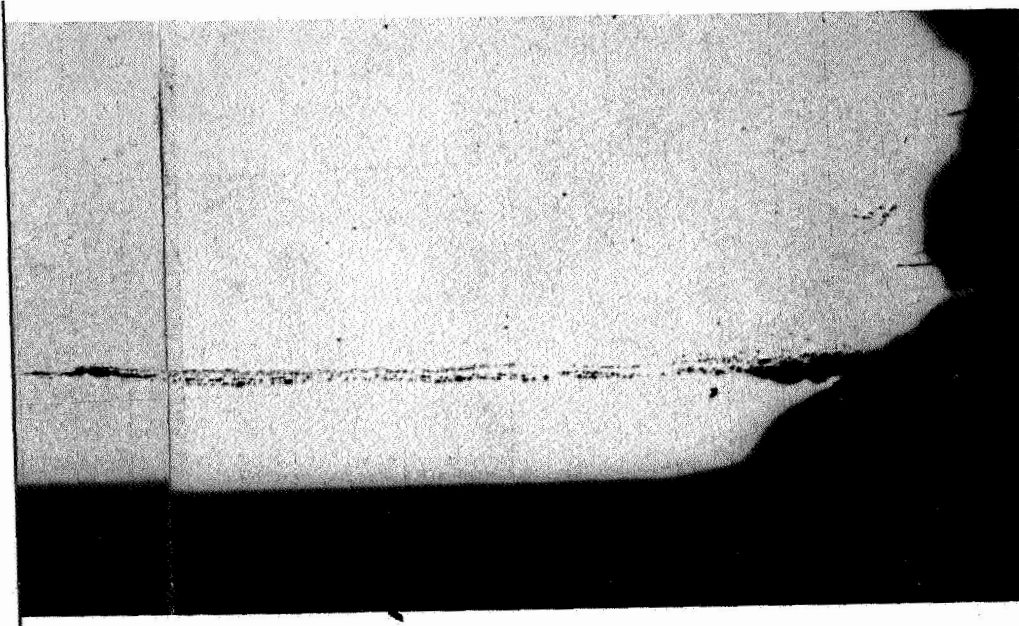
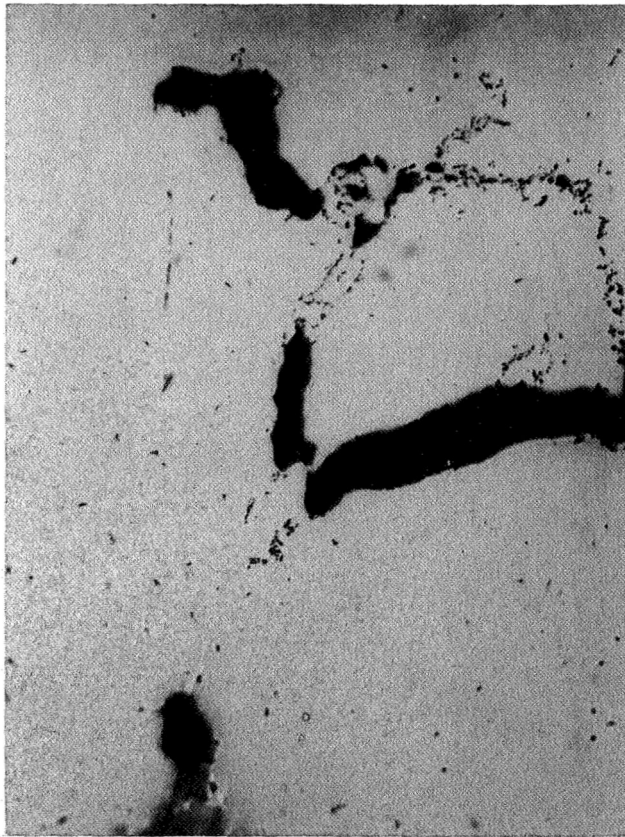


FIGURE VII-1

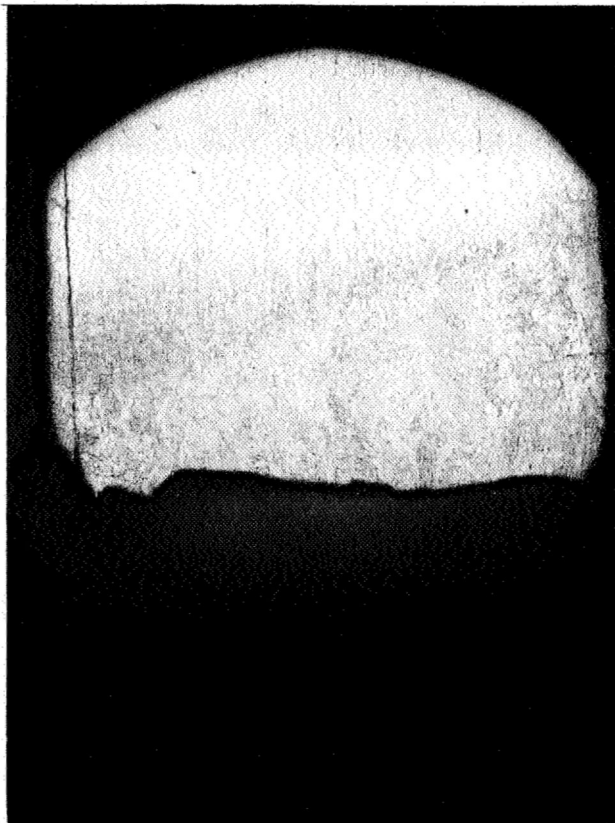
Laminar Slag Inclusion from the
Helium Sphere S/N 2 P/N D3590

Mag 100X

Unetched.



Saturn S IV B Helium S/N 2
Storage Vessel
Section of green protrusion
on fracture face
200X 10% Oxalic Acid



Saturn S IV B Helium
S/N 2 Storage Vessel
Section of laminar inclusion
25X 10% Oxalic Acid

Figure VII-2

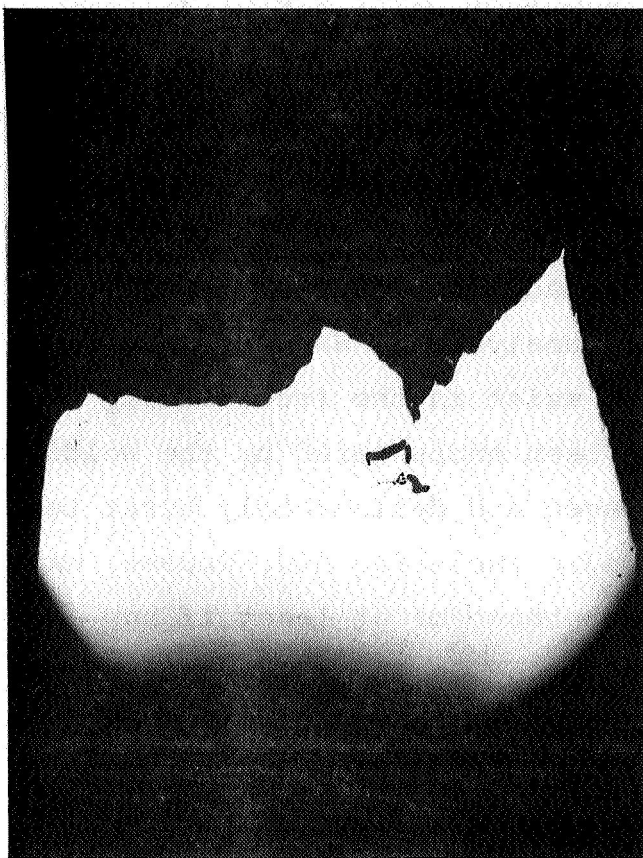
inches from the I.D. surface of the hemisphere. The thickness of the thickest part of the inclusion is approximately .0005 inches.

The location of the defects in the weld metal, adjacent to the green protrusion, is shown by Figure VII-3a. A high magnification view of non-metallic material in the laminar inclusion is shown in Figure VII-3b.

It is interesting to note in Figure VII-2b that the edge of the weld did not appear to disturb the inclusions. However, it is suspected that the inclusions in Figure VII-2a were washed up by the weld from the laminar inclusion shown in Figure VII-1. Figure VII-2b is on the opposite side of the fracture face from Figure VII-3a. The section in Figure VII-3a was taken about 1/4 inch in the direction of welding from the section in Figure VII-2b.

It was concluded from these observations that the premature stretch pit failure of S/N 2 resulted from the interaction of a large laminar inclusion in the base metal with the weld. As was previously noted, laps had been observed during the hydroforming of hemispheres made from this same heat of material. Sectioning of one of these laps showed the same type of laminar inclusion.

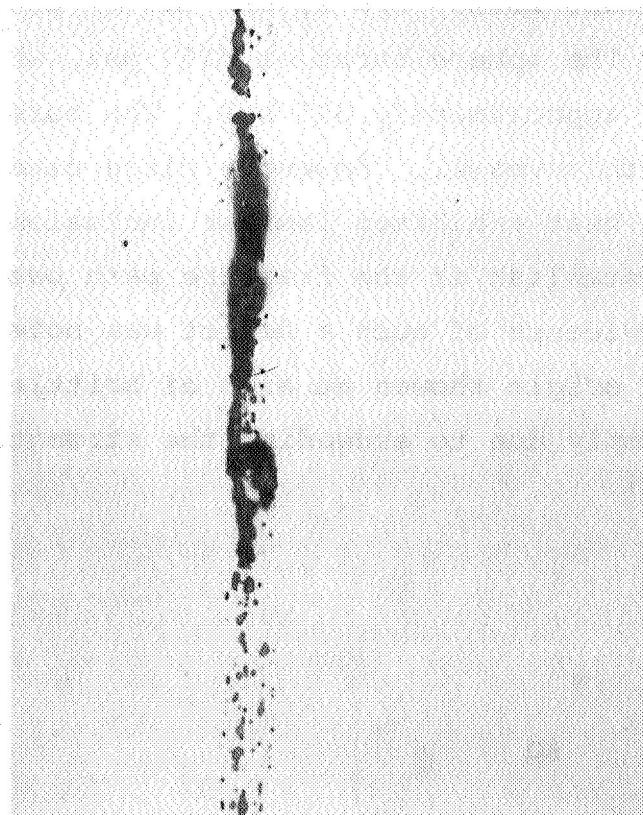
Routine microsections during incoming material inspection had not detected this type of slag inclusion. Since the



Saturn S IV B Helium
S/N 2 Storage Vessel
Section through green
protrusion.

25X

Unetched



Saturn S IV B Helium
S/N 2 Storage Vessel
High magnification photo
of portion of laminar
inclusion

500X

Unetched

Figure VII-3

distribution of these material defects is quite sparse, the likelihood of detection by microsection of sample sheet is limited. The laminar nature of these inclusions, and the fact that they are so thin makes them undetectable by radiographic inspection. Sphere S/N 1 had already been successfully stretched although it had been made from this same heat. It was suspected from the failure analysis of S/N 2 sphere that some of these inclusions might exist in the successfully stretched sphere, but had not been encountered by the welding. Sphere S/N 1 was, therefore, aged and deliberately burst tested at -320F to determine if the slag inclusion did, indeed, exist in the successfully stretched sphere; or at least if any deleterious effect could be observed in the mechanical properties of a completed, successfully stretched sphere.

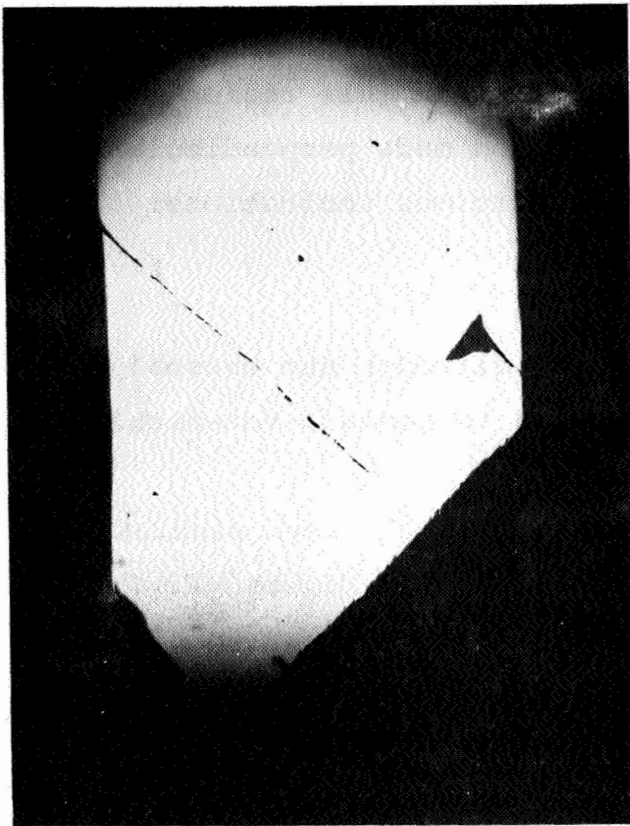
C. Analysis of Sphere S/N 1 Burst Tested at -320F

NASA helium sphere, Part No. D3590, S/N 1, was tested at -320F after stretching and aging. The sphere burst at 6250 psi, which represents a stress level of approximately 325 ksi. The burst stress was satisfactory for this vessel. However, since other vessels fabricated from this heat exhibited laminar inclusions, the vessel was examined to establish if the fracture path passed through such a defect. No evidence of such a defect was noted at the fracture origin. The origin showed no sign of brittle failure, and fracture was simply due to exceeding the strength of the material.

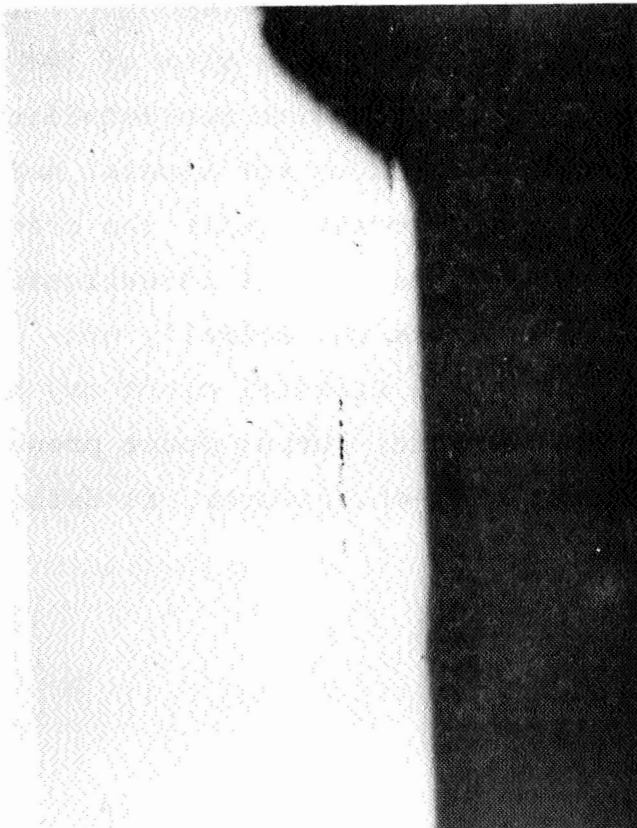
Examination of the fracture face showed a region some six inches from the fracture origin which exhibited laminar splitting. A view of one of a section in this region is shown at 25X in Figure VII-4a (section made perpendicular to the fracture edge) showed three suspicious indications:

1. A large triangular hole.
2. A diagonal crack which, although not unusual near a fracture edge, appears to contain non-metallic material.
3. A laminar inclusion about .010" long, similar to that observed in vessel S/N 2. Figure VII-4b shows the laminar inclusion at a magnification of 100X. Figure VII-5a shows a triangular hole at 200X. It should be noted that the hole appears clean and probably is a result of material pulled out during fracture. This sort of thing is not unusual near a fracture edge.

Figures VII-5b, VII-6a, and VII-6b show a view of the diagonal crack. It appears to be associated with non-metallic material. Although the presence of a crack is not unusual near a fracture, the non-metallic material associated with the crack are unusual. It was not definitely established by the investigation whether the material in the diagonal crack was actually non-metallic inclusions. The material in the diagonal crack may have been artifacts from the polishing operation during mount preparation. The laminar slag inclusion in Figure VII-4b, however, is definitely not an artifact.

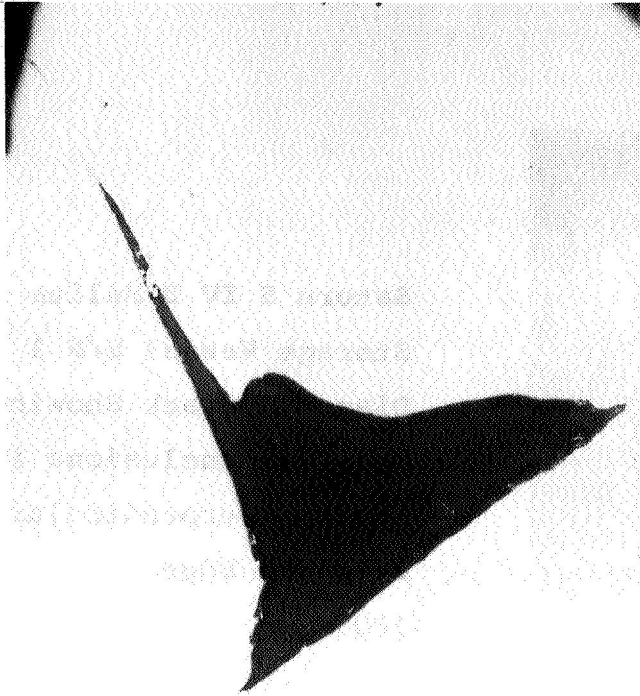


Saturn S IV B Helium
Storage Vessel S/N 1
Overall View of Section
Perpendicular to Fracture
Edge
25X Unetched



Saturn S IV B Helium
Storage Vessel S/N 1
Laminar Inclusion in Section
Perpendicular to Fracture
Edge Near I.D.
100X Unetched

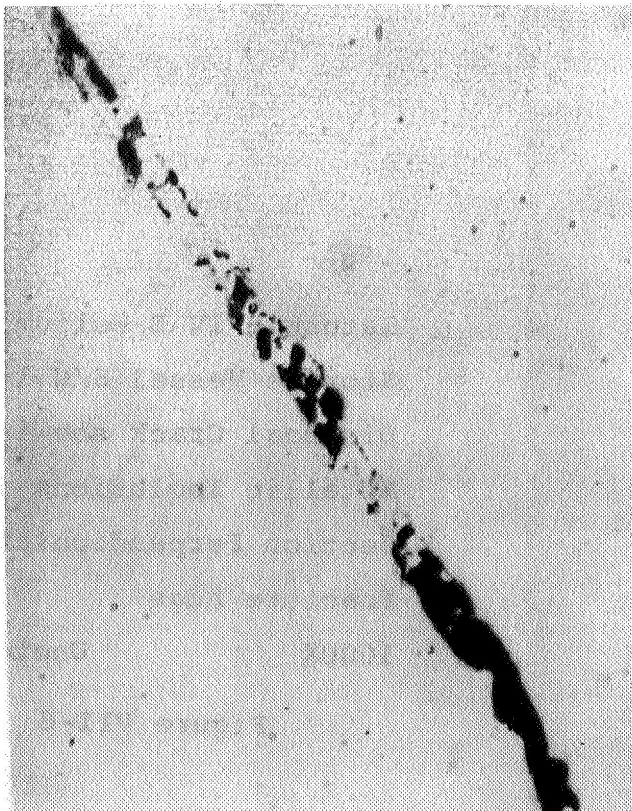
Figure VII-4



Saturn S IV B Helium
Storage Vessel S/N 1
Triangular Hole in Section
Perpendicular to Fracture
Edge, Near O.D.

200X

Unetched

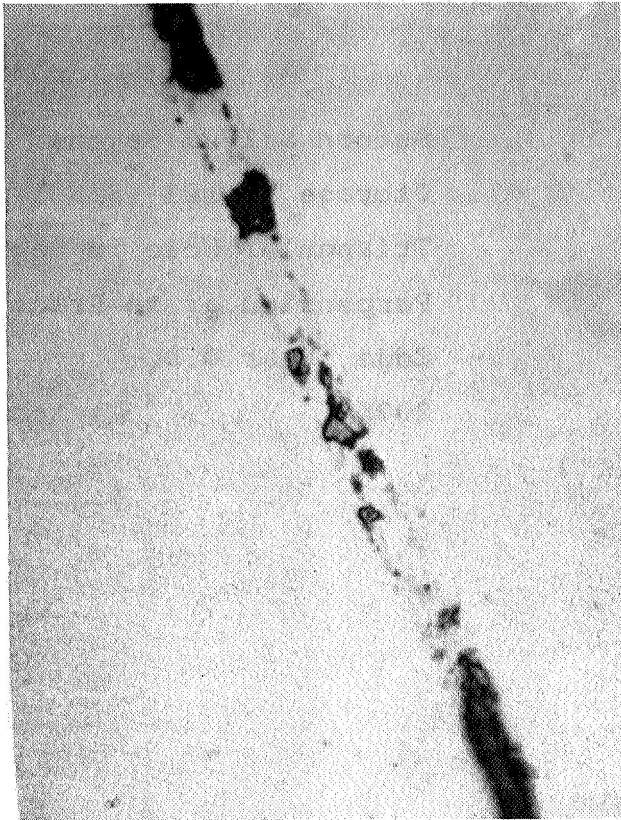


Saturn S IV B Helium
Storage Vessel S/N 1
Diagonal Crack Showing
Non-Metallic Inclusions
in Section Perpendicular
to Fracture Edge

500X

Unetched

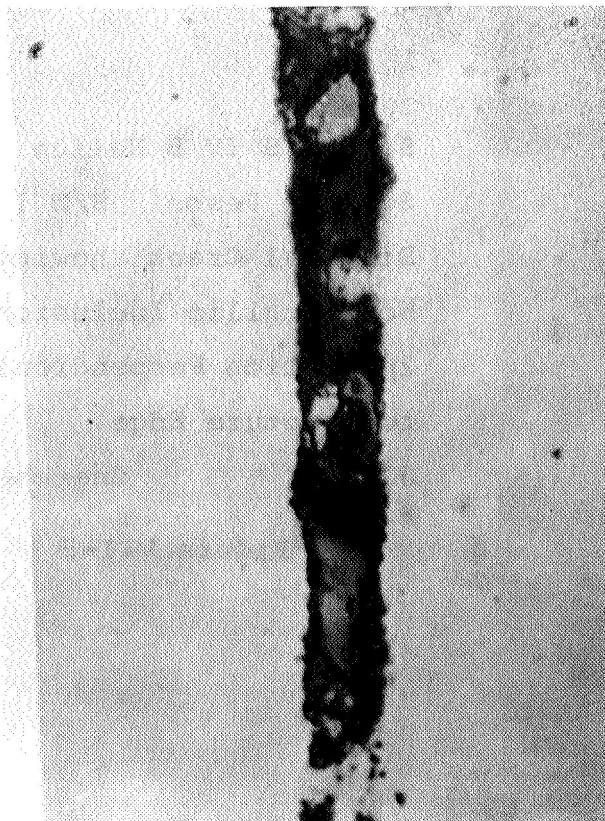
Figure VII-5



Saturn S IV B Helium
Storage Vessel S/N 1
Diagonal Crack Showing Non-
Metallic Inclusions in
Section Perpendicular to
Fracture Edge

1000X

Unetched



Saturn S IV B Helium
Storage Vessel S/N 1
Diagonal Crack showing Non-
Metallic Inclusions in
Section Perpendicular to
Fracture Edge

1000X

Unetched

Figure VII-6

Several conclusions could be drawn from the results observed with the two spheres, S/N 1 and S/N 2. These were as follows:

1) The laminar slag inclusions caused failure during stretch forming where a weld passed over them.

2) The slag inclusion noted in the base metal of a successfully stretched and aged sphere did not affect performance at -320F.

3) The slag inclusion noted in sphere S/N 2, which burst during cryogenic stretch forming was not a singular occurrence but probably existed in any of the hemispheres in which the previously described surface laps were observed during hydroforming. The entire heat 97058, therefore, was suspect.

4) The cryogenic stretch forming process was apparently capable of self inspection; that is, vessels in which a weld passed over an inclusion would fail in the cryogenic stretch operation, thus weeding out most unreliable vessels. If they did not fail during stretch, at least those defects which were present would enlarge and be detectable by radiographic inspection.

5) A test of a completed vessel at -320F indicated no deleterious effect of inclusions in the base metal.

It was decided that for utmost reliability heat 97058 should be discarded and an inspection method worked out, which would detect these defects if they existed in another heat which was available.

D. Methods for Detection of Slag Inclusions

In order to detect the type of thin laminar inclusion observed in the two vessels fabricated from heat 97058, it was felt that a suitable ultrasonic inspection technique would have to be evolved. Arrangements were made with Magna-flux Corp., Materials Testing Laboratory to conduct the necessary experiments. The objective of the experiments was to detect defects which could be verified by metallographic sectioning. Earlier ultrasonic inspection of the hemispheres which constituted S/N 1 and S/N 2 spheres, had been made with a 1/2" diameter transducer. This inspection detected no defects where it was definitely shown after failure that defects did exist. However, through the use of a focusing beam transducer, which covers an area about 1/8" in diameter, indications were noted on some of the suspect hemispheres. Sectioning of a heat at an indication verified that a laminar inclusion did in fact exist at the location detected by the transducer.

The heads were immersed in water for transmission of the ultrasonic vibration from the transducer to the parts. Because of the part shape, the transducer was manually traversed over the surface of the hemisphere rather than automatically traversed. The oscilloscope gain was set to give 85% saturation for the standard which was again a 3/64" diameter flat bottomed hole. All indications of any applicable level above background were reported. It is interesting to note that no more than one or two indications were noted on any head made from heat 97058. This

explained why it was unlikely that such defects could be detected by microsectioning of incoming sheet material. As was previously stated, the thickness of the laminar inclusions was small. This made them undetectable by radiographic techniques.

As a result of this work, Arde is revising their material acceptance specifications in order to avoid material of this nature in the future. The new specifications will call for sampling inspection of each batch of sheet stock by means of the ultrasonic technique used on the hemispheres described above. For sheet material, automatic inspection can be utilized. The transducer is automatically traversed over the entire sheet with overlapping of each pass. A permanent inspection record is also obtained as the instrument output is recorded. Arde's present specification calls for radiographic sampling inspection of incoming batches of sheet. However, the experience reported here, with the laminar slag inclusion indicates that radiographic inspection is not satisfactory for this type of defect.

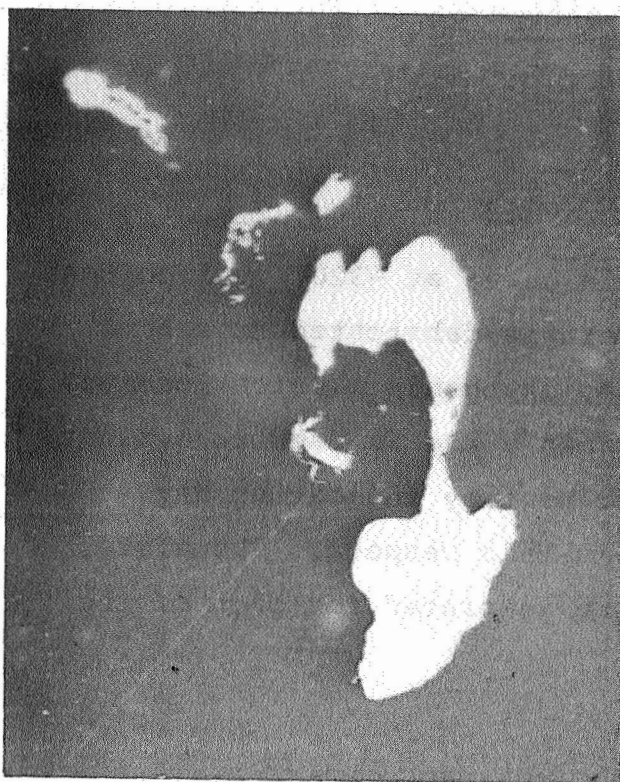
E. Inspection of Deliverable Vessels

Using the ultrasonic focusing beam transducer inspection technique, heads formed from another heat, 97107, were scanned and found to be free from this type of defect. These hemispheres were used in fabricating the spheres deliverable under the contract. After fabricating preforms from these heads, the stretch forming process acted as a self-inspection technique, assuring that no defects of a size sufficient to cause bursting in the stretch pit were present. Finally, after stretching, and helium leak testing under pressure, an additional radiographic inspection

was performed. The four vessels which were delivered were found to be free of defects at all stages of the inspection indicated above. Two additional vessels made from heat 97107, however, did exhibit crescent shaped indications upon final radiographic inspection and were accordingly rejected and not shipped to NASA. Thus, in summary, the four vessels from Heat 97107 which were delivered, were considered free from defects which can deteriorate their performance at -423F.

F. Metallographic Examination of X-Ray Detected Weld Defects

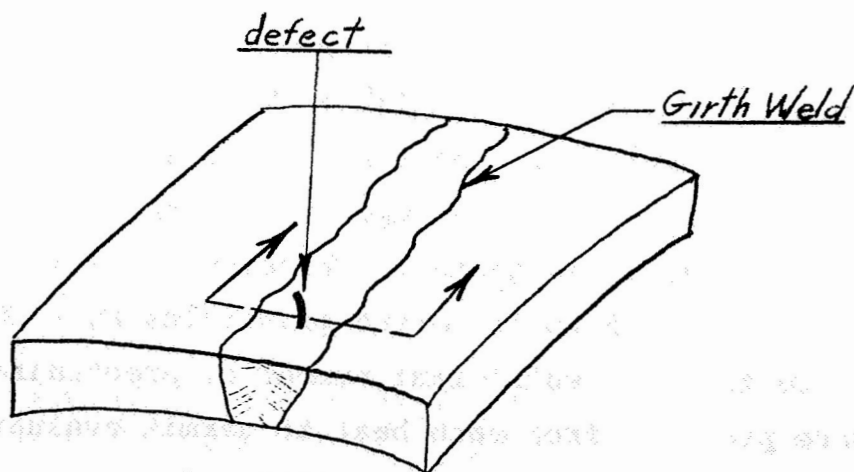
Two vessels S/N 3 and S/N 7 fabricated from Heat 97107 were successfully stretched but were nevertheless rejected on the basis of weld defects detected by radiographic inspection. The X-ray photographs showed crescent shaped defects in the center of the girth weld after cryoforming. These defects were not detectable prior to stretching. In order to determine the nature of these defects, a piece of the weld from sphere S/N 3 was cut out and a metallographic section made. Examination under the microscope revealed no solid non-metallic inclusions, but showed gas pockets. These voids are shown in Figure VII-7. The similarity between these defects and those seen in S/N 2 (Figure VII-2a) is striking. However, none of the hard particles seen in S/N 2 (Figure VII-2a) were noted. In addition, further sectioning along the weld in the vicinity of the defect in S/N 3 did not show direct evidence of the laminar inclusion seen in S/N 2 (Figure VII-2b). The defect in the S/N 3 weld, in conclusion, is gas porosity. The source of the defect could not be determined, however. It is possible that such a defect could occur if a small slag inclusion were encountered by the weld. However, weld porosity can also be caused by any number of other factors unrelated to the laminar slag inclusions noted on the previous vessels. The defect, fortunately, was readily detectable by radiographic inspection after cryoforming.



Saturn S IV B Helium Storage
Vessel.

Section of Weld from S/N 3

150X Unetched



Location of Microsection

Figure VII-7

VIII MATERIAL PROPERTIES

A. Mechanical Test Procedures

1. Description of Mechanical Tests

The uniaxial stress-strain curve at -320F is important in predicting the behavior of preforms fabricated from a particular heat of material during cryogenic stretch forming. In addition, the -320F stress-strain curve is used to evaluate the acceptability of a particular heat by indicating any departures from normal behavior in this respect. Therefore, stress-strain curves at -320F were generated for each of the heats available for this program.

In addition to the uniaxial stress-strain curves at -320F, mechanical testing was conducted to establish the strength of the materials after stretching and aging. During the cryogenic stretch forming operation, the material undergoes a transformation from austenite to martensite which results in increased strength. Further augmentation of this strength can be obtained by aging the material at 790F for 20 hours after cryogenic deformation. The response of each heat to -320F stretching and aging is dependent upon the amount of stretching to which the material is subjected. Therefore, specimens from each heat were subjected to different prestrains at -320F prior to aging and testing. A sufficient number of prestrained specimens were prepared from each heat to permit evaluation of its performance at room temperature, -423F and in some cases at -320F. Yield and tensile strengths were determined at the three temperatures.

In addition, notched specimens were prepared from additional pretrained specimens and these were tested to evaluate the behavior of the material in the presence of mechanical defects. The notch specimens were tested at the three temperatures previously indicated. Finally, welded specimens from two of the heats were notched and tested at room temperature and at -423F.

2. General Test Procedures and Specimen Preparation

Because of the variety of tests performed, a number of specimen types were utilized. All specimens, however, were processed in accordance with the following sequence:

1. Specimens were cut from sheet stock with the sheet rolling direction parallel to the tension direction of the specimen. Gage sections, approximately two and one half inches long, were machined into each specimen.
2. Specimens were then solution annealed, pickled and passivated in accordance with the Arde specifications applied to Ardeform parts.
3. The annealed specimens were then pretrained at -320F in a cryostat mounted on a 60,000 lb. hydraulic universal testing machine. The annealed specimens used to establish the -320 stress-strain curve were simply pulled to failure in the cryostat, while a load-strain curve was automatically plotted using an X-Y recorder.

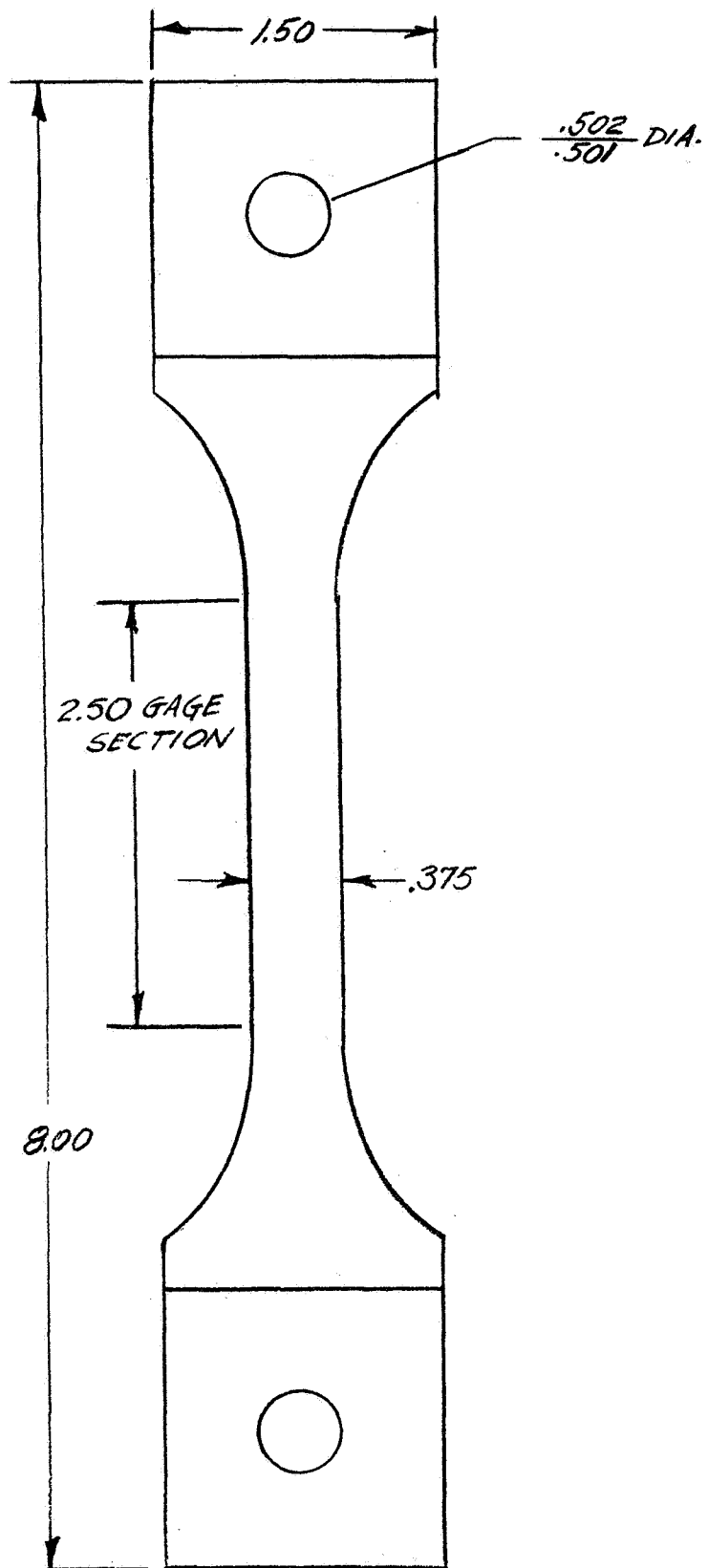


FIGURE VIII-1

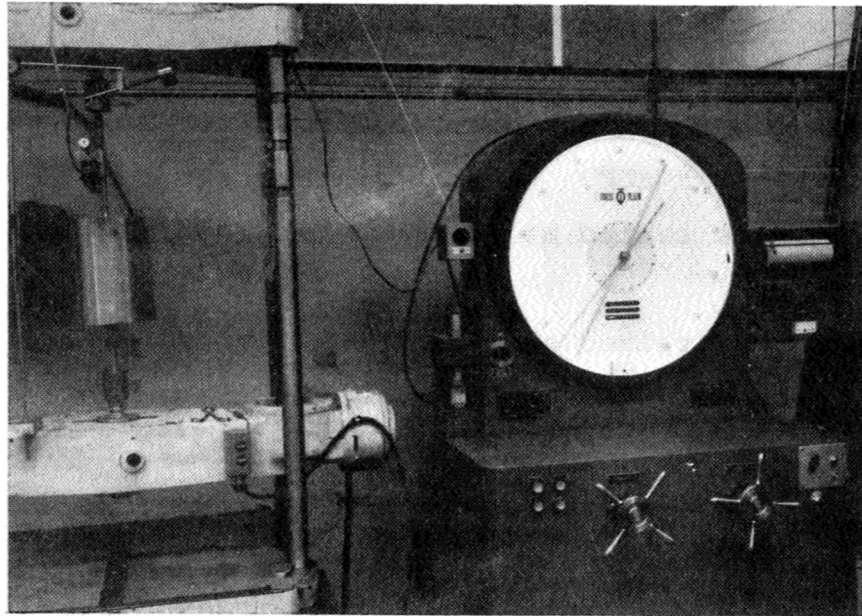
Tensile Specimen, P/N D104167

4. The prestrained specimens used for smooth tension tests were then aged for 20 hours at $790\text{F} \pm 10\text{F}$. After aging, smooth specimens were tested at the required test temperatures.
5. Prestrained specimens used for machined notch testing were notched in the unaged condition and then aged at $790\text{F} \pm 10\text{F}$ for 20 hours. Notched specimens were then tested at the three test temperatures at -423F , 320F and room temperature.

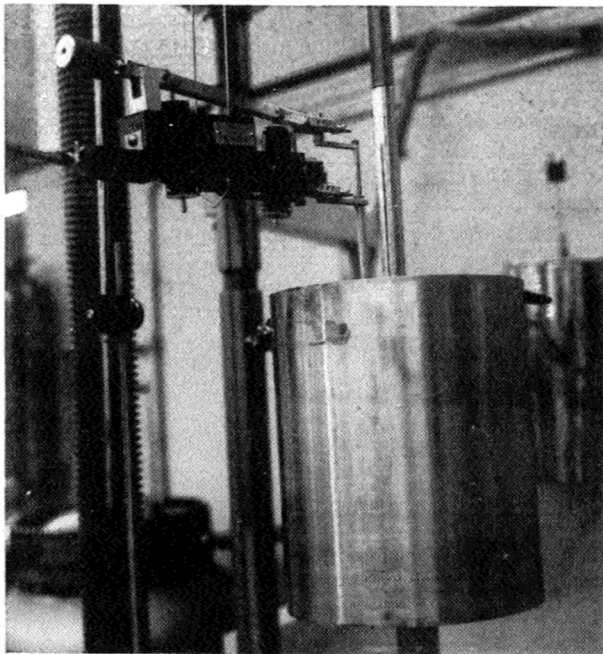
B. Tensile Testing

1. Description of Tensile Tests

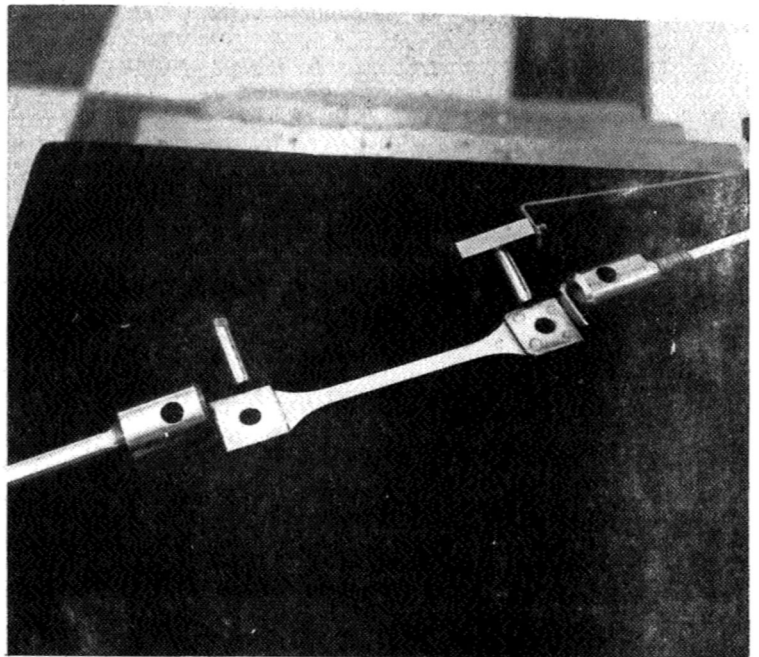
The first specimen from each heat was pulled to failure at -320F in the annealed condition in order to evaluate the performance of each heat during transformation from the austenite (annealed) to martensite. One smooth tensile test specimen (Figure VIII-1) from each heat was placed in a liquid nitrogen filled cryostat that had been set up on a Tinius Olsen tensile test machine. An extensometer was connected to the gage section of the specimen. The specimen was then pulled to failure while a load-strain curve was automatically plotted. The set up used for generating -320F stress-strain data, and for prestraining the specimens is shown in Figure VIII-2.



TINIUS OLSEN TESTING MACHINE WITH EQUIPMENT
FOR CRYOGENIC TENSILE TESTING



CLOSE-UP OF CRYOSTAT
AND EXTENSOMETER



TYPICAL TENSILE TEST SPECIMEN

Figure VIII-2

In order to evaluate the heats for their strength after prestraining and aging, six specimens from each heat were cryogenically prestrained to somewhat less than the failure strain of the first specimen. The stress-strain curve generated from the first specimen was used to establish the prestress levels for these six specimens. Generally, two of the six specimens were pulled to a high cryogenic prestress level, two specimens were pulled to a moderate prestress level, and two were pulled to a low prestress level. Load-strain curves were plotted for all specimens during prestraining at -320F and these curves were used to check the -320F stress-strain curve from the initial specimen. Area measurements were taken at nine different places along the gage section of each specimen, both before and after each tensile test. A two inch gage length was also lightly scribed on each specimen. Mechanical measurements of this gage length were taken before and after each test. The gage elongations measured, using this technique, were used to check the elongations in the 2" gage length recorded by the automatic plotter.

All the prestrained specimens were then aged for twenty (20) hours at 790F. Three of the specimens, each prestrained to a different cryogenic prestress level, were then subjected to a room temperature tensile test. The three remaining prestrained specimens from each heat were tested in tension at -320F.

The -320F and room temperature strength data from the testing described above was evaluated and a tentative design prestrain selected. The -423F strength of the spherical pressure

vessels to be built during the program had to be the basis for selection of the tentative design prestrain. At the time the design was initiated, no -423F data on the heats purchased was available. Therefore, an estimate of the prestrain required for the desired -423F strength was made by extrapolation of the tensile test data obtained at -320F and room temperature. The extrapolation was based on -423F data available from low silicon material previously tested.

In order to confirm the validity of the selected prestrain, two additional specimens from each heat were prepared for -423F testing. These two specimens were prestrained to the selected level and aged at 790F for 20 hours before testing at -423F. The tensile tests at -423F were performed at Wylie Laboratories inasmuch as Arde has no facilities for -423F testing. Automatic plots of the load strain relationships were made for each -423F test. The -423F test data obtained confirmed the extrapolated values.

2. Reduction of Data from Tensile Tests

The following raw data was obtained for each heat tested:

- 1) -320F load-strain curve.
- 2) Load strain curves from the tensile tests of cryogenically prestrained and aged specimens at room temperature, -320F and -423F.

This raw data was converted to more useful plots and data which defined the characteristics of the material. The converted information is as follows:

- a) A -320F true stress vs true strain curve for each heat in the annealed condition.
- b) The yield strength at the test temperatures of -423F, -320F and room temperature as a function of cryogenic prestress.
- c) The nominal tensile strength at the same test temperatures as a function of cryogenic prestress.

It should be noted that in many cases only one prestress was utilized for testing at -423F and therefore strength levels as a function of -320F prestress was not completely defined at this temperature.

The load strain curve generated from the -320F tensile test of annealed material from each heat was converted into a true stress ($\bar{\sigma}$) vs true strain ($\bar{\epsilon}$) curve where:

$$\bar{\sigma} = \frac{\text{Load (1+unit elongation)}}{\text{Specimen area before test}} \quad (1)$$

$$\text{and } \bar{\epsilon} = \ln (1+\text{unit elongation}) \quad (2)$$

In the above equation the true stress is based on the assumption of constancy of volume, using specimen elongation as a measure of the cross-sectional area reduction under load. The curves generated from the above calculations were plotted for each heat and are presented on Figures VIII-3 to VIII-7.

The yield point at .2% offset, and the nominal tensile strength were calculated for each test of a prestrained specimen.

TRUE STRESS VS. TRUE STRAIN AT -320F

HEAT 97056

UNIAXIAL - ANNEALED SPECIMEN

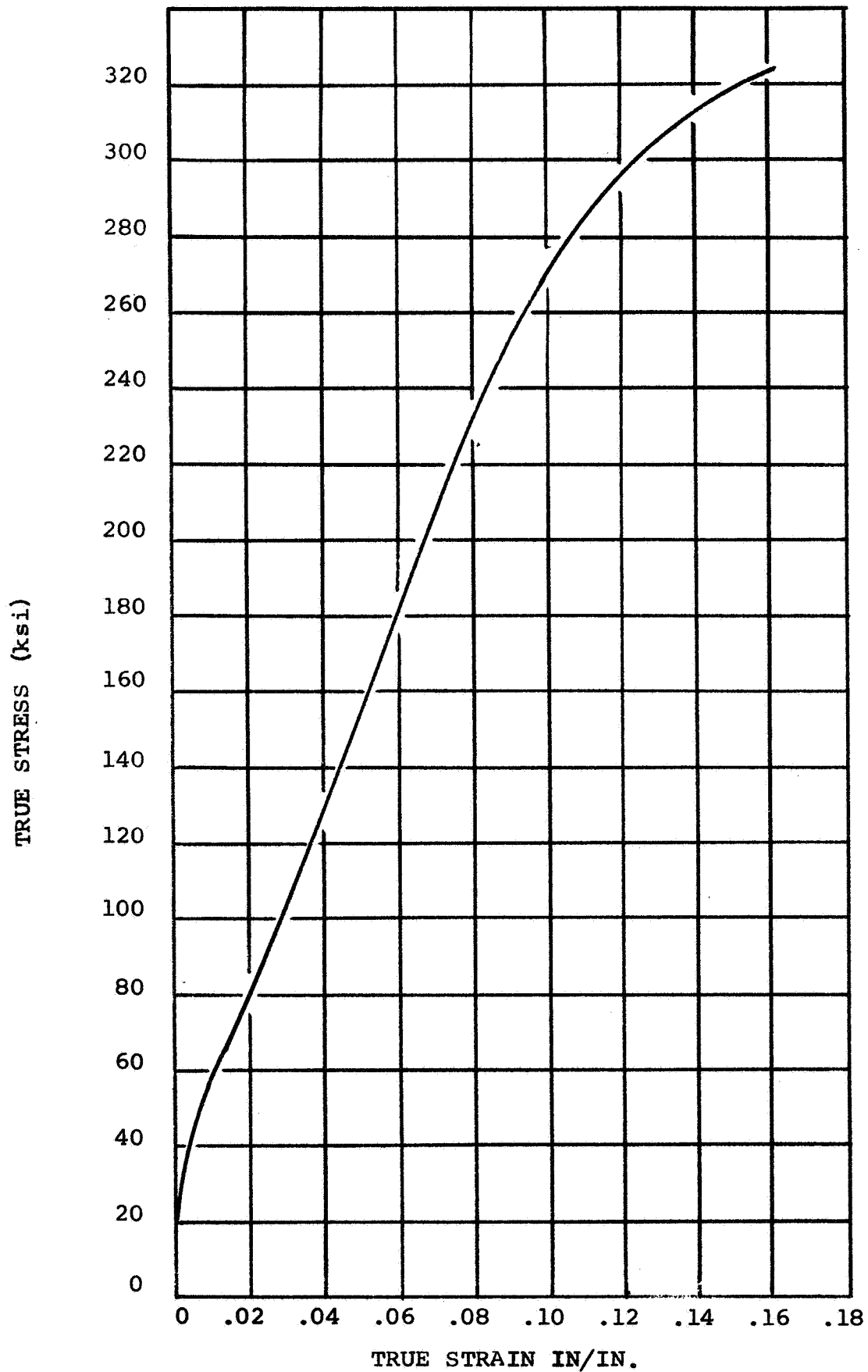


Figure VIII-3

TRUE STRESS VS. TRUE STRAIN AT -320F

HEAT 97057

UNIAXIAL - ANNEALED SPECIMEN

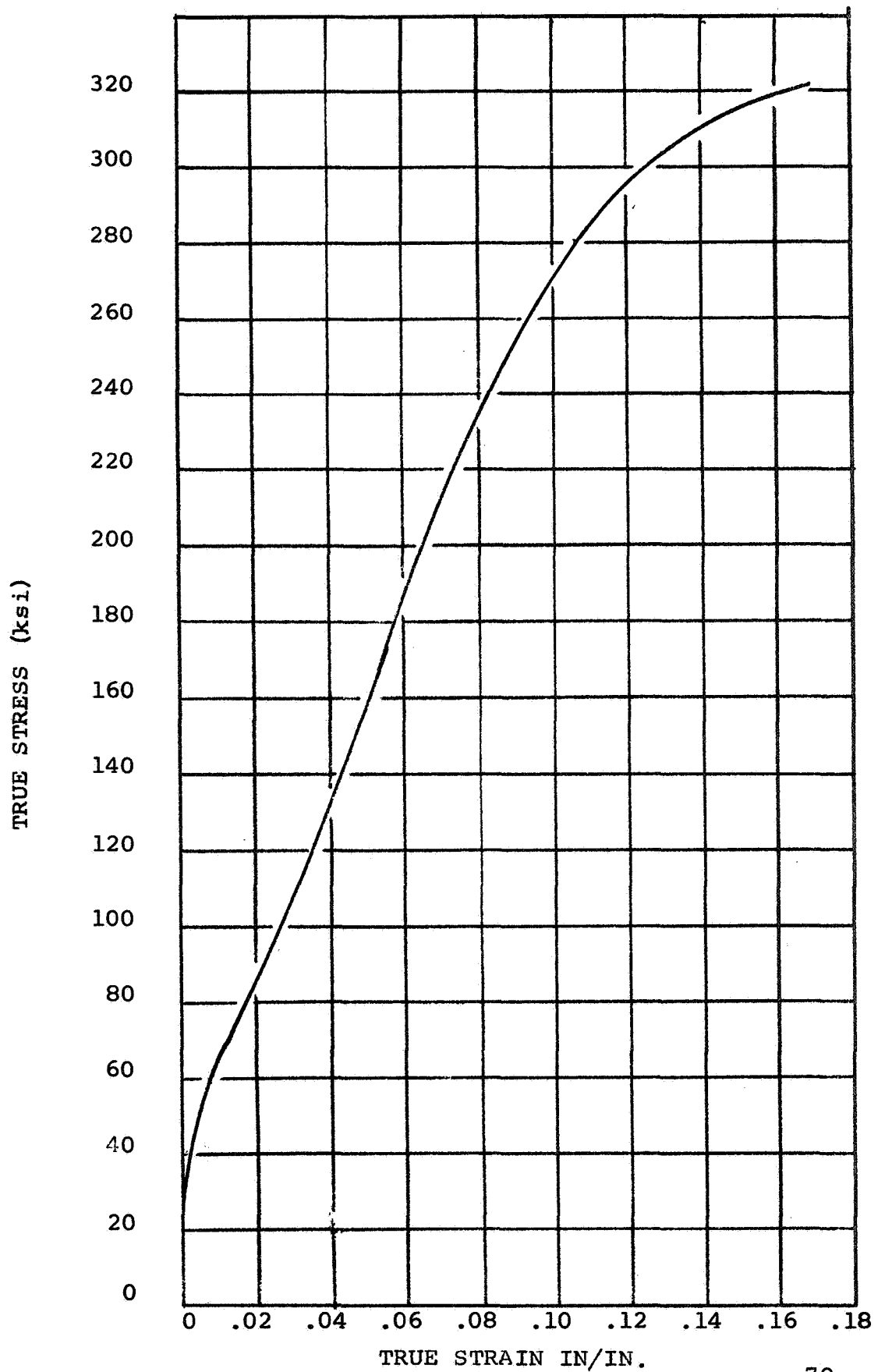


Figure VIII-4

TRUE STRESS VS. TRUE STRAIN AT -320F

HEAT 97058

UNIAXIAL - ANNEALED SPECIMEN

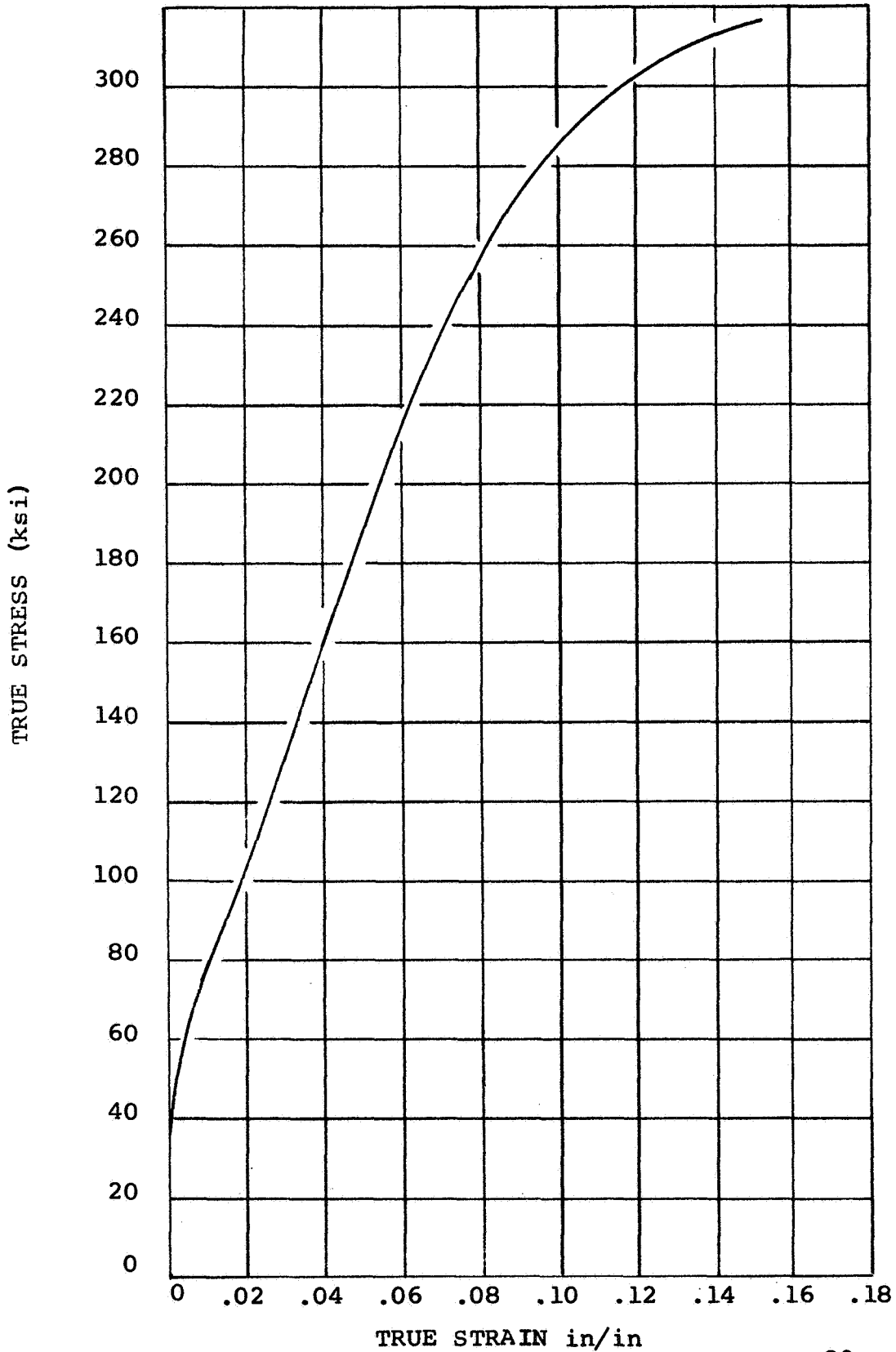


Figure VIII-5

TRUE STRESS VS. TRUE STRAIN AT -320F

HEAT 97106

UNIAXIAL - ANNEALED SPECIMEN

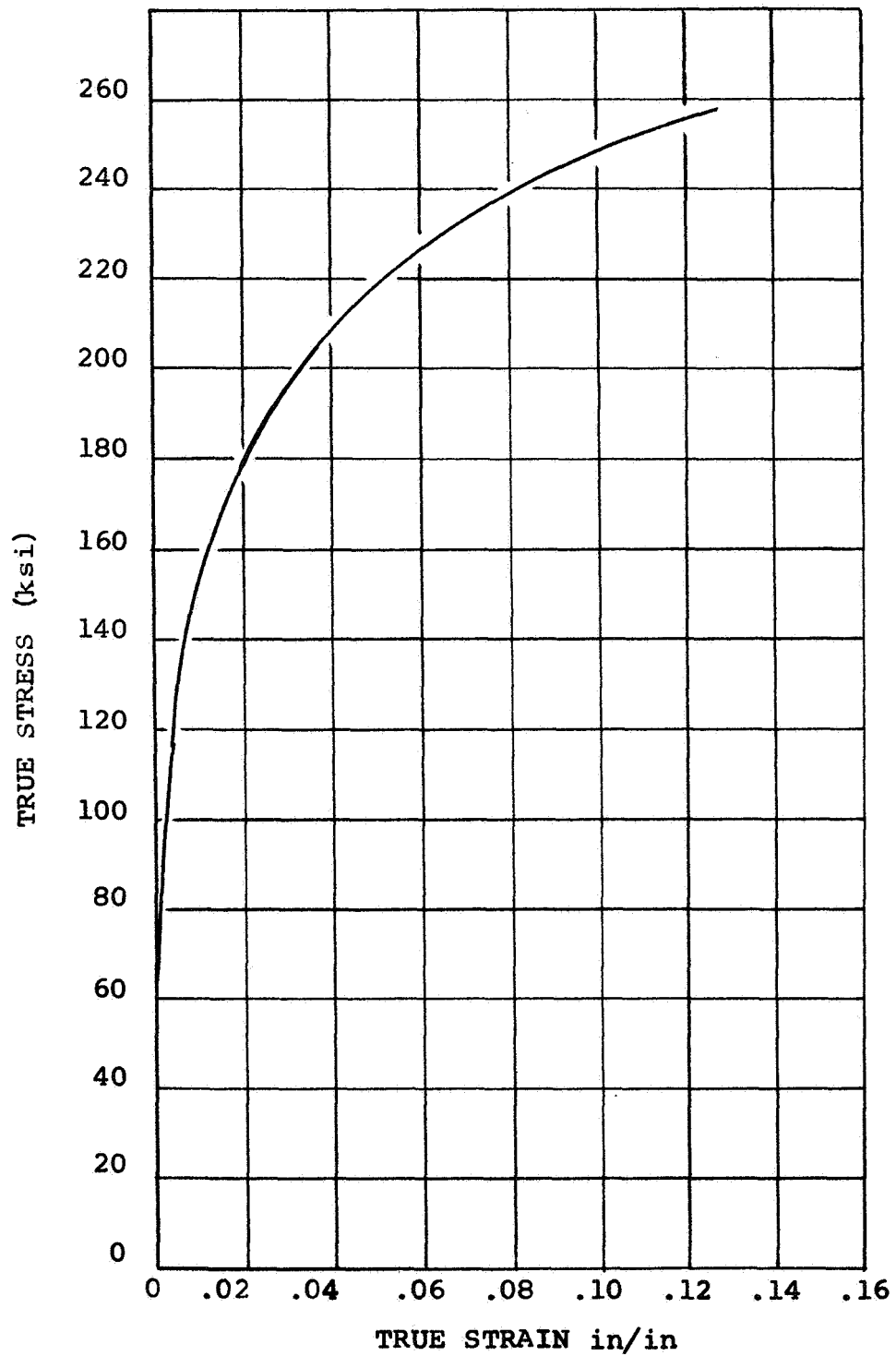


Figure VIII-6

TRUE STRESS VS. TRUE STRAIN AT -320F

HEAT 97107

UNIAXIAL - ANNEALED SPECIMEN

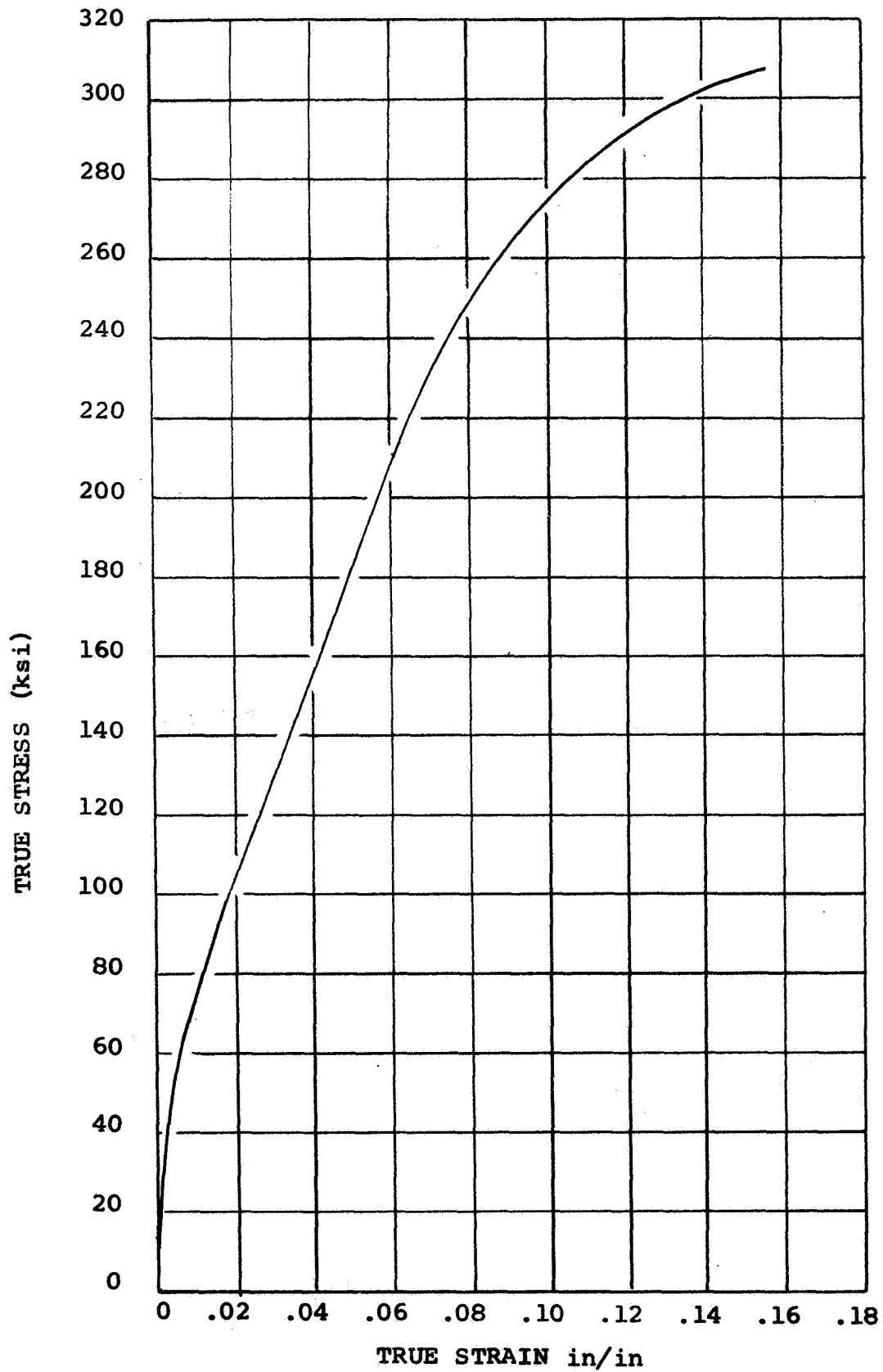


Figure VIII-7

The yield point was established using the offset method specified in ASTM Specification E8-57T. The nominal ultimate strength (S) was calculated using:

$$S = \frac{\text{Failure Load}}{\text{Specimen Area Prior to Test}} \quad (3)$$

The yield and nominal ultimate strength for each tensile test, at each test temperature, are tabulated on Tables VIII-1 to VIII-5. The -320F true prestress of each specimen is listed with its strength level. It should be noted that for these tests the true prestress was calculated using

$$\bar{\sigma} = \frac{\text{Prestress Load}}{\text{Area after Test}} \quad (4)$$

In the true prestress calculation in Equation (4), the elastic deformation is not taken into account since area measurements are made after the specimen is unloaded. However, the error is of the order of less than 1% in the prestress.

The yield and tensile strength is plotted as a function of true prestress for each heat at room temperature and -320F in Figures VIII-8 to VIII-17.

3. Evaluation of Tensile Test Data

Four of the five heats tested under this program demonstrated similar behavior during cryogenic transformation

TABLE VIII-1

MECHANICAL PROPERTIES OF LOW SILICON
ARDEFORM MATERIAL - AGED CONDITION

Heat 97056

Test No.	<u>-320F Prestrain Cond.</u>		<u>Final Test to Failure</u>			
	% Elong. in 2"	True Stress ksi	Yield Strength at .2% Offset	Tensile Strength ksi	% Elong. in 2"	Test Temp.
46	14.1	301.9	276.0	277.1	1.3	Room
47	9.1	240.7	252.3	255.6	1.45	Room
48	6.0	166.5	215.1	219.7	1.75	Room
43	14.0	298.0	350.0	351.0	1.7	-320F
44	9.0	232.7	*	322.4	2.3	-320F
45	6.0	169.4	272.9	297.6	13.3	-320F
49	10.4	259.3	328.7	333.4	2.05	-320F
3	9.1	246.0	362.0	369.0	-	-423F
4	9.1	245.0	354.0	363.0	-	-423F

* Extensometer slipped

TABLE VIII-2

MECHANICAL PROPERTIES OF LOW SILICON
ARDEFORM MATERIAL - AGED CONDITION

Heat 97057

Test No.	<u>-320F Prestrain Cond.</u>		<u>Final Test to Failure</u>			
	% Elong. in 2"	True Stress ksi	Yield Strength at .2% Offset	Tensile Strength ksi	% Elong. in 2"	Test Temp.
55	13.0	293.2	270.8	271.8	1.37	Room
56	8.7	237.0	250.7	254.5	1.6	Room
57	5.6	170.2	216.2	223.6	1.6	Room
52	13.7	295.3	343.6	345.6	1.4	-320F
53	8.4	236.5	321.2	324.1	1.67	-320F
54	5.6	171.1	277.7	301.0	12.0	-320F
5	8.7	237.0	**	362.0	-	-423F
6	8.6	237.0	359.0	363.0	-	-423F

** Failed before yield

TABLE VIII-3

MECHANICAL PROPERTIES OF LOW SILICON
ARDEFORM MATERIAL - AGED CONDITION

Heat 97058

Test No.	<u>-320F Prestrain Cond.</u>		<u>Final Test to Failure</u>			
	% Elong. in 2"	True Stress ksi	Yield Strength at .2% Offset	Tensile Strength ksi	% Elong. in 2"	Test Temp.
4	11.0	277.3	261.1	263.5	1.5	Room
5	8.5	247.5	252.7	254.7	1.25	Room
9	14.5	298.8	265.5	268.2	1.35	Room
6	14.5	298.0	338.8	342.9	1.7	-320F
7	13.5	291.6	338.3	340.7	-	-320F
8	8.0	231.1	*	320.0	-	-320F
1	11.3	284.0	381.0	384.0	-	-423F
2	11.5	285.0	**	381.0	-	-423F

* Extensometer slipped

** Failed before yield

TABLE VIII-4

MECHANICAL PROPERTIES OF LOW SILICON
ARDEFORM MATERIAL - AGED CONDITION

Heat 97106

Test No.	<u>-320F Prestrain Cond.</u>		<u>Final Test to Failure</u>			
	% Elong. in 2"	True Stress ksi	Yield Strength at .2% Offset	Tensile Strength ksi	% Elong. in 2"	Test Temp.
8	9.0	239.0	212.9	212.9	.95	Room
9	7.5	230.0	209.3	209.3	.90	Room
10	4.0	207.2	200.0	200.4	1.2	Room
11	4.1	209.9	*	273.0	-	-320F
12	10.7	243.8	*	281.7	-	-320F
13	8.0	236.6	*	280.6	-	-320F

* Extensometer slipped

TABLE VIII-5

MECHANICAL PROPERTIES OF LOW SILICON
ARDEFORM MATERIAL - AGED CONDITION

Heat 97107

Test No.	<u>-320F Prestrain Cond.</u>		<u>Final Test to Failure</u>			
	% Elong. in 2"	True Stress ksi	Yield Strength at .2% Offset	Tensile Strength ksi	% Elong. in 2"	Test Temp.
3	11.0	269.0	249.3	251.2	1.4	Room
4	9.3	253.5	243.2	247.4	1.6	Room
5	6.1	202.6	221.9	228.8	1.6	Room
6	11.0	271.3	*	324.2	-	-320F
7	9.5	260.0	316.1	320.0	1.65	-320F
8	6.0	200.2	286.6	293.7	1.65	-320F
9	11.0	272.5	324.2	328.6	1.65	-320F
1	9.8	259.0	367.0	369.0	-	-423F
2	9.3	252.0	352.0	363.0	-	-423F

* Extensometer slipped

ROOM TEMPERATURE STRENGTH AS A FUNCTION OF -320F PRESTRESS

HEAT 97056

AGED @ 790F 20 HOURS

○ YIELD

□ TENSILE STRENGTH

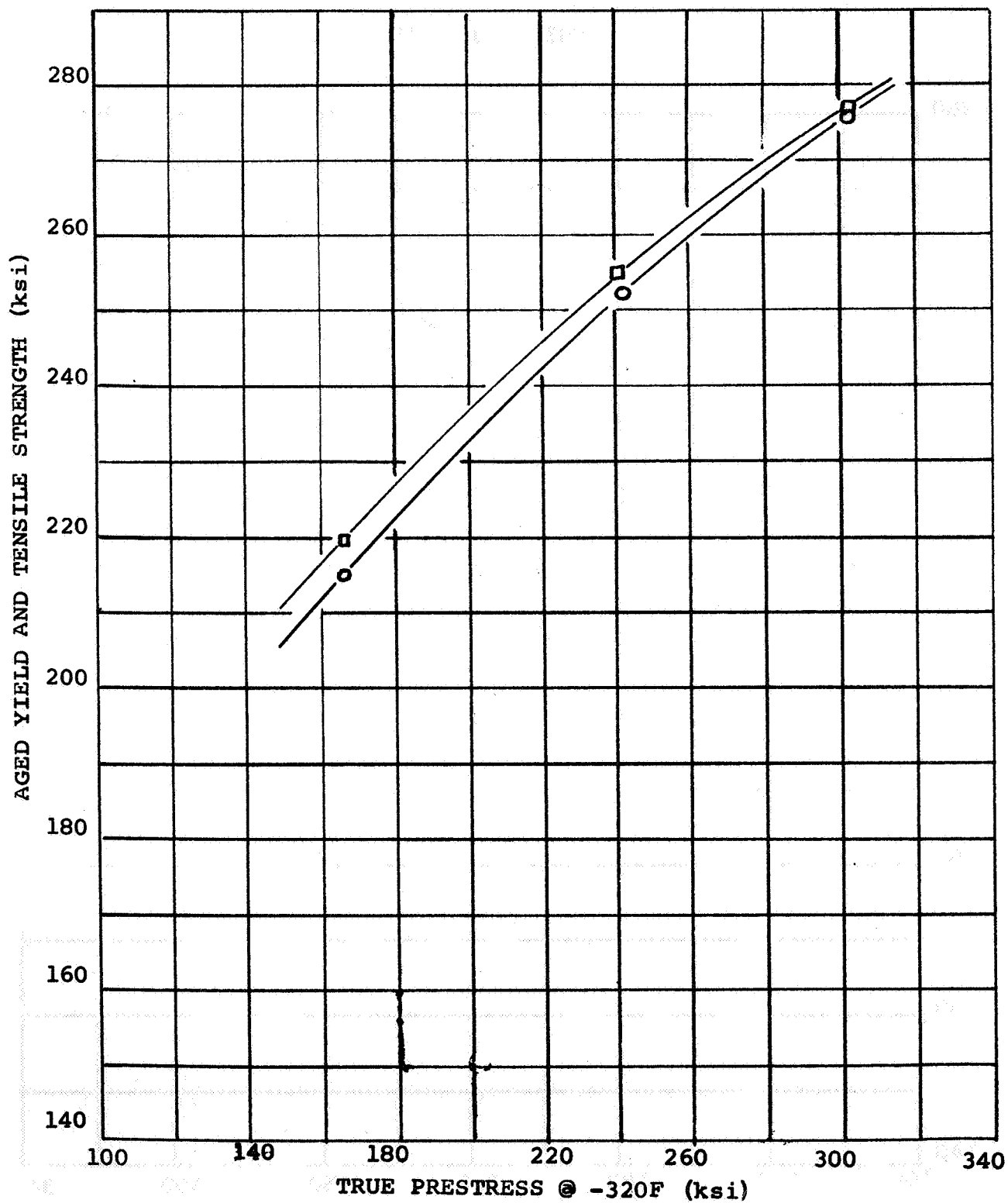


Figure VIII-8

ROOM TEMPERATURE STRENGTH AS A FUNCTION OF -320F PRESTRESS

HEAT 97057

AGED @ 790F 20 HOURS

○ YIELD

□ TENSILE STRENGTH

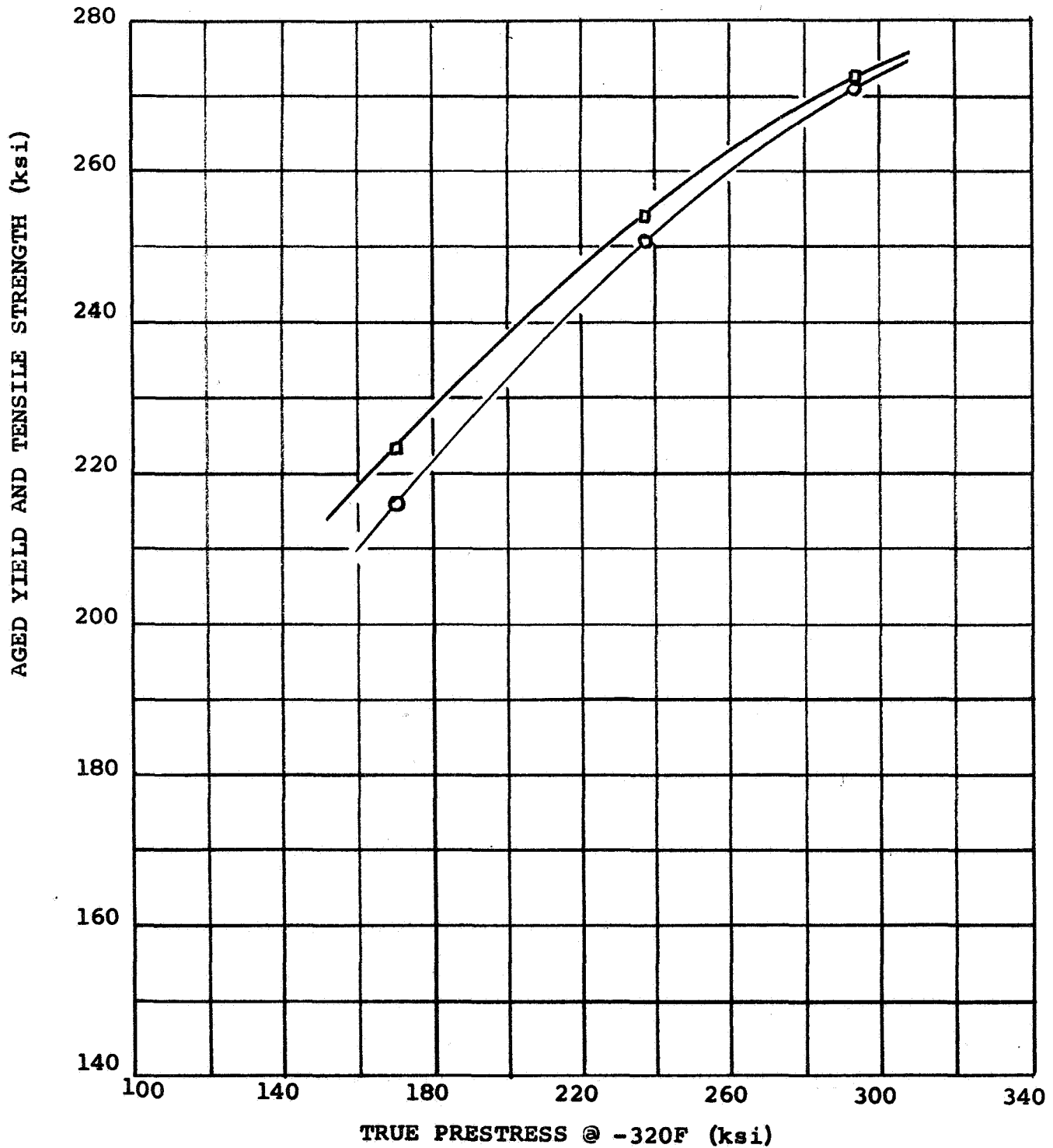


Figure VIII-9

ROOM TEMPERATURE STRENGTH AS A FUNCTION OF -320F PRESTRESS

HEAT 97058

AGED @ 790F 20 HOURS

○ YIELD

□ TENSILE STRENGTH

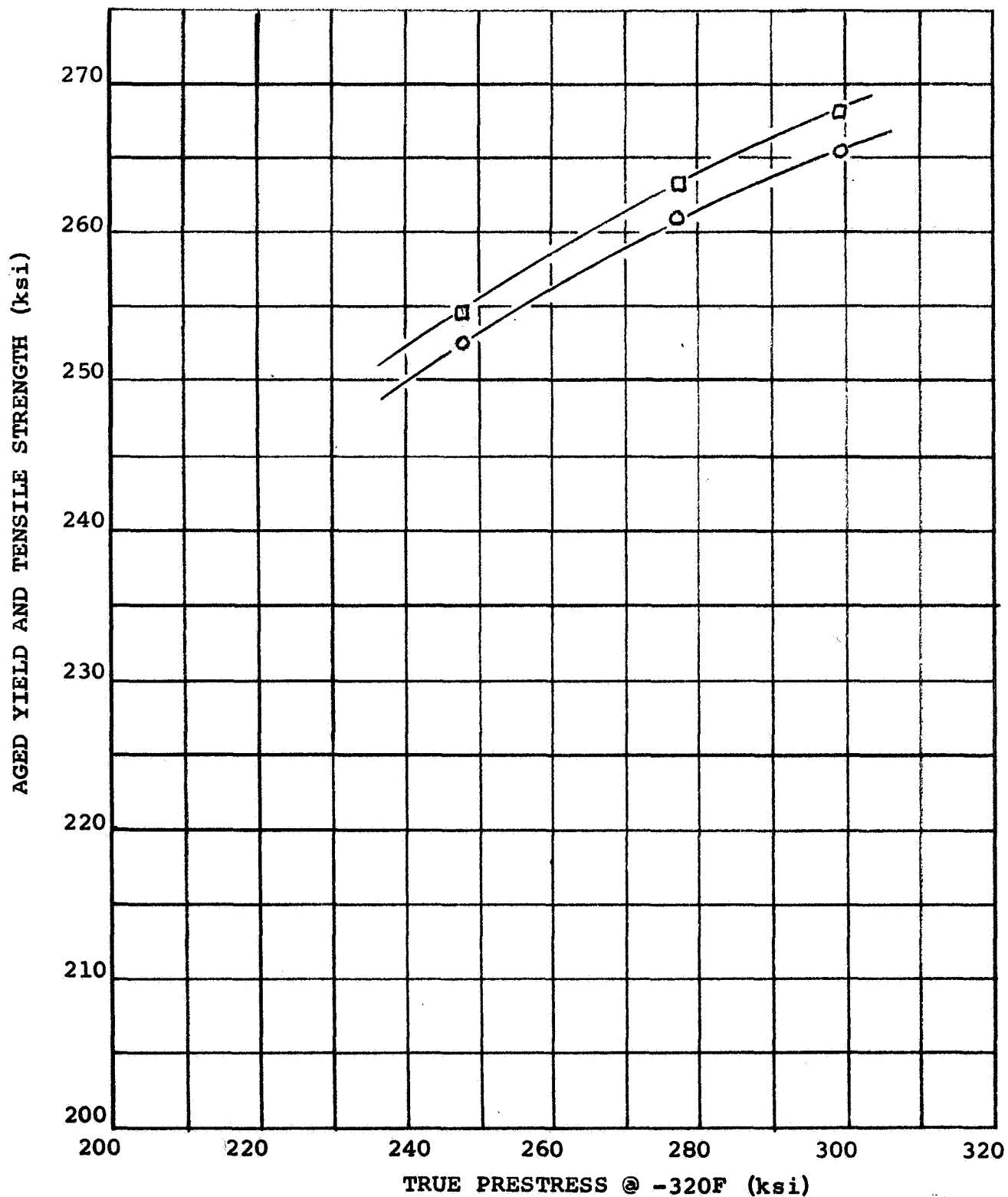


Figure VIII-10

ROOM TEMPERATURE STRENGTH AS A FUNCTION OF -320F PRESTRESS

HEAT 97106

AGED @ 790F 20 HOURS

○ YIELD

□ TENSILE STRENGTH

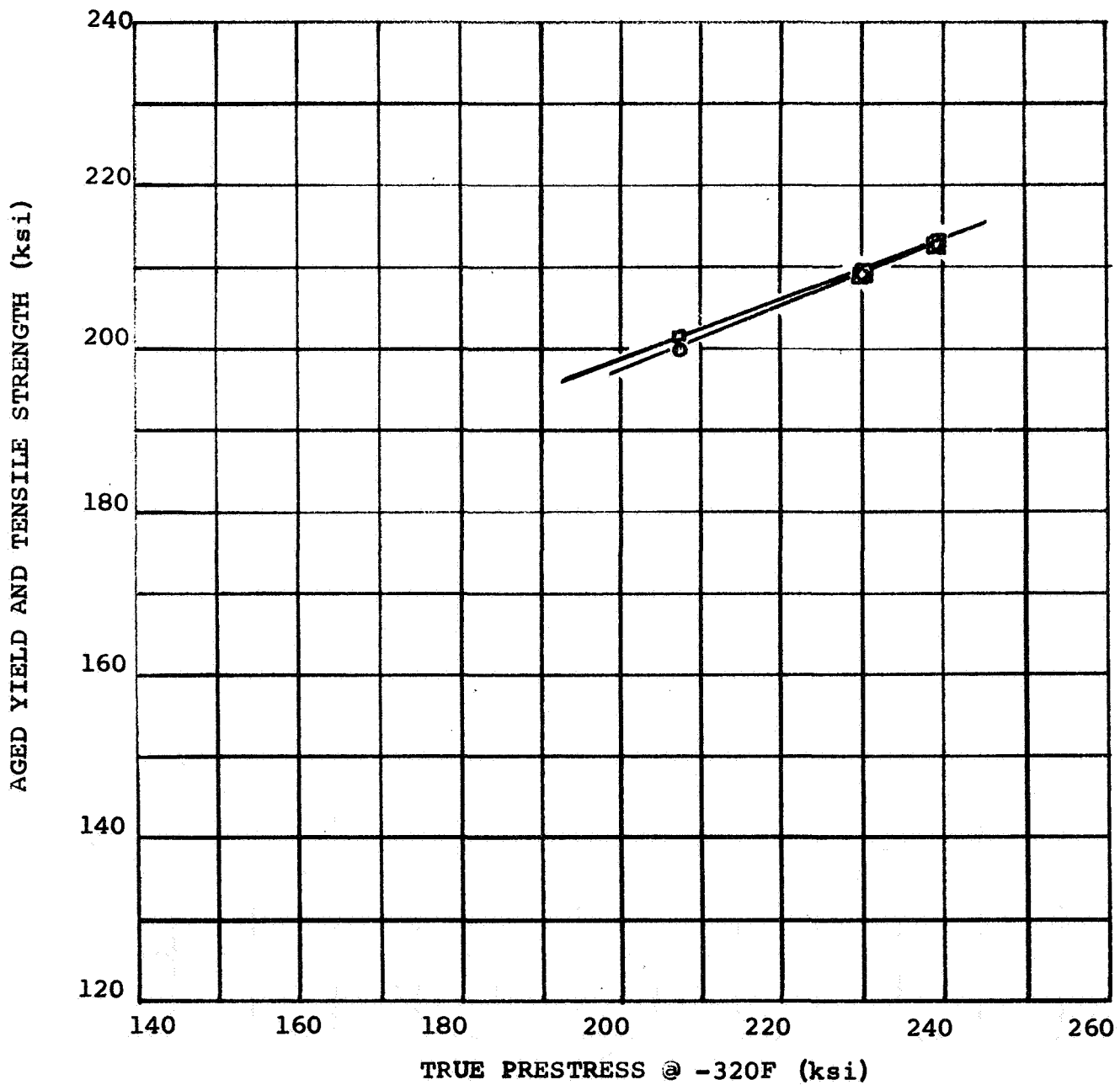


Figure VIII-11

ROOM TEMPERATURE STRENGTH AS A FUNCTION OF -320F PRESTRESS

HEAT 97107

AGED @ 790F 20 HOURS

○ YIELD

□ TENSILE STRENGTH

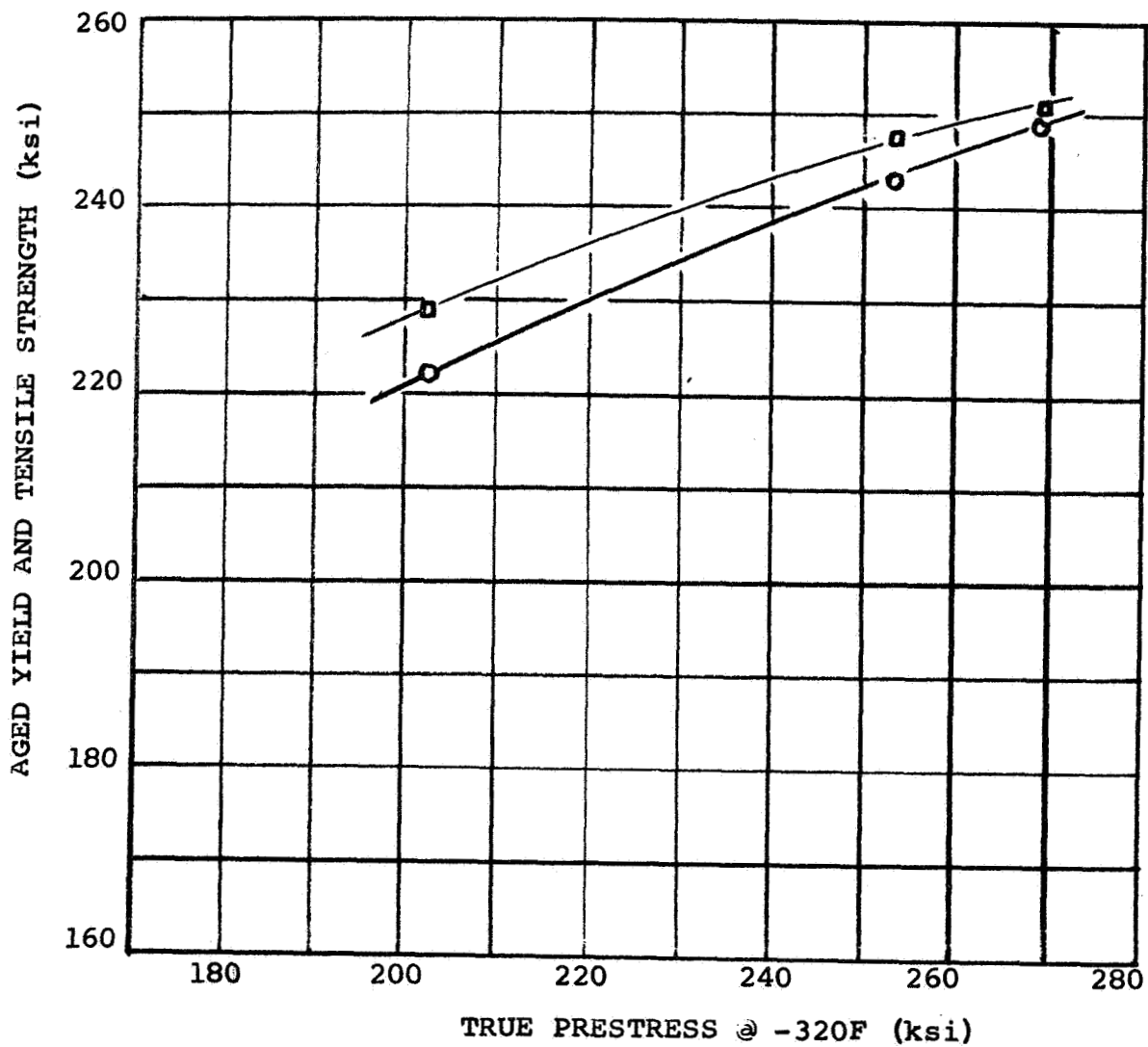


Figure VIII-12

STRENGTH @ -320F AS A FUNCTION OF -320F PRESTRESS

HEAT 97056

AGED @ 790F, 20 HOURS

O YIELD

□ TENSILE STRENGTH

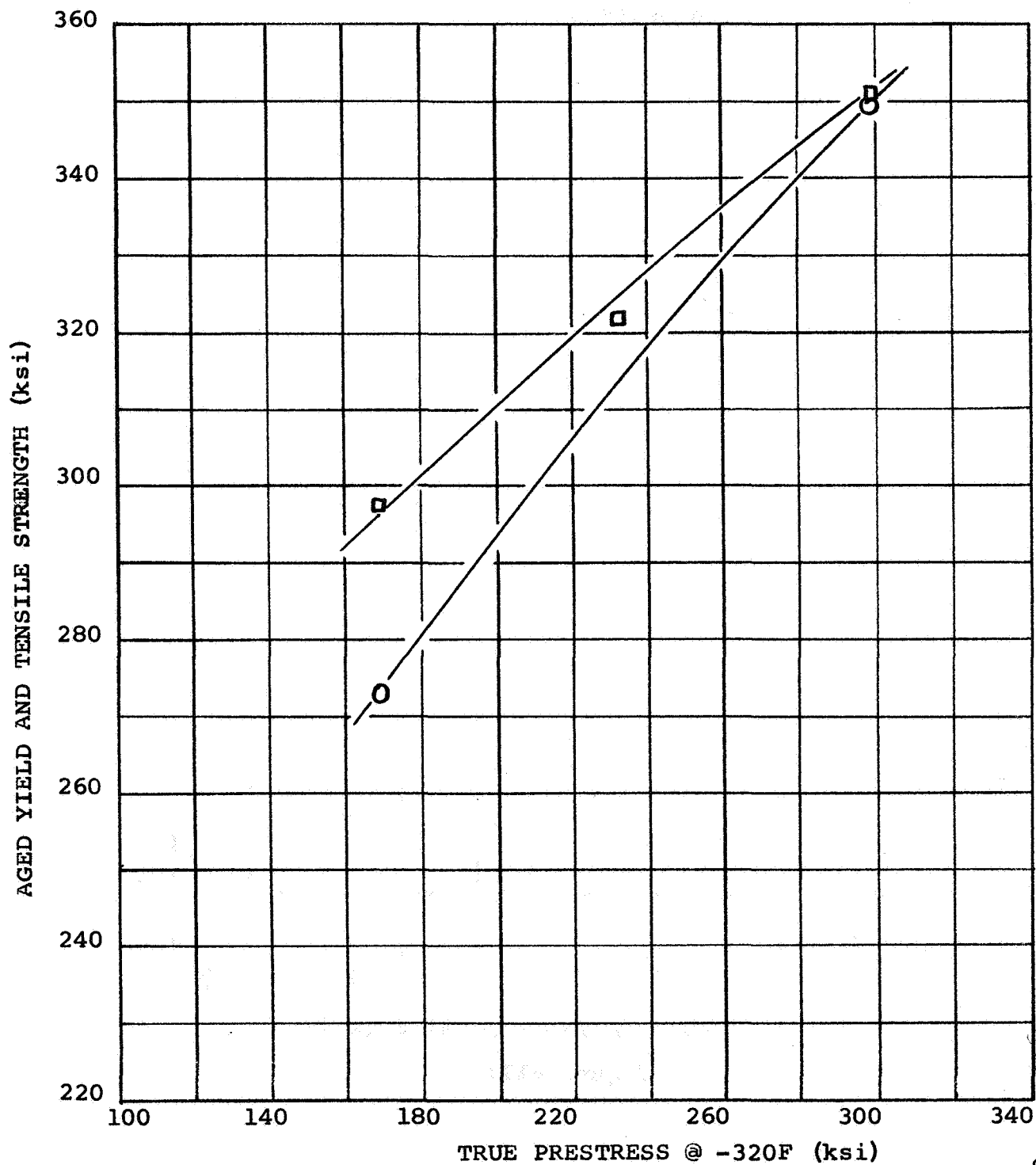


Figure VIII-13

STRENGTH @ -320F AS A FUNCTION OF -320F PRESTRESS

HEAT 97057

AGED @ 790F, 20 HOURS

○ YIELD

□ TENSILE STRENGTH

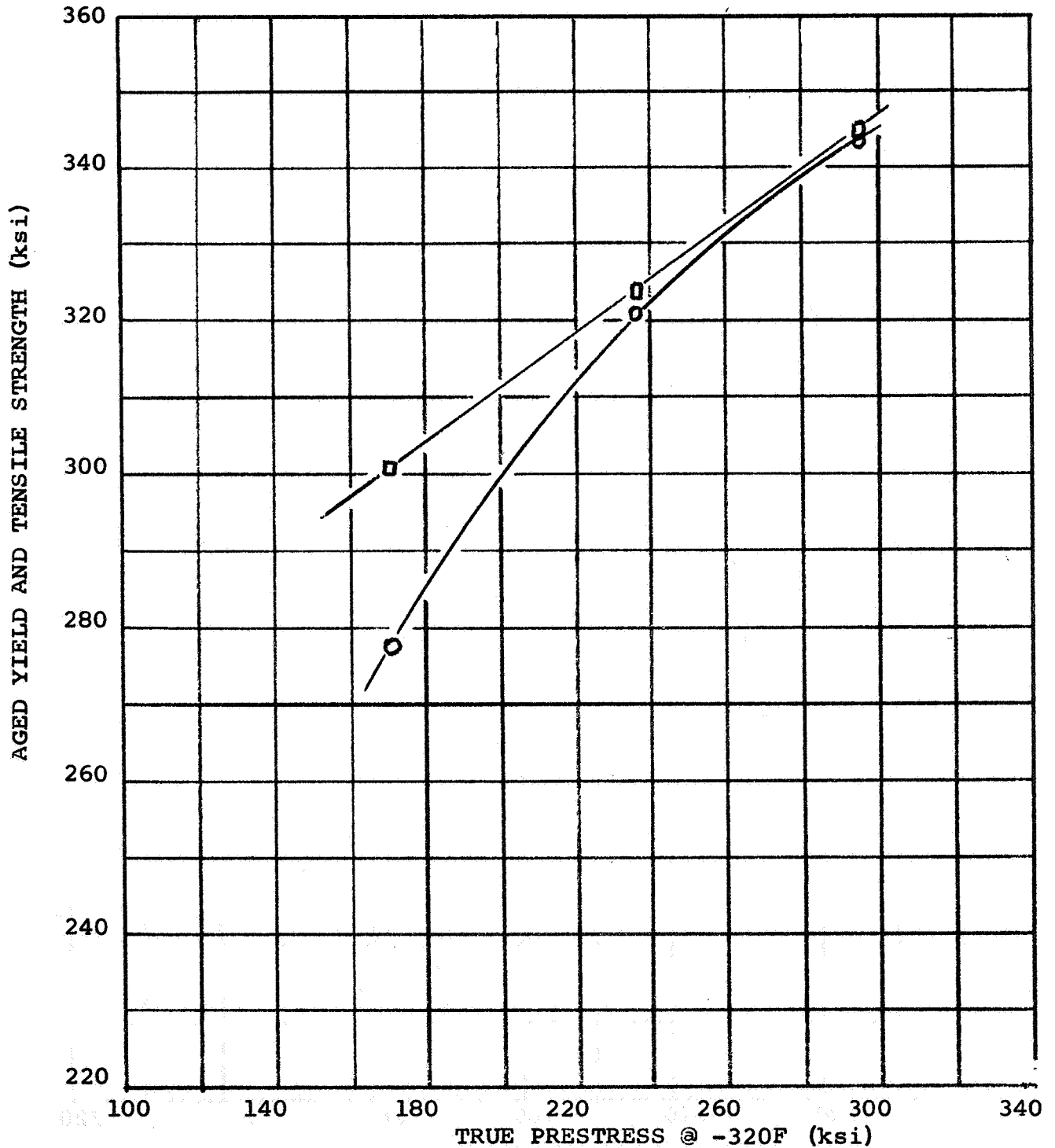


Figure VIII-14

STRENGTH @ -320F AS A FUNCTION OF -320F PRESTRESS

HEAT 97058

AGED @ 790F, 20 HOURS

○ YIELD

□ TENSILE STRENGTH

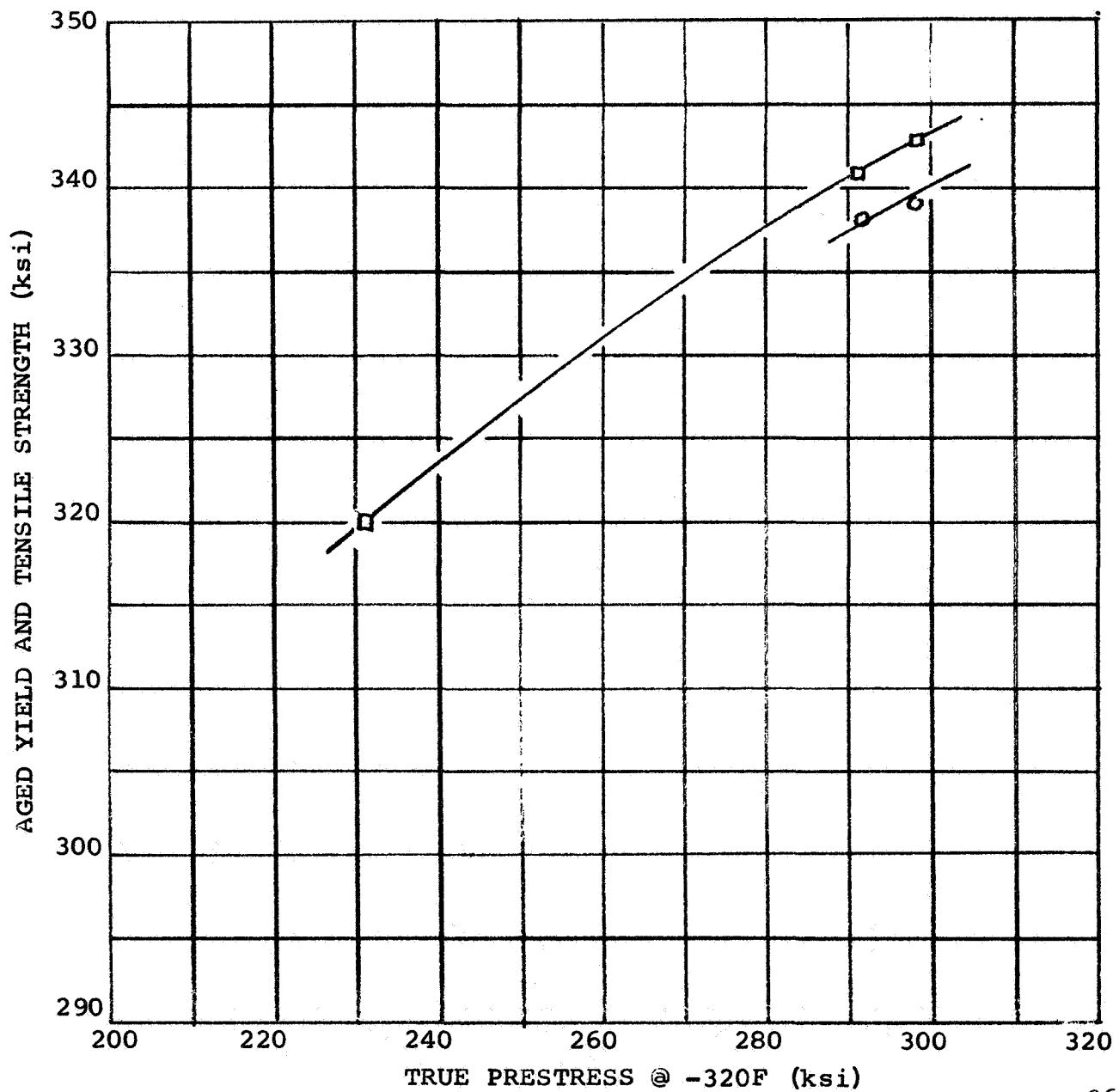


Figure VIII-15

STRENGTH @ -320F AS A FUNCTION OF -320F PRESTRESS

HEAT 97106

AGED @ 790F, 20 HOURS

○ YIELD

□ TENSILE STRENGTH

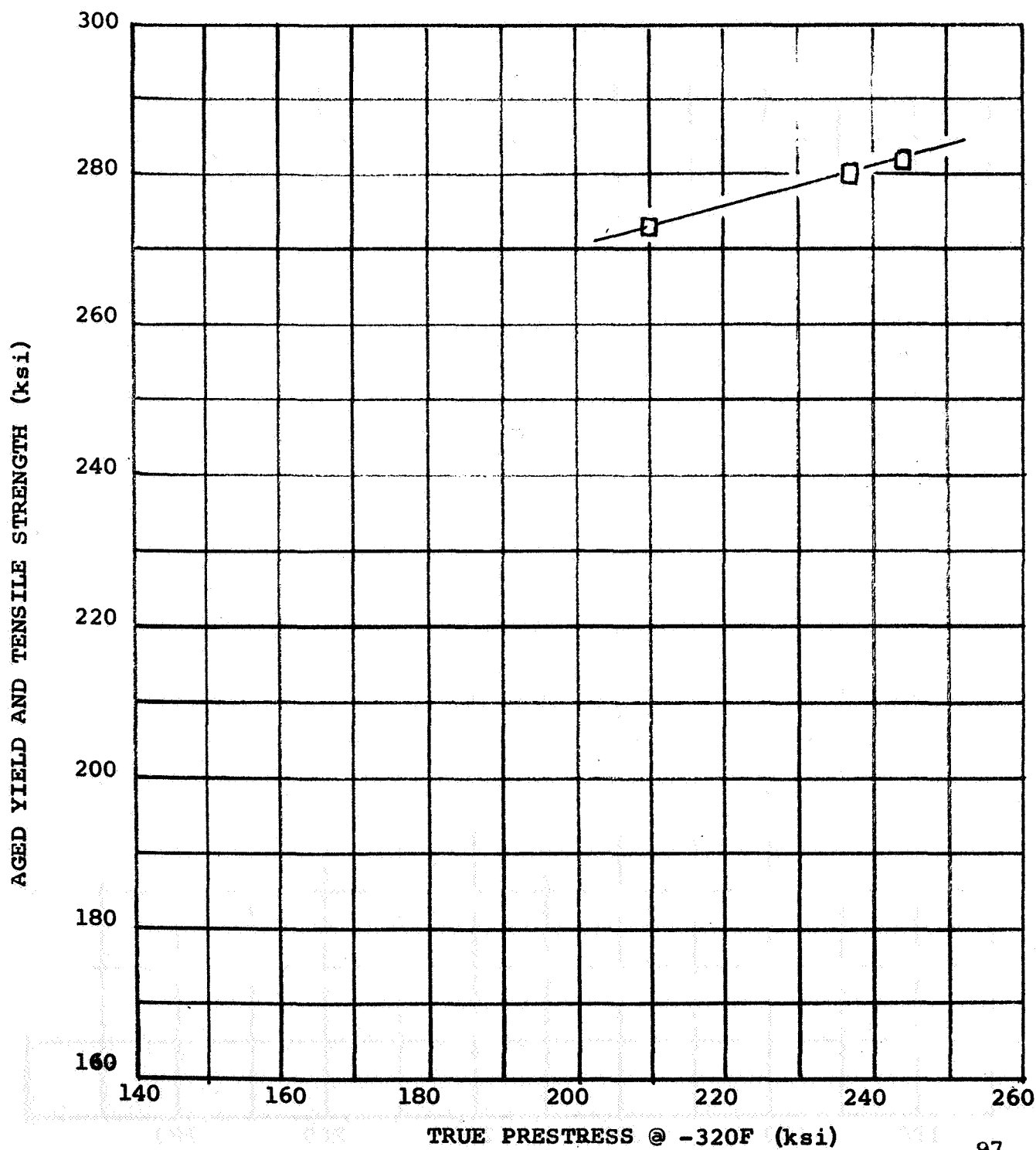


Figure VIII-16

STRENGTH @ -320F AS A FUNCTION OF -320F PRESTRESS

HEAT 97107

AGED @ 790F, 20 HOURS

○ YIELD

□ TENSILE STRENGTH

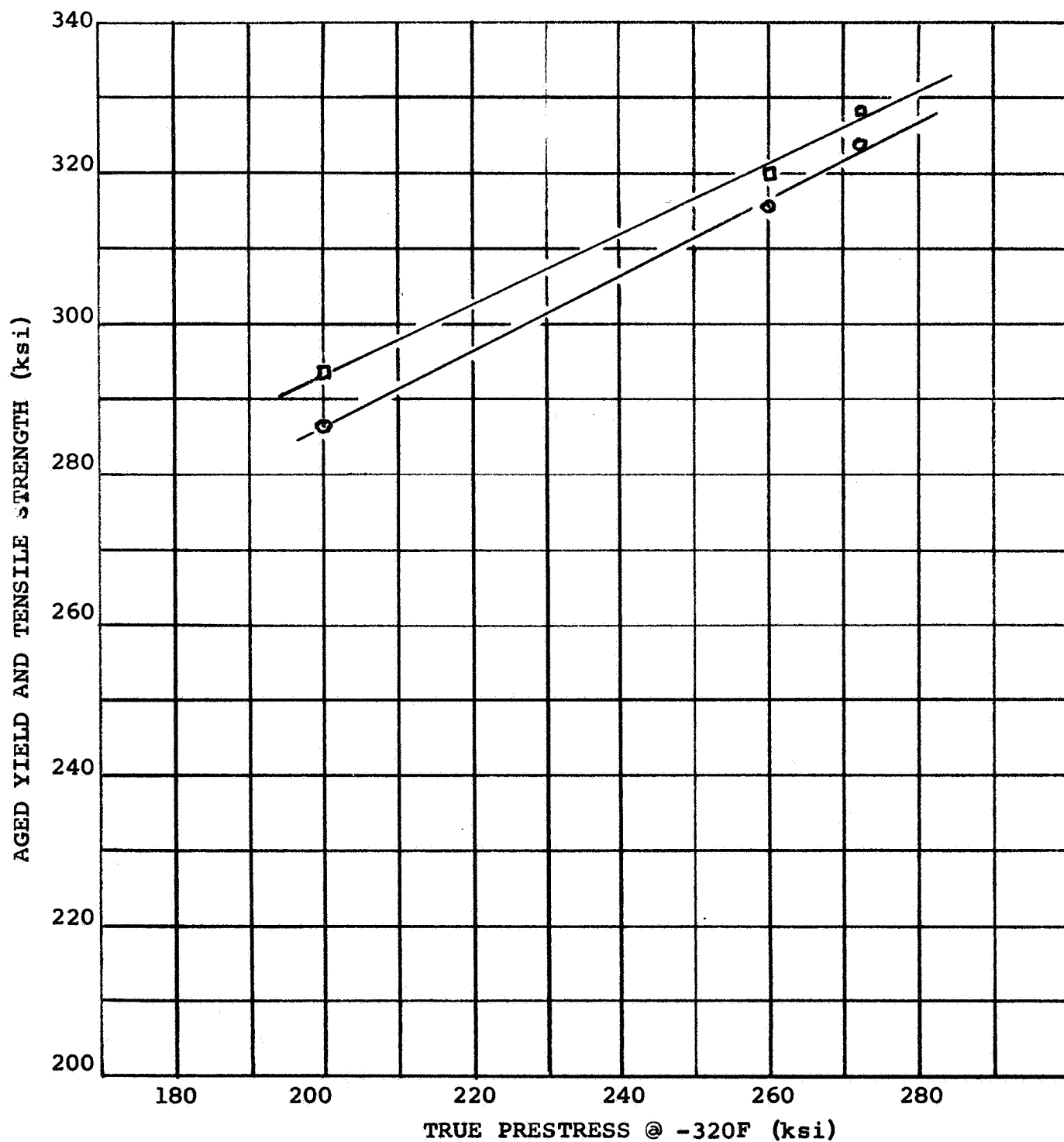


Figure VIII-17

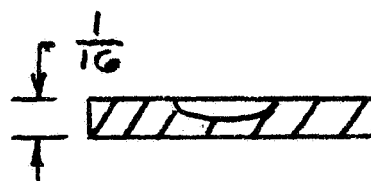
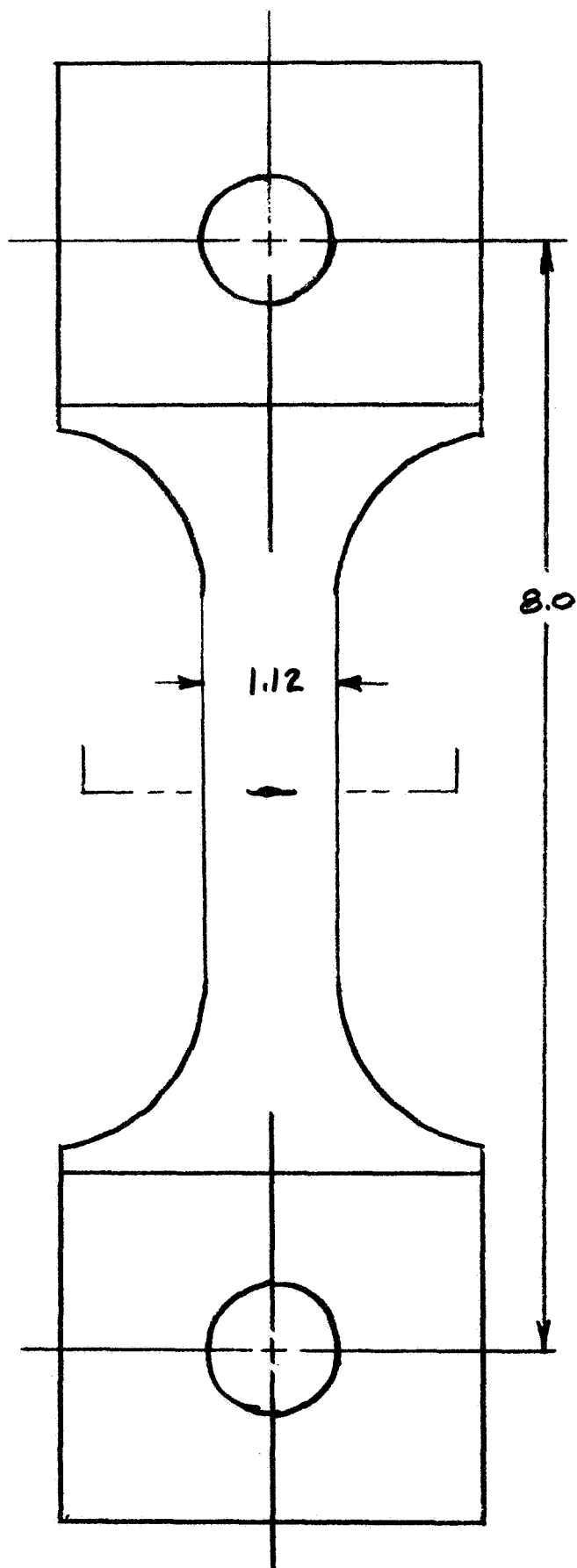
from the austenite to martensite. These four heats, numbers 97056, 97057, 97058 and 97107 also showed good strength levels after prestraining and aging. Three of these, 97056, 97057 and 97058 have almost identical strength levels at room temperature, -320F and -423F. Heat 97107 shows an aged strength response that, while very adequate, is approximately 10 ksi below those demonstrated by the first three heats.

Heat 97106 has a poor response to cryogenic strain induced transformation. The prestrained and aged room temperature and -320F strength of the material was low. The poor performance of this heat 97106 probably is caused by its low chromium content which is outside the specification requirements and which caused rejection of this heat. Tests of this heat were conducted to determine if the low chrome level would affect the material behavior, and was indeed sufficient cause for rejection. Because of the requirements for material early in the program it was felt advantageous to determine if the heat was usable. MRB review resulted in the decision to reject unless tensile data could show that the properties were acceptable. The tensile test results indicated above, of course, definitely eliminated this heat.

C. Notch Testing

1. Notch Tensile Test Procedure

All heats were notch tested using a type D3517 specimen (see Figure VIII-18). Each notch test specimen was measured and cryogenically prestrained in a manner similar to the smooth specimens. The specimens for each heat were all subjected to



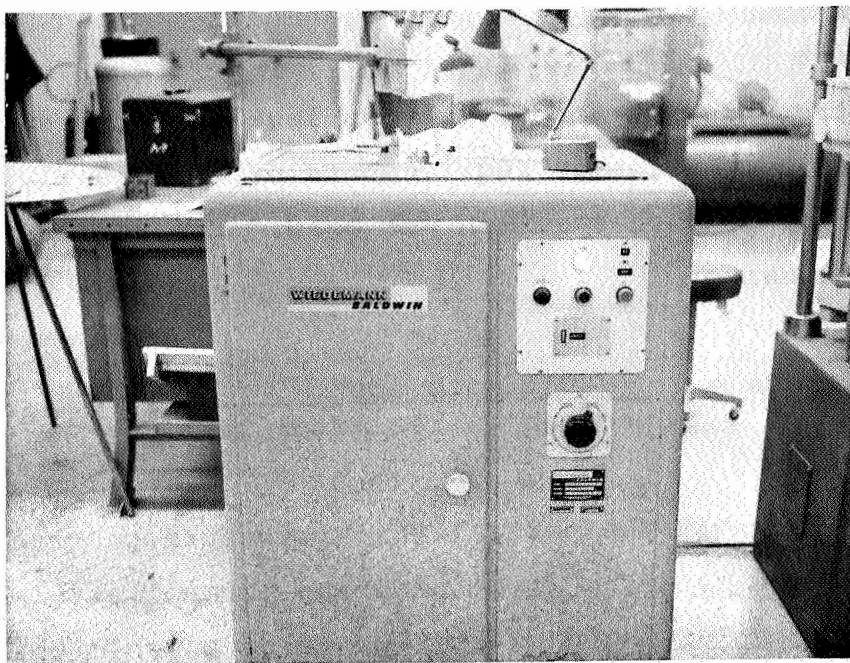
Notch Specimen

Figure VIII-18

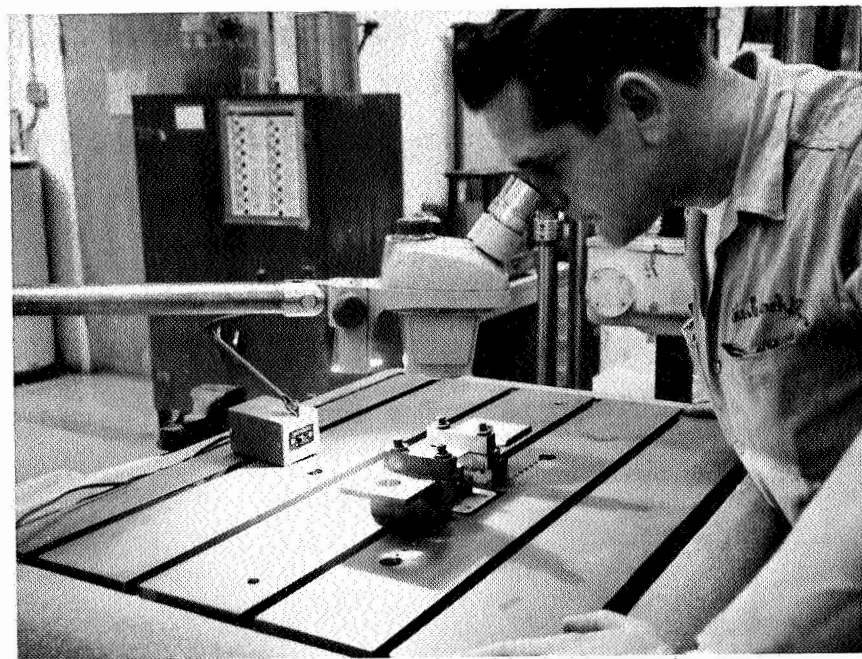
similar prestress levels; the prestress levels of the specimens being dictated by the design requirements of the vessel. After prestraining, each specimen was aged. The true prestress was calculated using:

$$\text{Prestress} = \frac{\text{Ultimate Load}}{\text{Specimen's Area After Test}}$$

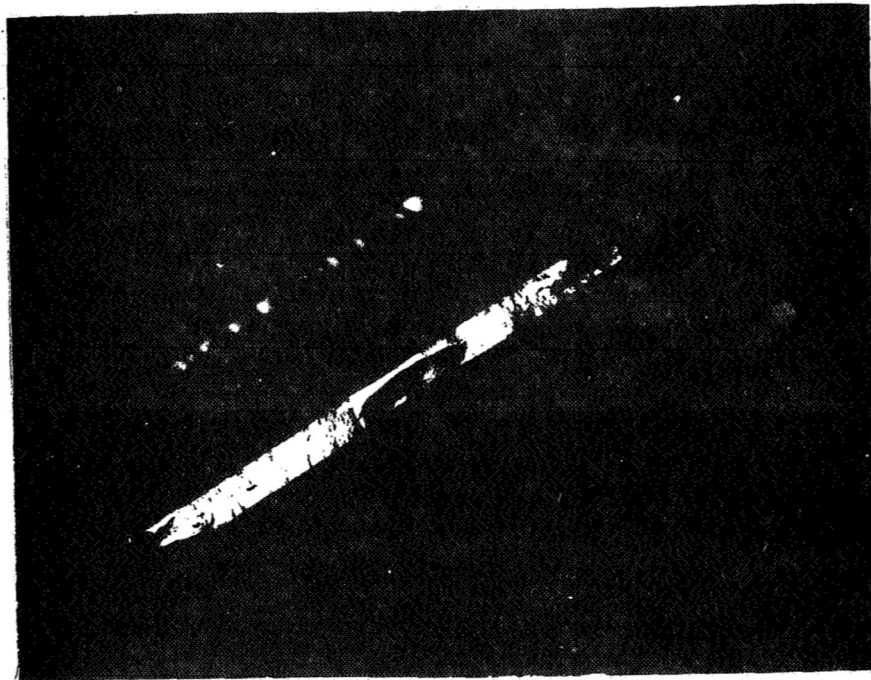
The cracks in the partial thickness surface cracked specimens were generated by first punching a small starter notch in the center of the gage section using a small chisel shaped tool. The specimens were then fatigue cracked in bending on a Wiedemann-Baldwin fatigue tester. See Figure VIII-19. Approximately 10,000 cycles at a computed bending stresses of about 45% of yield strength was required to produce a fatigue crack at each tip of the wedge shaped starter notch. This type of cyclic loading produced a crack transverse to the tension direction of the specimen and partially through the specimen thickness. The crack was viewed through a 10X microscope as it was propagated. When the crack reached the desired length, the loading was stopped. Each notched specimen was then pulled to failure. Measurements of the notch size and specimen cross-sectional area was made. Figure VIII-20 shows close-up cross-section view of a crack in a tested tensile specimen.



Fatigue Cracking Machine



Specimen Undergoing Fatigue Cracking
Figure VIII-19



Surface Fatigue Crack in Uniaxial Specimen

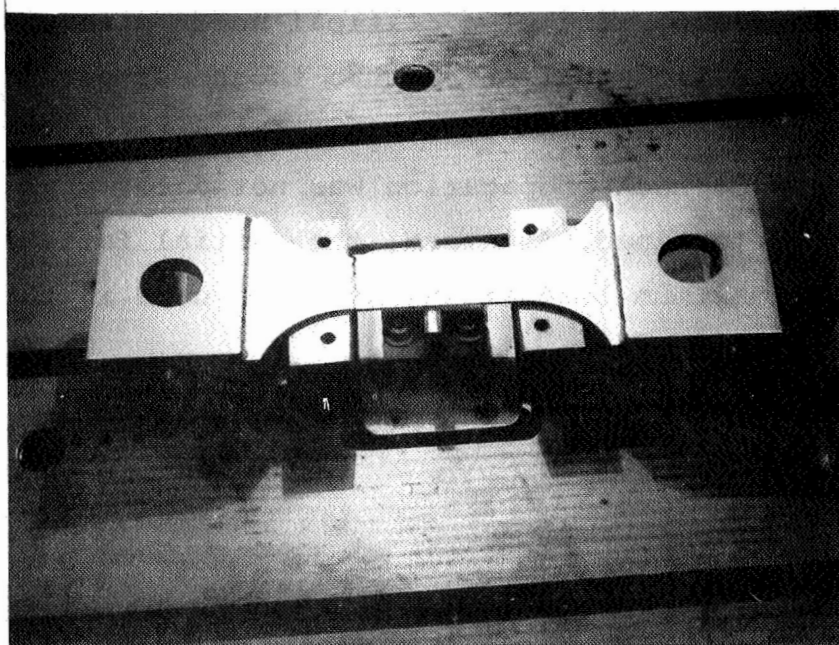
Figure VIII-20

Six tensile specimens from heat 97058, and six specimens from heat 97107 were prepared in the above manner. These specimens were tested at room temperature, -320F and -423F; two specimens from each heat being tested at each temperature. Four additional specimens were prepared, two each from heats 97056 and 97057. Inasmuch as -423F is the most critical operating condition, these four specimens were tested at this temperature. Testing at room temperature and -320F was conducted by ARDE. Testing at -423F was conducted by Wyle Labs in Corona, California. Those specimens which were sent to Wyle Labs were vacu-blasted, cleaned and passivated after aging.

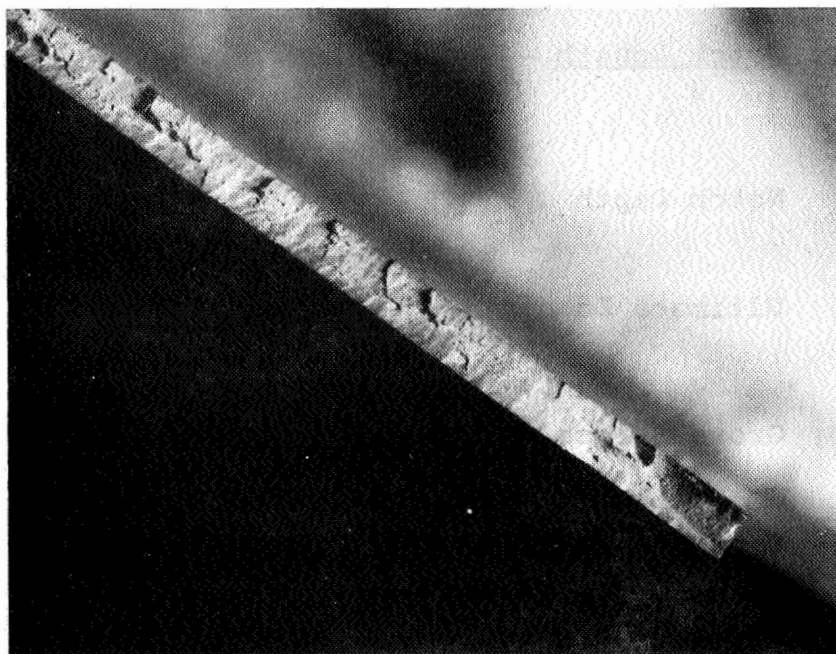
One specimen from heat 97056, did not fail in the center notch area during the -423F testing. Failure occurred near the end of the specimen gage section. This area is adjacent to the section of the specimen which was clamped to the fatigue cracking machine (see Figure VIII-21a). Apparently, the crack was started at the specimen edge in this region during the fatigue cycling. The specimen failed at this crack rather than at the central crack during liquid hydrogen testing. A photograph of this crack is shown in Figure VIII-21b.

2. Reduction of Notch Test Data

The notch test results were evaluated on the basis of nominal K_{Ic} values. The notch testing was intended primarily



Specimen 10N
Heat 97056
On Fatigue Cracking
Machine, Showing
Fail Area Next to
Clamp Support



Specimen 10N
Heat 97056
Failure Edge
Showing Edge
Crack

Figure VIII-21

to evaluate the -423F behavior of the material used in this program by comparison with their behavior at room temperature, as well as to obtain some idea of a critical notch size under design operating conditions. The fracture toughness parameter measured here is considered nominal in that the exact notch size at the onset of rapid crack propagation was not determined nor was a pop-in load determined. Instead, the initial fatigue crack dimensions and the maximum load at failure were used in the equation below:

$$K_{IC} = \sigma_G \sqrt{\frac{1.21 \pi A_m}{E^2 - .212 (\sigma_G / \sigma_Y)^2}}$$

where $E^2 = \int_0^{\pi/2} \sqrt{1 - k^2 \sin^2 \theta} d\theta$

$$k^2 = \frac{A_m^2 - C_m^2}{A_m^2}$$

$$A_m = \frac{\text{Notch Length}}{2}$$

$$C_m = \text{Notch Depth}$$

$$P = \text{Ultimate Load}$$

$$\sigma_G = \text{Gross Stress} = \frac{P}{\text{Gross Specimen Area}}$$

$$\sigma_Y = \text{Equivalent smooth yield stress of material}$$

In addition, difficulty is ordinarily experienced in specimens of this type in limiting the depth of the initial crack to less than 1/2 the sheet thickness.

Under these conditions, the notch is inadequately restrained and plane strain conditions are not met.

In addition, the net fracture stress (σ_N) and the notch ratio for each specimen was calculated using

$$\sigma_N = \frac{P}{WB - A_m C_m}$$

where W = specimen width

and B = specimen thickness

$$\text{Notch ratio} = \frac{\sigma_N}{\sigma_y}$$

All notch data is presented in Table VIII-6. Average notch values for each heat are plotted in Figures VIII-22, VIII-23 and VIII-24. It should also be noted that in most instances at room temperature and -320F the ratio of the gross notch strength to yield strength exceeded .8. Under these conditions, of course, accurate K_{Ic} value cannot be obtained. Such data merely indicates the high tolerance of the material to notches of the type introduced and an approximation to actual K_{Ic} value for the material. At -423F all gross fracture stress ratios are less than .8; this indicates that the specimen design is satisfactory for K_{Ic} determination at -423F.

TABLE VIII-6

Heat	Spec. S/N	-320F Prestress		Test Temp. °F	Equiv. Smooth Yield Stress σ_y ksi	Gross Notch Strength σ_g ksi	σ_g/σ_y	Nominal Notch Tensile Stress σ_N ksi	Nominal Notch Ratio σ_N/σ_y	Nominal K_{Ic} ksi $\sqrt{in.}$
97056	11N	223	237	-423	354	220	.62	251	.71	77
97057	6N	224	236	-423	359	244	.68	268	.75	80
	7N	224	237	-423	359	214	.60	250	.70	77
97058	5N	261	285	Room	266	239	.90	272	1.02	85
	6N	260	283	Room	265	228	.86	261	.99	82
	12N	260	279	-320	335	250	.75	293	.87	91
	13N	261	281	-320	336	300	.89	358	1.07	109
	14N	260	281	-423	381	233	.61	260	.68	80
	15N	260	284	-423	381	255	.67	274	.72	78
97107	1N	239	253	Room	243	246	1.01	260	1.07	75
	2N	239	252	Room	243	241	.99	256	1.05	74
	3N	241	254	-320	314	305	.97	329	1.05	98
	14N	239	252	-320	313	305	.97	335	1.07	103
	4N	240	253	-423	352	195	.55	218	.62	65
	5N	239	252	-423	352	280	.80	301	.85	95

NOMINAL K_{IC} KSI \sqrt{in}

VS

TEMPERATURE

ARDE FORM LOW SILICON
STAINLESS STEEL

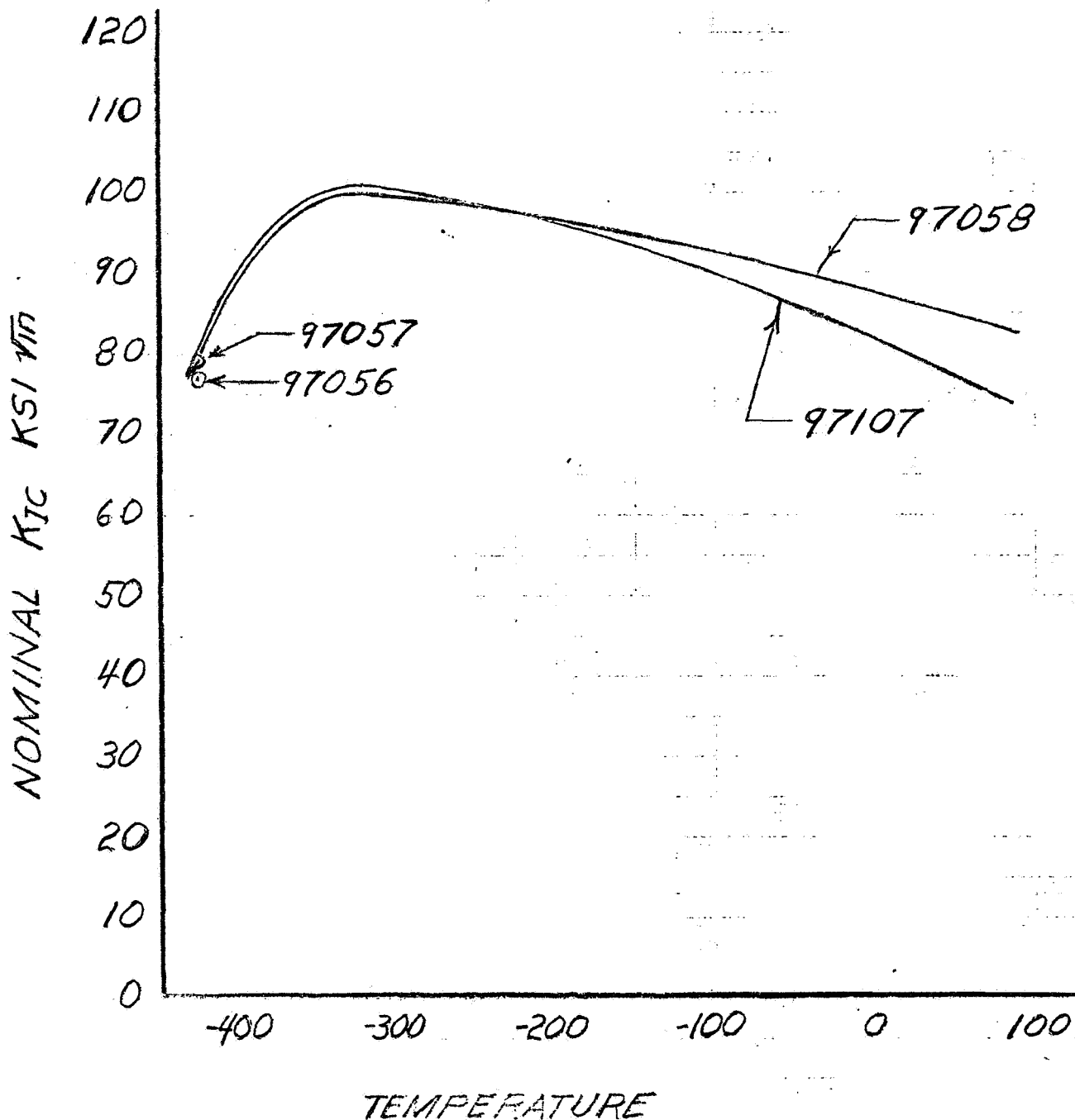


FIGURE VIII-22

NOTCHED/UNNOTCHED STRENGTH
VS
TEMPERATURE
AR DEFORM LOW SILICON STAINLESS
STEEL - FATIGUE CRACKED SPECIMENS
SPECIMEN WIDTH ≈ 1.12
PARTIAL THICKNESS CRACK
AVERAGE VALUES PLOTTED
CRACK LENGTH .150/.210

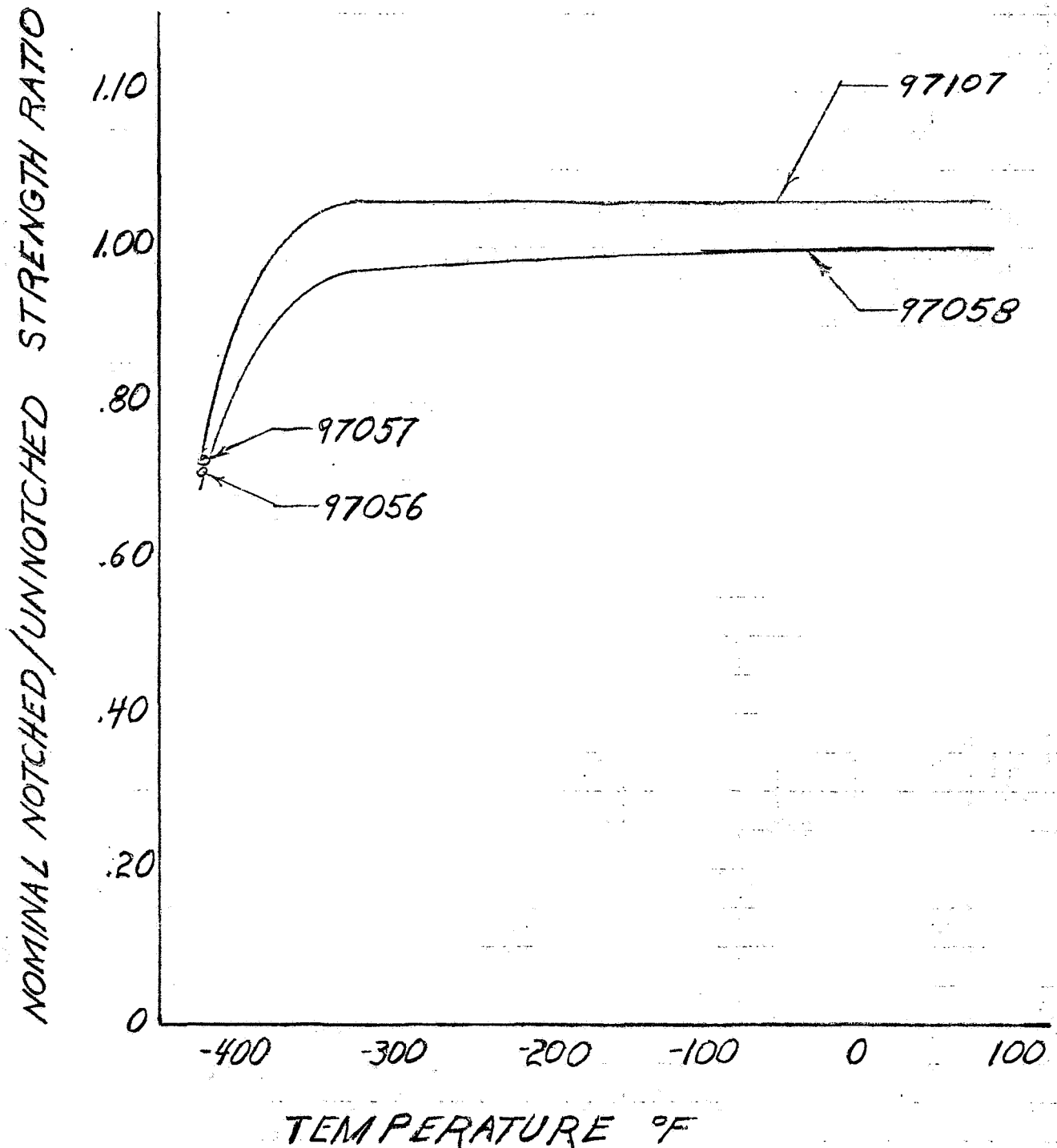


FIGURE VIII-23

NOMINAL NOTCHED TENSILE STRENGTH
VS
TEMPERATURE
ARDE FORM LOW SILICON STAINLESS STEEL
FATIGUE CRACKED SPECIMENS:
SPECIMEN WIDTH ≈ 1.12
PARTIAL THICKNESS CRACK
AVERAGE VALUES PLOTTED
CRACK LENGTH .150/.210

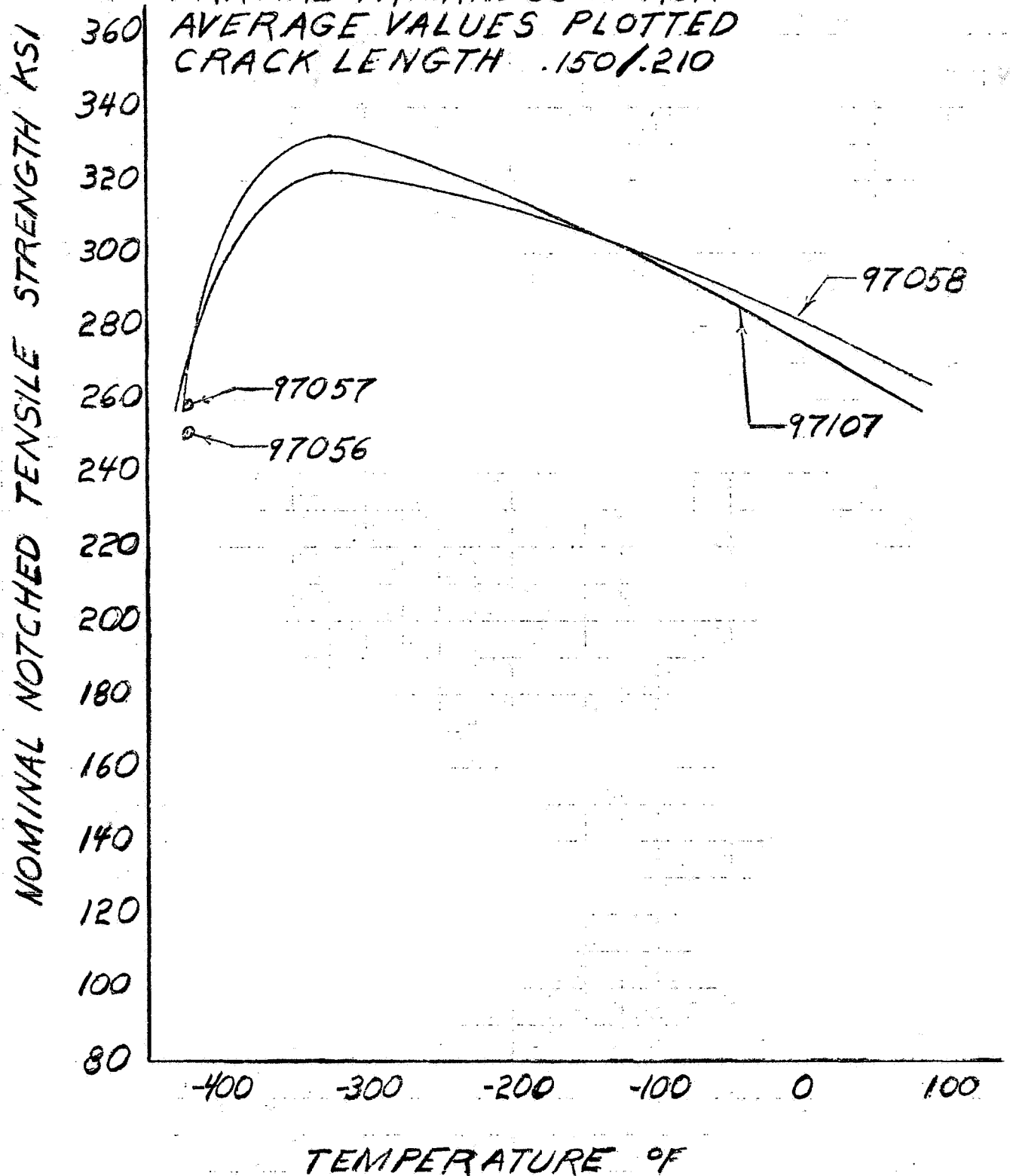


FIGURE VIII-24

D. Mechanical Testing of Welds

1. Test Specimens and Procedure

In addition to the previously described smooth and notch testing conducted to evaluate the basic material, the weld strength of the material was also evaluated by NASA at Marshall. Twenty-four (24) type D3617 (See Figure VIII-25) specimens were prepared by Arde for the testing program. Twelve (12) specimens were fabricated from a .060 nominal thickness sheet of heat 97058, and twelve (12) specimens from heat 97107. All specimens were cut with the rolling direction of the sheet stock parallel to the specimen gage length. Prior to cutting, each sheet of material was welded with a full penetration TIG weld bead. Welds were not machined flush to the material surface but were left with the slight under and over bead normal to the process.

After all machining was completed, each specimen was cleaned in mild alkaline detergent, annealed, pickled and passivated.

The specimens were all subject to similar cryogenic prestress levels. The prestrain of the specimens were dictated by the design requirements of the vessel. The true prestress of each specimen was calculated using

$$\bar{\sigma} = \frac{\text{Load}}{\text{Specimen Area After Prestrain and Prior to Machining}}$$

The weld bead was not included in the specimen thickness measurement.

After prestraining, each specimen gage section was remachined to a .500 inch width. All machining was done with sufficient quantities of coolant to prevent overheating the specimen. Each specimen was aged for 20 hours at 790F, vacuum blasted to remove aging oxides, cleaned in detergent and passivated.

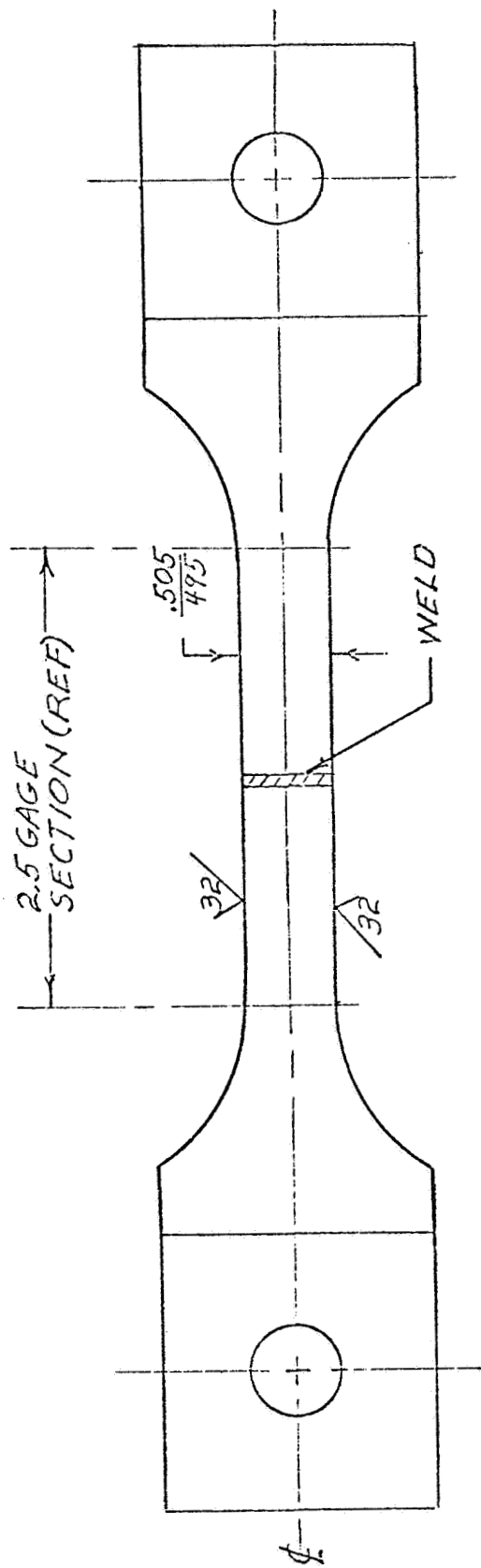
Each specimen was bagged in plastic. All the specimens were shipped to NASA for notching and testing. Figure VIII-25 shows the prestrained, remachined specimen before notching.

At NASA the weld bead was left intact and edge notches were machined as nearly as possible on the centerline of the weld. The notches were designed to produce a K_T of 10. Tests were made at room temperature and at -423F. Test results obtained in the NASA Laboratories are reproduced in Table VIII-7 and VIII-8.

E. Stress Corrosion Susceptibility Testing of Welded Ardeform Material

1. Specimen Fabrication History

Ten (10) type D3617 specimens were prepared for the stress corrosion testing program at NASA's Marshall Space Flight Center. All specimens were fabricated from a .060 nominal thickness sheet of Arde low silicon material heat 97058. All specimens were cut with the rolling direction of the sheet stock parallel to the specimen gage length. Prior to cutting, the



Welded Tensile Specimen

Figure VIII-25

TABLE VIII-7

MECHANICAL PROPERTIES OF ARDEFORMED LOW Si
STAINLESS STEEL WELDED TENSILE SPECIMENS

Heat and Spec. No.	True Cryo Prestress ksi	Test Temp. (°F)	U.T.S. (psi)	0.2 Per- cent Y.S. (psi)	Elongation Percent in in 2"
97058- 7	281	R.T.	259,090	258,390	--
- 8	281	R.T.	249,320	246,960	3.5
- 2	277	-423	379,125	370,030	1.5
- 3	281	-423	383,665	374,000	1.5
-11	282	-423	382,650	374,690	1.5
-14	280	-423	384,350	379,590	1.5
97107-10	254	R.T.	243,110	240,990	3.0
-18	253	R.T.	238,360	236,300	3.5
-11	254	-423	364,810	353,310	1.5
-12	255	-423	364,110	349,130	1.5
-16	254	-423	366,900	353,310	1.5
-19	269	-423	373,500	359,150	1.5

TABLE VIII-8

NOTCHED TENSILE PROPERTIES OF ARDEFORMED LOW Si
STAINLESS STEEL WELDED TENSILE SPECIMENS

Heat and Spec. No.	True Cryo Prestress ksi	Test Temp. °F	Notched Tensile Strength (psi)	N/UN Ratio (Kt=10)
97058- 1	280	R.T.	302,955	Average 1.16
-10	278	R.T.	289,640	
- 5	279	-423	277,780	High - 0.74 Low - 0.69 Average -0.72
- 9	278	-423	269,410	
-12	283	-423	266,930	
-13	282	-423	281,500	
97107- 9	255	R.T.	304,110	Average 1.27
-20	255	R.T.	306,370	
-13	253	-423	260,740	High - 0.90 Low - 0.69 Average - 0.82
-14	255	-423	329,100	
-15	256	-423	293,830	
-17	255	-423	317,660	

sheet material was welded with a full penetration TIG weld. The weld was made using argon gas back-up. The welds in these specimens were also left with the slight under and over bead which is normal for the welding process.

After all machining was completed, each specimen was cleaned in mild alkaline detergent, annealed, pickled and passivated in hot nitric acid-sodium dichromate solution.

Each specimen was placed in a bath of liquid nitrogen and prestressed to a true stress ($\bar{\sigma}$) of approximately 279 ksi. The gage width and thickness of the specimens were measured both before and after prestraining, and areas calculated. The weld bead was not included in thickness. The true prestress was calculated using the area of the specimen after prestraining.

$$\text{Prestress} = \frac{\text{Load}}{\text{Area After Prestrain}}$$

The cryogenic prestress level and predicted room temperature yield stress of each specimen is shown in Table VIII-9. Each specimen was aged for 20 hours at 790F, vacu-blasted to remove aging oxides, cleaned in detergent and passivated. Specimens were bagged in plastic and shipped to NASA for stress corrosion testing.

TABLE VIII-9

Cryogenic Prestrain of Corrosion Test Specimens

Serial Number	Heat Number	Cryogenic Prestress ksi	Predicted R.T. Yield Stress ksi
15	97058	282	262
16		278	261
17		284	263
18		282	262
19		279	261
20		281	262
21		279	261
22		284	263
23		283	263
24	V	282	262

2. Test Procedure and Results

The specimens were stressed by constant deflection using a fixed span snap-in frame. Three specimens were loaded in tension to 190 ksi (75% Y.S.) and three to 227 ksi (90% Y.S.). The test environment consisted of alternate immersion in a neutral 3 1/2 percent solution of sodium chloride at ambient temperature. A Ferris wheel type tester was used which cycled in such a manner that the specimens were immersed in the solution for ten minutes, followed by fifty minutes of drying above the solution. This material was found to be resistant to stress-corrosion cracking under the test conditions in that no failures were encountered at either stress load (190 and 227 ksi) after six months of exposure.

F. Data Addendum

The data curves for heat 50793, which is applicable to the material used in the fabrication of the S/N 10 and 11 vessels is provided in Appendix F.

IX. SATURN S IV B HELIUM STORAGE VESSELS, RECOMMENDED HANDLING PROCEDURES DURING QUALIFICATION TESTING

1. Introduction

The combined influence of stress and corrosion can cause premature failure in most metals and alloys. Such failures can occur below the design stress, even in those environments where general corrosion may not be noticeable. Fortunately, the conditions of service and the service environments which may result in such failures, tend to be specific for each material. For these reasons, it is important that the Saturn S IV B Helium Storage pressure vessels be projected from the specific service conditions and service environments which can degrade the performance of ARDEFORM material.

2. Hydrogen Embrittlement and Stress Corrosion

It has long been known that embrittlement of high yield strength alloy steels may be caused by penetration of the metal by atomic hydrogen. Austenitic stainless steels, on the other hand, show little, if any, tendency toward embrittlement by atomic hydrogen. ARDEFORM pressure vessels are fabricated by a process which transforms austenitic stainless steel to a low carbon martensite of very high yield strength. Therefore, it must be expected that transformed material will behave in a manner similar to that of the high strength alloy steels in the presence of atomic hydrogen. Since the stainless steel surface of ARDEFORMed pressure vessels are passivated, they have excellent resistance to general corrosion.

However, if attachments to the vessel provide a crevice where condensed water vapor can accumulate, local oxygen concentration cells may be set up as a result of the difference between the oxygen concentrations of the condensation exposed to the air and the moisture trapped in the crevice. Such cells break down the passivation and cause a very slow, highly localized pitting attack, which in itself is not serious except over very long periods of service. Unfortunately, atomic hydrogen is a product of the pitting corrosion and may cause embrittlement under such service conditions.

The hydrogen embrittlement of ARDEFORM material has, in all cases, been traced to the release of hydrogen as a result of either galvanic action or local electromechanical corrosion. In all cases it has been possible to modify the application or use conditions to eliminate the cause of the embrittlement.

ARDEFORM material shows, in general, good resistance to stress corrosion in the presence of various environments. Users, however, are urged to consult Arde, Inc. concerning any test procedure or application which will subject the vessel to environments not contemplated in the design of vessels.

In order to protect the Saturn S IV B Helium Storage vessels from moisture during shipment they were purged with dry nitrogen gas and placed in a plastic bag which was also purged with dry nitrogen gas prior to being heat sealed.

3. Recommendations

1) Straps or similar crevice forming devices should not be used to hold the Saturn S IV B Helium Storage vessels. Instead, test stands should be designed and built with appropriate support fittings to match the bosses and clevises of the vessel. See Figure IX-1 and IX-2.

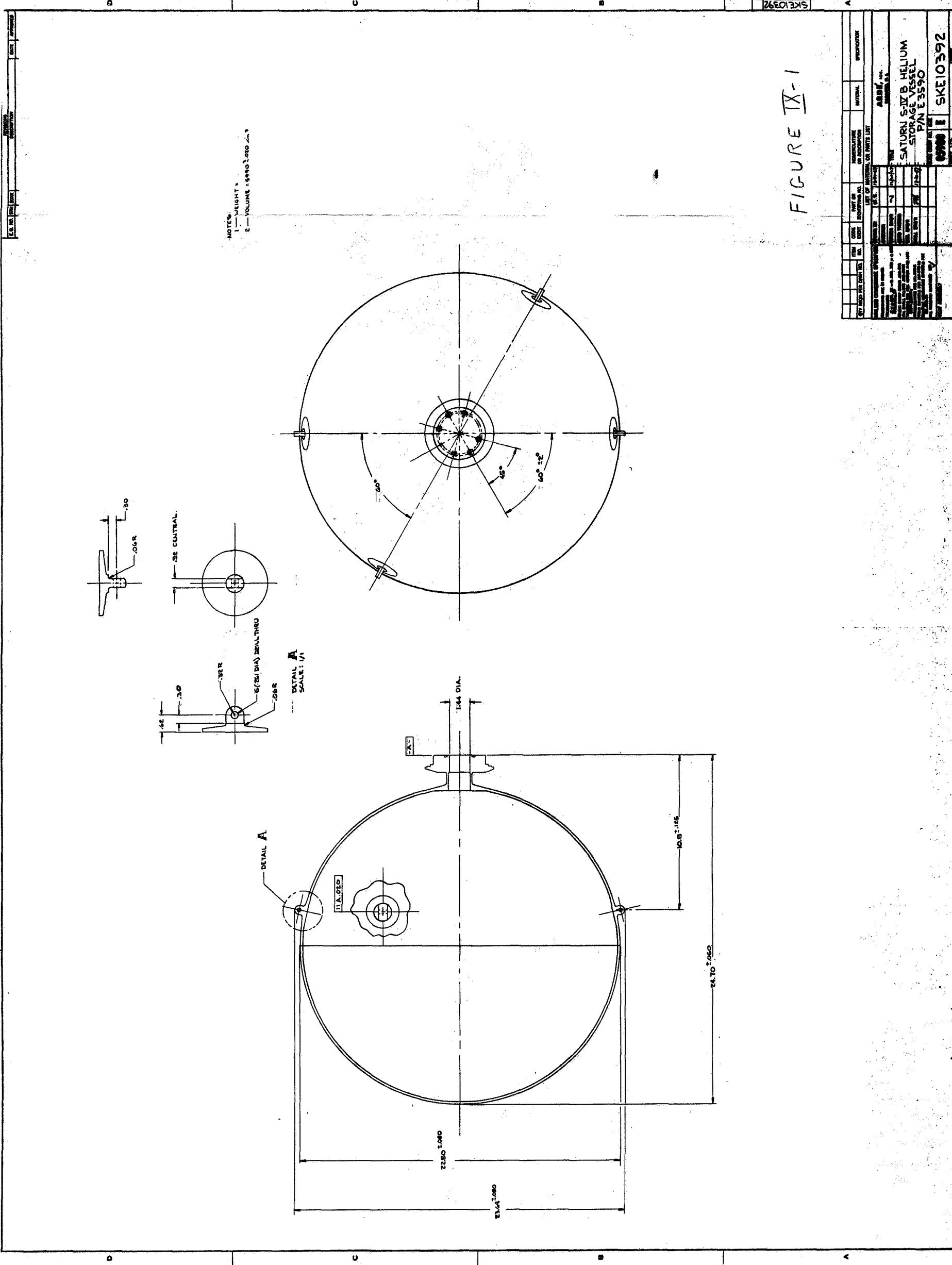
2) Only type 300 series stainless steel shall be used for all mounting hardware and fixtures which will come in contact with the vessel. All hardware, fixtures, etc. should be thoroughly washed and cleaned prior to use with these vessels.

3) Avoid the application of substances containing chlorides, sulfides, organic amines to the surface of ARDEFORM vessels. Substances of unknown composition should not be applied indiscriminately. Consult ARDE before using any adhesive, coating, or waterproofing material on the surface of ARDEFORM vessels. It is suggested that "Duco" cement be used to affix strain gages to the vessels. Strain gages should be removed after test and all cement should be cleaned from the vessel using acetone.



4) The vessels should not be allowed to come into contact with oil or grease of any sort.

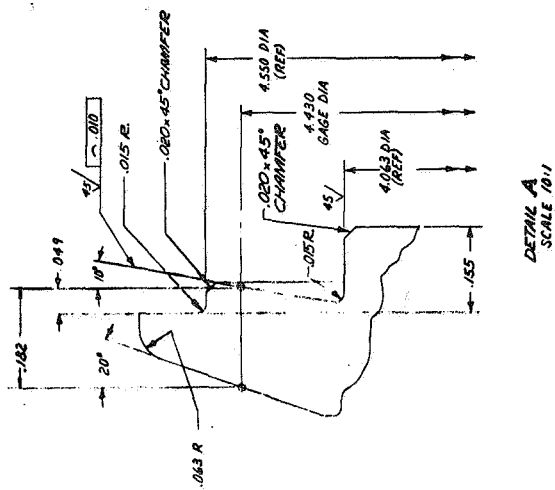
5) White gloves should be worn whenever the vessels are handled.

6) Avoid placing the vessels directly on any metallic surface, such as aluminum or zinc, which might create an electrolytic cell.

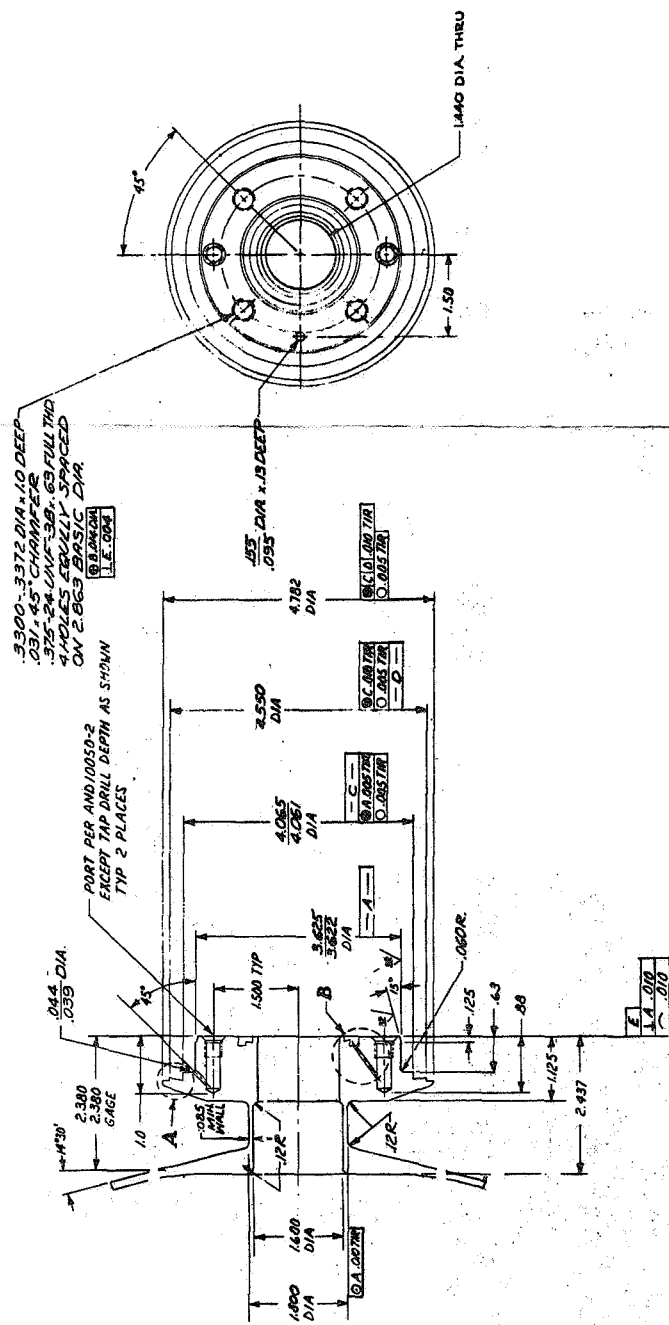


ITEM NO.	QTY	DESCRIPTION	UNIT	REMARKS
1	1	SATURN S-IV B HELIUM STORAGE VESSEL		
2	1	P/N E3590		
3	1	SKE10392		

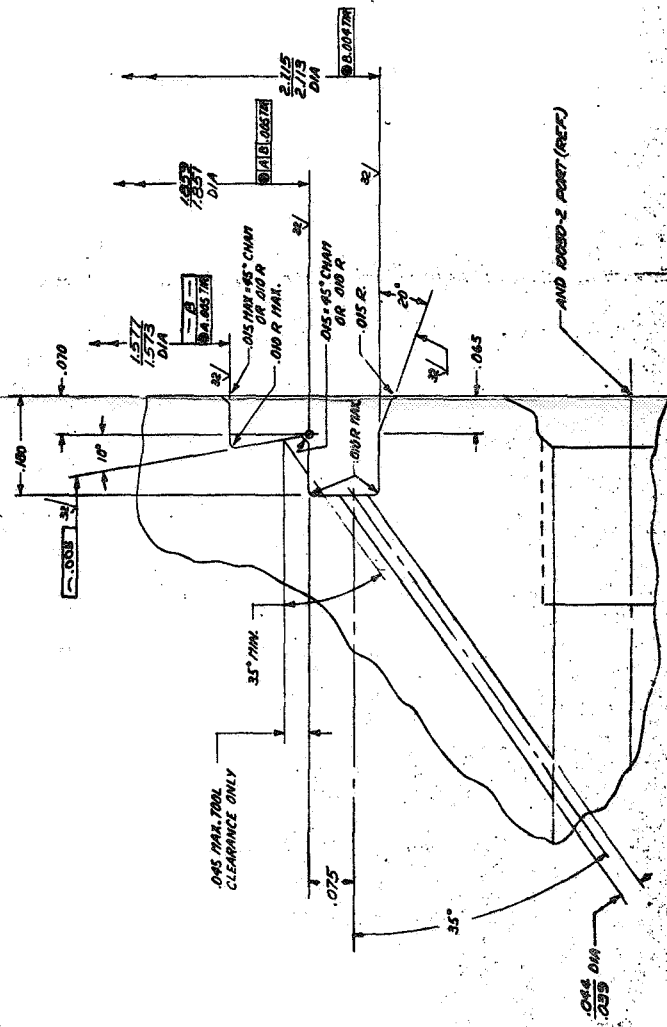
RETURNING			DATE	APPROVED
S.O. NO.	SCORE	DESCRIPTION		
A		1) 41 WAS 412 (1) 1191 WAS 1409/150 2) 2726 WAS 2357. (0) REVISED NOTE P.	1955 F.I.L.	
B		1) 4587/4588 WAS 6404/6410. 2) 2760 WAS 2726. (0) WAS 195	1955 F.I.L.	



DETAIL A
SCALE 10:1



NOTES:



DATE

FIGURE IX-2

[illegible]

7) Vessels should be stored in clean plastic bags. If vessels are to be stored for any long duration of time (more than a month) they should be dry nitrogen gas purged and placed in plastic bags, the bags should be dry nitrogen gas purged and heat sealed.

X. CONCLUSIONS

The program indicated that pressure vessels of reasonable complex configuration could be fabricated from low silicon material for -423F service. Also, that ARDE's inspection techniques and the self inspecting characteristics of the cryogenic stretch forming process can result in the production of reliable hardware. The scrap rates due to the inclusions in the material were fairly high but this can be remedied through the use of ultrasonic inspection techniques and double vacuum melted raw material.

XI. APPENDIX

APPENDIX A

Uniaxial - Biaxial Correlation

APPENDIX A

Uniaxial - Biaxial Correlation

In the theory of elasticity⁽¹⁾ the strain in a given direction can be expressed quite simply by "Hooke's Law",

$$\epsilon_1 = \frac{1}{E} (\sigma_1 - \nu (\sigma_2 + \sigma_3))$$

Therefore a stress state exists that does not describe yielding or plastic flow and the material expands or contracts as a function of the condition of loading. Hence, problems are relegated to considerations of small strains with either small or large deflections, a constant modulus of elasticity, E, is used and two solutions can be superimposed in suitable proportions to obtain the correct answer.

In the theory of plastic deformation, it is necessary to use graphical solutions in considering large strains (as well as large deflections) that cause changes of shape while the volume of material remains basically constant. This plastic deformation, as applied to the ARDEFORM process, results in a 10-14% reduction in thickness throughout all highly stressed surfaces in the vessel, and a corresponding elongation of approximately 10-14% primarily in the hoop direction for cylinders, and a 5-7% elongation in each of two mutually perpendicular axes for spheres. With plastic deformation the Poisson's ratio used = .5. It is necessary to introduce an arbitrary constant $1/D$ ⁽¹⁾, analogous

(1) NADAI, A. "Plasticity" McGraw Hill - 1931

to $1/E$ in Hooke's Law. The value of $1/D$ is directly related to the portion of the stress-strain curve under consideration. The essential plasticity stress-strain relation for a tensile coupon, pressurized sphere, and a pressurized cylinder are shown in Table I.

Line 1 lists the principal stresses. The tensile coupon has only one principal stress. For the sphere, two principal stresses are equal, and the third is assumed zero because the pressure is negligible next to the strength of the material.

In Line 2, the formula for the stress invariant σ^* is used. This relationship defines the conditions for a state of yielding in the material for any stress state in terms of a stress invariant σ^* . Note that the invariant stress σ^* , equals the tensile stress in a tensile coupon and the meridional or hoop stress in a sphere; it is somewhat smaller than the hoop stress in the cylinder.

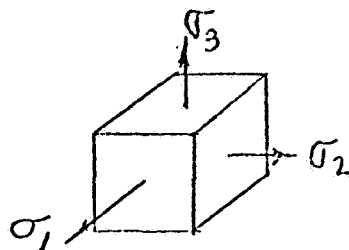
Line 3 represents a simple algebraic conversion from σ_1 to σ^* .

Line 4 defines D , and Line 5 defines ϵ^* . Well established⁽¹⁾ relationships are quoted and used in Line 6; here the relations of Line 3 have been substituted. Now using relations of Lines 4 and 5 in Line 6, one obtains Line 7. In accordance with theory, constancy of volume is maintained by $\epsilon_1 + \epsilon_2 + \epsilon_3 = 0$.

(1) NADAI, A. "Plasticity" McGraw Hill - 1931

TABLE I PLASTICITY RELATIONS APPLIED TO TENSILE COUPONS
AND INTERNALLY PRESSURIZED SPHERES AND CYLINDERS

Line No.	Type of Member	Tensile Coupon	Sphere	Cylinder
	Loading	Axial	Pressure	Pressure
1	Given principal Stresses, in terms of Maximum Principal Stress, σ_1	σ_1 (axial) $\sigma_2 = 0$ $\sigma_3 = 0$	σ_1 (hoop) σ_1 long. 0	σ_1 (hoop) $\frac{1}{2} \sigma_1$ long. 0
2	Stress invariant in terms of maximum principal stress, σ_1 $\sigma^* = \sqrt{\frac{1}{2} [(\sigma_1 - \sigma_2)^2 + (\sigma_2 - \sigma_3)^2 + (\sigma_3 - \sigma_1)^2]}$	σ_1	σ_1	$\frac{\sqrt{3}}{2} \sigma_1$
3	Principal stresses in terms of stress invariant, σ^*	$\sigma_1 = \sigma^*$ $\sigma_2 = 0$ $\sigma_3 = 0$	σ^* σ^* 0	$\frac{2}{\sqrt{3}} \sigma^*$ $\frac{1}{\sqrt{3}} \sigma^*$ 0
4	Invariant stress-strain relation	$\sigma^* = D \epsilon^*$	$\sigma^* = D \epsilon^*$	$\sigma^* = D \epsilon^*$
5	Strain invariant relation	$\epsilon^* = \sqrt{\frac{2}{3} [\epsilon_1^2 + \epsilon_2^2 + \epsilon_3^2]}$		
6	Principal strains in terms of stress invariant $D \epsilon_1 = \sigma_1 - .5(\sigma_2 + \sigma_3)$ $D \epsilon_2 = \sigma_2 - .5(\sigma_3 + \sigma_1)$ $D \epsilon_3 = \sigma_3 - .5(\sigma_1 + \sigma_2)$	σ^* $-.5 \sigma^*$ $-.5 \sigma^*$	$\frac{1}{2} \sigma^*$ $\frac{1}{2} \sigma^*$ $-\sigma^*$	$\frac{\sqrt{3}}{2} \sigma^*$ 0 $-\frac{\sqrt{3}}{2} \sigma^*$
7	Principal strains in terms of invariant strain, ϵ^* $\epsilon_1 = \ln \frac{L}{L_0}$ or $\epsilon_1 = \ln \frac{R}{R_0}$ $\epsilon_2 = \ln \frac{w}{w_0}$ $\epsilon_3 = \ln \frac{t}{t_0}$	ϵ^* $-\frac{1}{2} \epsilon^*$ $-\frac{1}{2} \epsilon^*$	$\frac{1}{2} \epsilon^*$ $\frac{1}{2} \epsilon^*$ $-\epsilon^*$	$\frac{\sqrt{3}}{2} \epsilon^*$ 0 $-\frac{\sqrt{3}}{2} \epsilon^*$



From the table it should be noted that for the tensile coupon $\epsilon_1 = \epsilon^*$ and $\sigma_1 = \sigma^*$ so that the σ^* vs. ϵ^* relation is nothing more than the conventional true-stress true-strain diagram for a tensile coupon. Since the principal stresses and strains for any stress state are related to the stress and strain invariants, σ^* and ϵ^* during plastic deformations, then it is clear that plastic strains and stresses in structures such as spheres may be related to the uniaxial stress strain curve.

A sphere may be related to a uniaxial specimen as follows:

$$\text{From line 3 of Table A-1, } \sigma_1 = \sigma^* = \bar{\sigma} \quad \text{Eq. (1)}$$

where σ_1 is the sphere hoop stress

σ^* is the stress invariant

$\bar{\sigma}$ is equivalent stress in a uniaxial tensile specimen

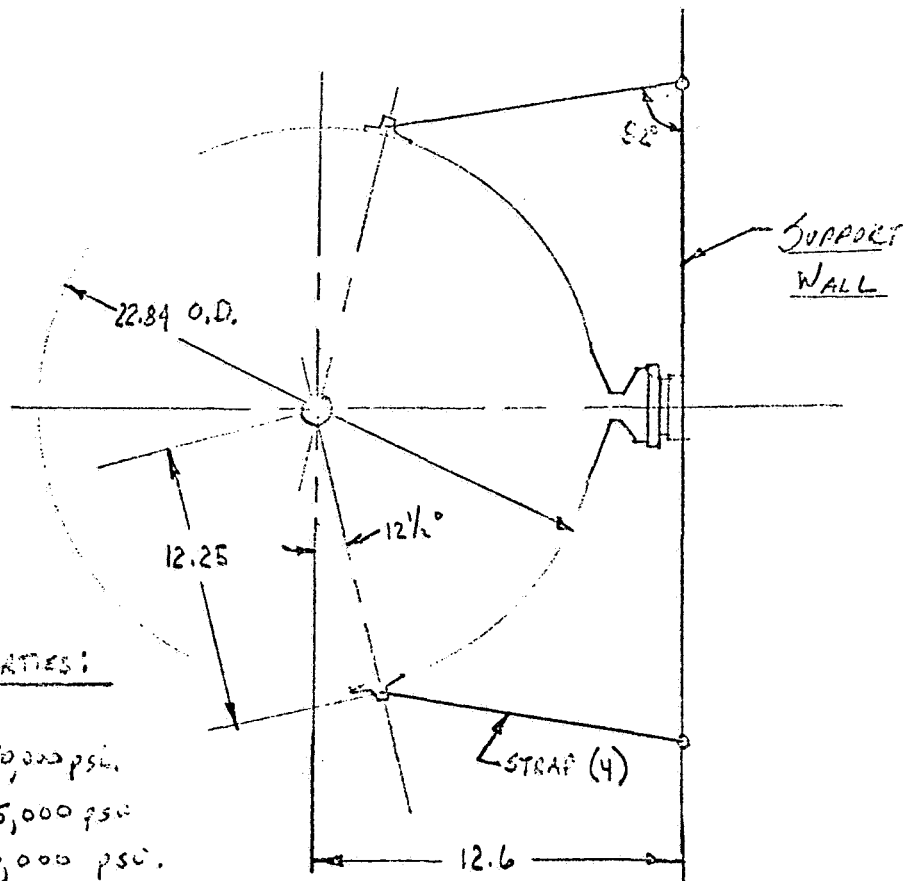
$$\text{From line 7 of Table A-1, } \epsilon_1 = 1/2 \epsilon^* = 1/2 \bar{\epsilon} \quad \text{Eq. (2)}$$

where the notation is the same as that in Equation 2 above.

APPENDIX B

Boss Analysis

TANK SUPPORT LOADS

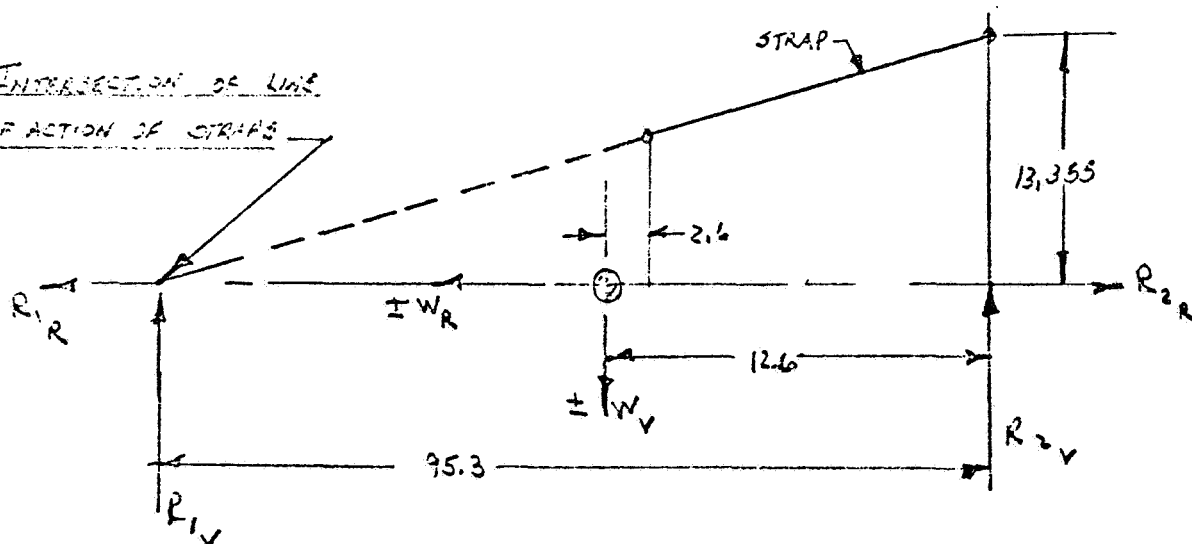


SHELL MAT'L. PROPERTIES:

$\sigma_y @ -423^\circ F = 550,000 \text{ psi.}$
 $\sigma_y @ -320^\circ F = 315,000 \text{ psi.}$
 $\sigma_y @ \text{R.T.} = 240,000 \text{ psi.}$

SUPPORT ARRANGEMENT

INTERSECTION OF LINE OF ACTION OF STRAPS



SUPPORT GEOMETRY

VIBRATION LOADS [REF.: NASA MEMO J.H. FARROW TO L.H. HEIN]

$$\left. \begin{array}{l} \text{THRUST AXIS} = \pm 1280^{\#} \\ \text{RADIAL AXIS} = \pm 1040^{\#} \\ \text{TANG. AXIS} = \pm 1600^{\#} \end{array} \right\} \text{EQUIVALENT STATIC LOADS}$$

$$\text{STATIC FLIGHT ACCELERATION} = 4.17 g$$

$$\text{EST. WT. OF TANK (FULL)} = 75^{\#} \quad \swarrow \text{DESIGN YIELD FACTOR}$$

$$\begin{aligned} \text{MAX. LOAD ALONG MISSILE THRUST AXIS} &= 1.25(1280 + 75 \times 4.17) \\ \text{(DESIGN YIELD)} &= 2000^{\#} \end{aligned}$$

$$\text{TANG. DESIGN LOAD} = (1.25)(1600) = 2000^{\#}$$

$$\text{RADIAL DESIGN LOAD} = (1.25)(1040) = 1300^{\#}$$

BOSS AND STRAP LOADS

$$R_{1V} = (2000) \left(\frac{12.6}{95.3} \right) = 265^{\#}$$

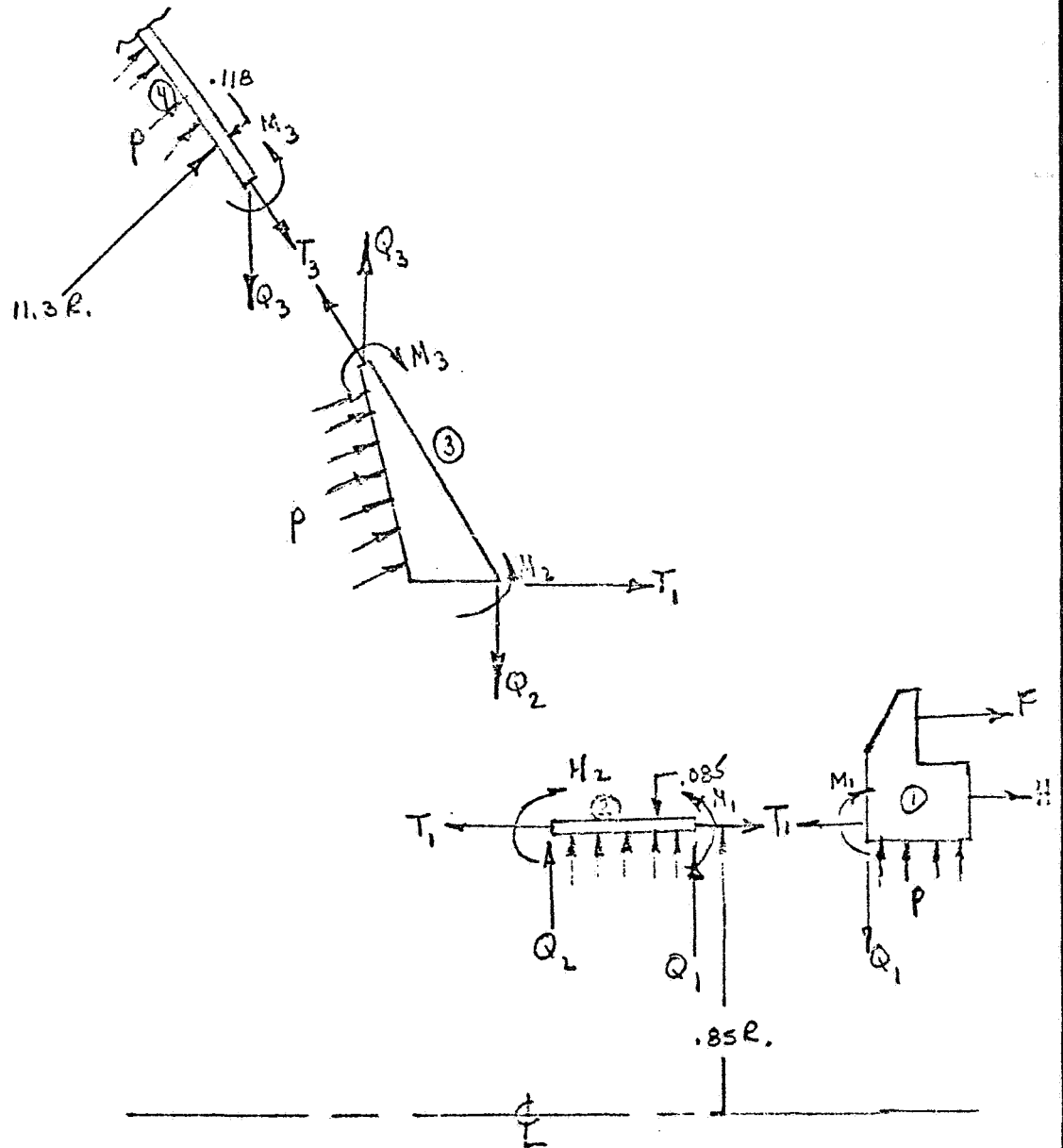
$$R_{2V} = 1735^{\#}$$

$$R_{1R} = R_{2R} = 1300^{\#}$$

$$\text{STRAP LOAD DUE TO } R_{1R} = 1300^{\#} = \frac{1300}{(4) \cos 8^{\circ}} = 328^{\#}$$

$$\text{STRAP LOAD DUE TO } R_{1V} = 265 = \frac{265}{2(\sin 45^{\circ})(\sin 8^{\circ})} = 1350$$

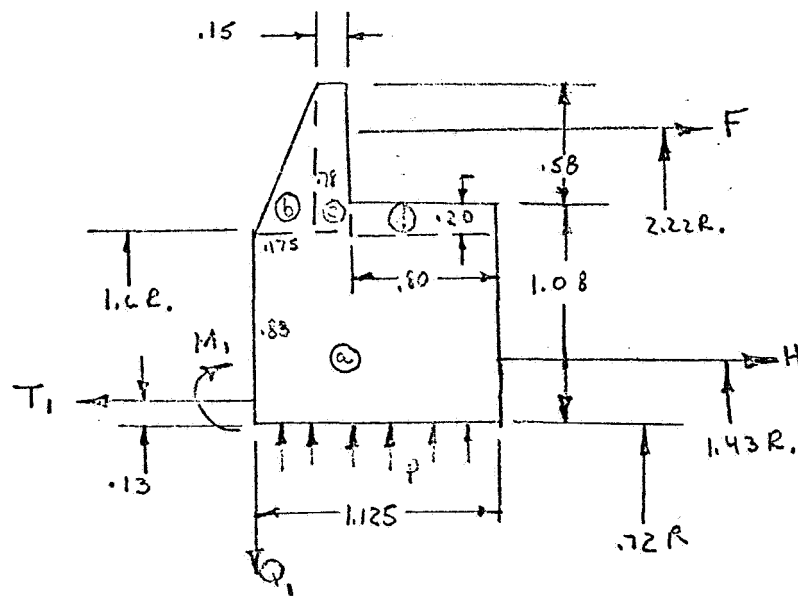
DISCONTINUITY ANALYSIS



FREE - BODY DIAGRAM

RING ①

$\uparrow +Q, +W$
 $\curvearrowright +M, +V$



SECTION PROPERTIES:

Item	A	x	y	Ax	Ay	Ax ²	I _{oy}
a	.990	.563	.440	.557	.436	.314	.1050
b	.068	.117	1.140	.008	.078	—	—
c	.117	.250	1.270	.029	.148	.007	.0003
d	.160	.725	.950	.116	.157	.084	.0085
	1.335	(.532)	(.613)	.710	.819	.405	.1138

$$I_y = .405 + .1138 - 1.335 (.532)^2 = .141 \text{ IN.}^4$$

$$R_{C.G.} = .72 + .613 = 1.333 \text{ IN.}$$

$$Q_{NET} = Q_1 \left(\frac{.85}{1.333} \right) - 1.125 p \left(\frac{.72}{1.333} \right) = .637 Q_1 - .608 p$$

$$M_{NET} = .532 Q_1 (.637) - .637 M_1 - .483 T_1 (.637) - .939 F \left(\frac{2.22}{1.333} \right) \\ - .097 H \left(\frac{1.43}{1.333} \right) + 1.125 p \left(\frac{.72}{1.333} \right) (.563 - .532) \\ = .340 Q_1 - .637 M_1 - .308 T_1 - 1.430 F - .104 H + .019 p$$

$$T_1 = H \left(\frac{1.43}{.85} \right) + F \left(\frac{2.22}{.85} \right)$$

$$T_1 = 1.682 H + 2.61 F$$

$$\text{Sub. FOR } H = .393 p :$$

$$T_1 = 2.61 F + .662 p$$

$$M_{NET} = .340 Q_1 - .637 M_1 - .804 F - .204 p - 1.480 F - .041 p + .019 p$$

$$M_{NET} = .340 Q_1 - .637 M_1 - .226 p - 2.284 F$$

$$\theta_1 = \frac{(1.332)^2}{(30 \times 10^6)(.141)} (.340 Q_1 - .637 M_1 - .226 p - 2.284 F)$$

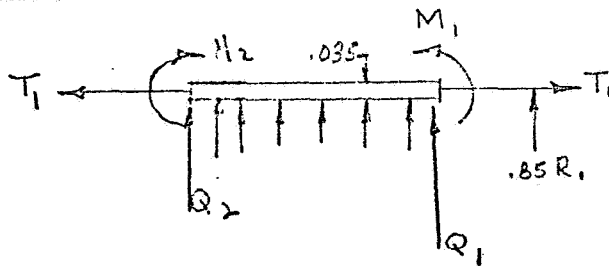
$$\theta_1 = 10^{-6} (.143 Q_1 - .269 M_1 - .0952 p - .962 F)$$

$$N_1 = \frac{(1.333)^2}{(35 \times 10^6)(1.335)} (.637 Q_1 - .603 p) + .532 \theta_1$$

$$w_1 = 10^{-6} (.0283 Q_1 - .0270 p + .0761 Q_1 - .143 M_1 - .0506 p - .511 F)$$

$$w_1 = 10^{-6} (.1044 Q_1 - .143 M_1 - .0776 p - .511 F)$$

CYL. ②



$$\beta_2 = \frac{1.285}{\sqrt{(.85)(.035)}} = 4.80$$

$$\beta l = (4.8)(.8) = 3.84 > \pi \quad \therefore \text{LONG CYLINDER}$$

$$D_2 = \frac{(30 \times 10^6)(.035)^3}{10.92} = .168 \times 10^4$$

$$W_{2R} = \frac{10^{-4}}{(2)(.168)(4.8)^3} \left(-Q_1 - 4.8 M_1 \right) - \left[\frac{(.85)^2 p - (.30)(2.61 F + .667 p)(.85)}{(30 \times 10^6)(.035)} \right]$$

$$W_{2R} = 10^{-4} (-.0269 Q_1 - .1292 M_1 - .00207 p + .0022 F)$$

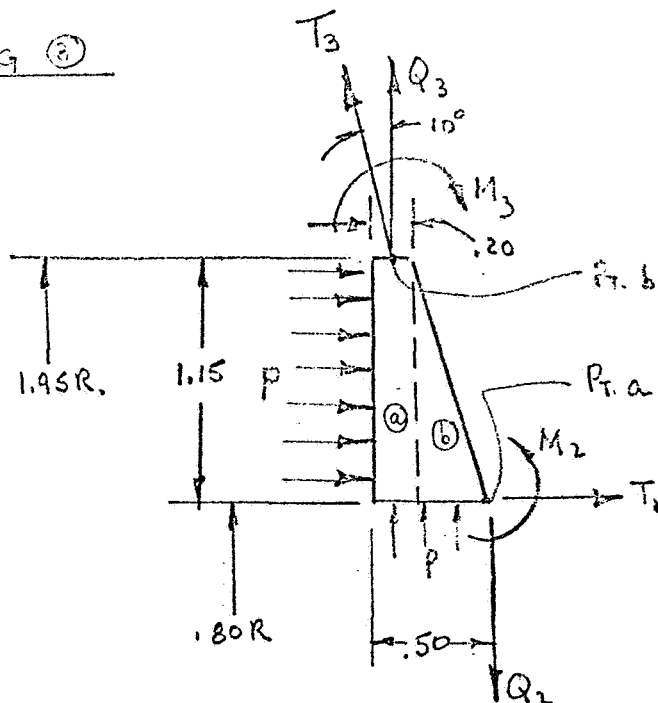
$$\theta_{2R} = \frac{10^{-4}}{(2)(.168)(4.8)^2} (Q_1 + 9.6 M_1)$$

$$\theta_{2L} = 10^{-4} (.1292 Q_1 + 1.240 M_1)$$

$$W_{2L} = 10^{-4} (-.0269 Q_2 - .1292 M_2 - .00207 p + .0022 F)$$

$$\theta_{2L} = 10^{-4} (-.1292 Q_2 - 1.240 M_2)$$

RING ②



<u>I_{cm}</u>	<u>A</u>	<u>x</u>	<u>y</u>	<u>Ax</u>	<u>Ay</u>	<u>Ax²</u>	<u>I_c</u>
w	.230	.10	.575	.023	.132	.0023	.00077
L	.173	.30	.333	.052	.066	.0156	.00086
	.403	(.184)	(.491)	.075	.198	.0179	.00163

$$I_y = .0179 + .00163 - .403 (.184)^2 = .0056 \text{ in.}^4$$

$$R_{c.g.} = .8 + .491 = 1.291 \text{ in.}$$

$$\begin{aligned} Q_{NET} &= Q_2 \left(\frac{.80}{1.291} \right) - 1.5 p \left(\frac{.80}{1.291} \right) - Q_3 \left(\frac{1.95}{1.291} \right) - T_3 \cos 10 \left(\frac{1.95}{1.291} \right) \\ &= .619 Q_2 - .310 p - 1.51 Q_3 - 1.49 T_3 \end{aligned}$$

$$T_3 \sin 10 = T_1 \left(\frac{.8}{1.95} \right) + p \left(\frac{1.95^2 - .8^2}{2 \times 1.95} \right) = .41 T_1 + .81 p$$

$$T_3 = 2.36 T_1 + 4.66 p = 6.22 p + 6.16 F$$

$$Q_{NET} = .619 Q_2 - 1.51 Q_3 - 9.57 p - 9.18 F$$

$$M_{NET} = -.619 Q_2 (.314) + (.619)(2.61F + .62p)(.491) + .619 M_2 \\ - (Q_3 + .985 T_3) \left(\frac{1.95}{1.291} \right) (.036) - 1.51 M_3 + .174 T_3 (.559) (.151) \\ + .50p (.619) \left(\frac{.264}{.25 - .186} \right) - 1.15p \left(\frac{1.50}{1.291} \right) (.209)$$

$$M_{NET} = -.194 \bar{Q}_2 + .793 \bar{F} + .202 \bar{p} + .619 \bar{M}_2 - .130 \bar{Q}_3 - .123 \bar{T}_3 \\ - 1.51 \bar{M}_3 + .173 \bar{T}_3 + .020 \bar{p} - .279 \bar{p}$$

$$M_{NET} = -.194 \bar{Q}_2 + .619 \bar{M}_2 - .130 \bar{Q}_3 - 1.51 \bar{M}_3 - .057 \bar{p} + .793 \bar{F} + .045 \bar{T}_3$$

$$M_{NET} = -.194 \bar{Q}_2 + .619 \bar{M}_2 - .130 \bar{Q}_3 - 1.51 \bar{M}_3 + .223 \bar{p} + 1.070 \bar{F}$$

$$\phi_{(3)} = \frac{(1.291)^2}{(30 \times 10^6)(1.0056)} (M_{NET}) = 9.93 \times 10^{-6} M_{NET}$$

$$\phi_{(3)} = 10^{-6} (-1.927 \bar{Q}_2 + 6.15 \bar{M}_2 - 1.292 \bar{Q}_3 - 15.0 \bar{M}_3 + 2.21 \bar{p} + 10.62 \bar{F})$$

$$W_{(3)a} = \frac{(1.291)^2}{(30 \times 10^6)(1.403)} (.619 \bar{Q}_2 - 1.51 \bar{Q}_3 - 9.57 \bar{p} - 9.18 \bar{F}) - .314 \phi_{(3)}$$

$$W_{(3)a} = 10^{-6} (.0855 \bar{Q}_2 - .2085 \bar{Q}_3 - 1.32 \bar{p} - 1.265 \bar{F} + .604 \bar{Q}_2 - 1.927 \bar{M}_2 \\ + .405 \bar{Q}_3 + 4.71 \bar{M}_3 - .694 \bar{p} - 3.34 \bar{F})$$

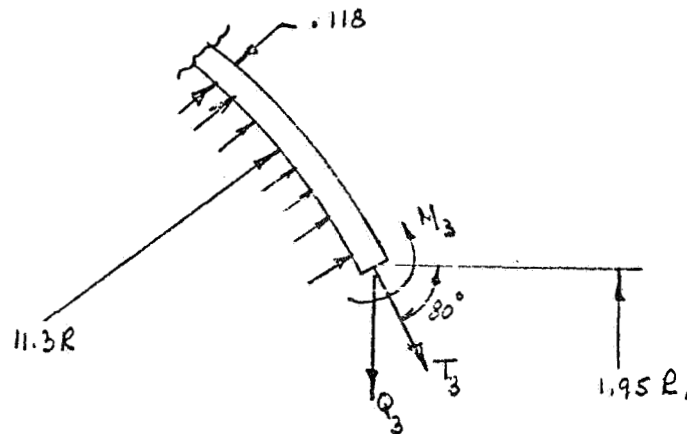
$$W_{(3)a} = 10^{-6} (.6975 \bar{Q}_2 - 1.927 \bar{M}_2 + 1.965 \bar{Q}_3 + 4.71 \bar{M}_3 - 2.014 \bar{p} - 4.605 \bar{F})$$

$$W_{(3)b} = 10^{-6} (.0855 \bar{Q}_2 - .2085 \bar{Q}_3 - 1.32 \bar{p} - 1.265 \bar{F}) + .096 \phi_{(3)}$$

$$w_{(3)_b} = 10^{-6} (.0855 Q_2 - .2085 Q_3 - 1.32 p - 1.265 F - .1655 Q_2 + .529 M_2 \\ - .1110 Q_3 - 1.292 M_3 + .190 p + .913 F)$$

$$w_{(3)_b} = 10^{-6} (-.0800 Q_2 + .529 M_2 - .3195 Q_3 - 1.292 M_3 - 1.130 p - .352 F)$$

SPHERICAL SECTOR (4)



$$(3)_4 = \frac{1.285}{\sqrt{(11.3)(.118)}} = 1.117$$

$$\phi = 10^\circ$$

$$\sin \phi = .174$$

$$\sin^2 \phi = .0303$$

$$D_{(4)} = \frac{(30 \times 10^6)(.118)^3}{10.92} = .452 \times 10^4$$

$$w_{(4)_R} = \frac{10^{-4}}{(2)(.452)(1.117)^3} \left[.0303 Q_3 - (.174)(1.117) M_3 \right] - \frac{(.15)p(1.95)(.113)}{(30 \times 10^6)(.118)} \\ + \frac{(.15)(1.75)(6.22p + 2 \times 6.16F)}{(30 \times 10^6)(.118)}$$

$$w_{(4)_R} = 10^{-4} (.0241 Q_3 - .1543 M_3 - .0260 p + .0102 F)$$

$$\phi_{\text{R}} = \frac{10^{-4}}{(2)(.452)(1.117)^2} \left[-.174 Q_3 + (2)(1.117) M_3 \right]$$

$$\phi_{\text{R}} = \frac{10^{-4}}{\dots} \left(-.1543 Q_3 + 1.980 M_3 \right)$$

$$w_{\text{I}} = w_{\text{R}}$$

$$.1044 Q_1 - .143 M_1 - .0776 p - .511 F = -2.690 Q_1 - 12.920 M_1 - .207 p + .22 F$$

$$2.7944 Q_1 + 12.777 M_1 = -.1294 p + .731 F$$

$$Q_1 + 4.56 M_1 = -.0463 p + .261 F \quad \text{--- (1)}$$

$$\phi_{\text{I}} = \phi_{\text{R}}$$

$$.143 Q_1 - .268 M_1 - .0952 p - .962 F = 12.92 Q_1 + 124.0 M_1$$

$$-12.777 Q_1 - 124.268 M_1 = .0952 p + .962 F$$

$$-Q_1 - 9.74 M_1 = .00756 p + .0754 F \quad \text{--- (2)}$$

$$Q_1 + 4.56 M_1 = -.0463 p + .2610 F \quad \text{--- (1)}$$

$$-5.18 M_1 = -.03874 p + .3364 F$$

$$M_1 = .00748 p - .0649 F$$

$$Q_1 = -.0534 p + .261 F - 4.56 (.00748 p - .0649 F)$$

$$Q_1 = -.0878 p + .557 F$$

$$\underline{w_{(3)u} = w_{(2)L}}$$

$$.6895 Q_2 - 1.927 M_2 + .1965 Q_3 + 4.71 M_3 - 2.014 p - 4.605 F =$$

$$- 2.64 Q_2 - 12.92 M_2 - .207 p + .22 F$$

$$3.3795 Q_2 + 10.993 M_2 + .1965 Q_3 + 4.71 M_3 = +1.307 p + 4.825 F \text{ --- (1)}$$

$$\underline{\theta_{(3)} = \theta_{(2)L}}$$

$$-1.927 Q_2 + 6.15 M_2 - 1.292 Q_3 - 15.0 M_3 + 2.21 p + 10.62 F = -12.92 Q_2 \\ - 124.0 M_2$$

$$10.993 Q_2 + 130.15 M_2 - 1.292 Q_3 - 15.0 M_3 = -2.21 p - 10.62 F \text{ --- (2)}$$

$$\underline{w_{(3)b} = w_{(3)L}}$$

$$-.0800 Q_2 + .529 M_2 - .3195 Q_3 - 11.292 M_3 - 1.130 p - 1.352 F = 2.41 Q_3 - 15.43 M_3 \\ - 2.60 p + 1.02 F$$

$$-.0800 Q_2 + .529 M_2 - 2.7295 Q_3 + 14.138 M_3 = -1.770 p + 1.372 F \text{ --- (3)}$$

$$\underline{\theta_{(3)} = \theta_{(3)L}}$$

$$-1.927 Q_2 + 6.15 M_2 - 1.292 Q_3 - 15.0 M_3 + 2.21 p + 10.62 F = -15.43 Q_3 + 143.0 M_3$$

$$-1.927 Q_2 + 6.15 M_2 + 14.138 Q_3 - 213.0 M_3 = -2.21 p - 10.62 F \text{ --- (4)}$$

SOLUTION OF EQUATIONS

Eq.	Q_2	M_2	Q_3	M_3	$K(p)$	\checkmark	$K(F)$	\checkmark
1	3,37950	10,99300	.19650	4,71000	1,80700	21,08600	4,82500	24,10400
2	10,999300	130,15000	-1,29200	-15,00000	-2,21000	122,64100	-10,62000	114,23100
3	-1,08000	.52900	-2,72950	14,13800	-1,47000	10,38750	1,37200	13,22950
4	-1,92700	6,15000	14,13800	-213,00000	-2,21000	-196,84900	-10,62000	-205,25900
	3,37950	3,25285	.05814	1,39370	.52019	6,22488	1,39517	7,09986
	10,999300	94,39142	-1,02045	-3,2122	-1,08397	.57432	-1,27499	.38332
	-1,08000	.78923	-2,70871	-5,35421	.50285	-3,85136	-1,62784	-4,98206
	-1,92700	12,41824	14,50399	-128,66794	.05796	1,05796	-1,03566	.96432
P	.55068	-1,04874	.81318	.05796				
F	2,47870	-1,30319	-1,81877	-1,03566				

STRESSES

Ex. 1

$$\begin{aligned}P_{OPER.} &= 3200 \text{ psi @ } -423^{\circ}\text{F} \\&= 3500 \text{ psi @ R.T.} \\P_{BURST} &= 7200 \text{ psi @ } -423^{\circ}\text{F} \\F &= \pm 94 \text{ #/in.}\end{aligned}$$

$$\begin{aligned}F_{TY} \text{ (301 ANNEALED)} &= 40,000 \text{ psi @ R.T.} \\&= 80,000 \text{ psi @ } -423^{\circ}\text{F} \\F_{T0} &= 150,000 \text{ psi @ } -423^{\circ}\text{F}\end{aligned}$$

@ -423°F

$$Q_1 = -(0.0878)(3200) \pm (0.557)(94) = -333 \text{ #/in.}$$

$$M_1 = (0.00748)(3200) \mp (0.0649)(94) = 30.1 \text{ in-#/in.}$$

$$Q_{NET} = (0.637)(-333) - (0.608)(3200) = -2160 \text{ #/in.}$$

$$\begin{aligned}M_{NET} &= (0.340)(-333) - (0.637)(30.1) - (0.226)(3200) - (2.284)(94) \\&= -113 - 19 - 723 - 215 = -1070 \text{ in-#/in.}\end{aligned}$$

$$\begin{aligned}f_{MAX.} &= \frac{(2160)(1.333)}{1.335} + \frac{(1070)(1.333)(0.532)}{0.141} \\&= 2200 + 5500 = 7700 \text{ psi} < 80000 \therefore \text{O.K.}\end{aligned}$$

@ R.T.

$$Q_1 = -(0.0573)(3500) = -307 \text{ #/in.}$$

$$M_1 = (0.00748)(3500) = 26 \text{ in-#/in.}$$

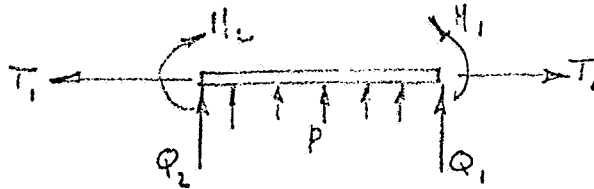
$$Q_{NET} = (0.637)(-307) - (0.608)(3500) = -2334 \text{ #/in.}$$

$$M_{NET} = (0.340)(-307) - (0.637)(26) - (0.226)(3500) = -723 \text{ in-#/in.}$$

$$f_{MAX.} = \frac{(2334)(1.333)}{1.335} + \frac{(723)(1.333)(0.532)}{0.141}$$

$$= 2300 + 4800 = 7100 \text{ psi} < 40,000 \text{ psi} \therefore \text{O.K.}$$

CYL (2) - STRESSES



$$t = .085$$

$$R = .85$$

$$p = 4.8$$

$$Q_1 = -.0878 p \pm .557 F \quad ; \quad M_1 = .00748 p \mp .0649 F$$

$$Q_2 = .5507 p \pm 2.479 F \quad ; \quad M_2 = -.04874 p \mp .3032 F$$

$$T_1 = .662 p \pm 2.61 F$$

LEFT END

$$T = -423^\circ F, \quad P_{OP} = 3200 \text{ psi.}$$

$$F_{TY} @ -423^\circ F = 350,000 \text{ psi.}$$

$$F_{TY} @ R.T. = 240,000 \text{ psi.}$$

$$F_{TY} @ -423^\circ F > 350,000 \text{ psi.}$$

$$Q_2 = (.5507)(3200) + (2.479)(94) = 1995 \text{ #/in}$$

$$M_2 = -(.04874)(3200) - (.3032)(94) = -185 \text{ #/in}$$

$$T_1 = 2365 \text{ #/in}$$

$$\sigma_L = \frac{2365}{.085} + \frac{(6)(185)}{(.085)^2}$$

$$\sigma_L = 27,800 + 154,000 = 182,000 \text{ psi.}$$

$$< 350,000 \text{ psi. } \therefore \text{O.K.}$$

$$\sigma_H = \frac{(3200)(.85)}{.085} + \frac{(2)(1995)(4.8)(.85)}{.085}$$

$$- \frac{(2)(4.8)^2(185)(.85)}{.085} + (.3)(154,000)$$

$$\sigma_H = 32,000 + 191,000 - 25000 + 46,000$$

$$\sigma_H = 184,000 \text{ psi. } \therefore \text{O.K.}$$

RIGHT END

$$T = -423^\circ F, \quad P_{OP} = 3200 \text{ psi.}$$

$$Q_1 = -(.0878)(3200) - (.557)(94) = -333 \text{ #/in}$$

$$M_1 = (.00748)(3200) + (.0649)(94) = 30.1 \text{ #/in}$$

$$T_1 = (.662)(3200) + (2.61)(94) = 2365 \text{ #/in}$$

$$\sigma_L = \frac{2365}{.085} + \frac{(6)(30.1)}{(.085)^2}$$

$$\sigma_L = 27,800 + 25,000 = 52,800 \text{ psi.}$$

$$< 80,000 \text{ psi. } \therefore \text{O.K.}$$

$$\sigma_H = \frac{(3200)(.85)}{.085} - \frac{(2)(4.8)(333)(.85)}{.085}$$

$$+ \frac{(2)(4.8)^2(30.1)(.85)}{.085} + (.3)(25000)$$

$$\sigma_H = 32,000 - 32,000 + 13,800 + 7500$$

$$\sigma_H = 21,300 \text{ psi. } \therefore \text{O.K.}$$

CYL. ① (CONT'D.)

LEFT END	RIGHT END
$T = -423^{\circ}\text{F}, P_{\text{PRESS}} = 5340 \text{ psi}$ $Q_2 = (.5507)(5340) = 2940 \text{ #/"}$ $M_2 = -(.04874)(5340) = -260 \text{ #-"}^2$ $T_1 = 3540 \text{ #/"}^2$ $\sigma_L = \frac{3540}{.085} + \frac{6(260)}{(.085)^2}$ $\sigma_L = 41,600 + 216,000 = 257,600 \text{ psi.}$ $< 350,000 \text{ psi. } \therefore \text{O.K.}$ $\sigma_{H_p} = 53,400 \text{ psi. } \therefore \text{O.K.}$	$T = -423^{\circ}\text{F}, P_{\text{PRESS}} = 5340 \text{ psi.}$ $Q_1 = (-.0878)(5340) = -469 \text{ #/"}^2$ $M_1 = (.00748)(5340) = 40 \text{ #-"}^2$ $T_1 = (.662)(5340) = 3540 \text{ #/"}^2$ $\sigma_L = \frac{3540}{.085} + \frac{(6)(40)}{(.085)^2}$ $\sigma_L = 41,600 + 33,200$ $= 74,800 \text{ psi. } < 80,000 \text{ psi. } \therefore \text{O.K.}$ $\sigma_{H_p} = \frac{(5340)(.85)}{.085} = 53,400 \text{ psi. } \therefore \text{O.K.}$ $\sigma_H \text{ NOT CRITICAL}$
$R.T., P_{\text{PRESS}} = 3500 \text{ psi.}$ $\sigma_L = (257,600)\left(\frac{3500}{5340}\right)$ $\sigma_L = 169,000 \text{ psi. } < 240,000 \text{ psi.}$ $\therefore \text{O.K.}$ $\sigma_{H_p} = 35,000 \text{ psi. } \therefore \text{O.K.}$	$R.T., P_{\text{PRESS}} = 3500 \text{ psi.}$ $\sigma_L = \left(\frac{3500}{5340}\right)(74,800) = 48,700 \text{ psi.}^*$ <p>*NOTE: THIS STRESS APPARENTLY EXCEEDS THE R.T. YIELD STRENGTH OF 40KSI. HOWEVER, THE MOMENT WILL YIELD OUT REDUCING THE STRESS TO THE YIELD POINT.</p> $\sigma_{H_p} = \frac{(3500)(.85)}{.085} = 35,000 \text{ psi.}$ $\therefore \text{O.K.}$
$T = -423^{\circ}\text{F}, P_{\text{BURST}} = 7100 \text{ psi}$ $\sigma_L = (257,600)\left(\frac{7100}{5340}\right)$ $\sigma_L = 340,000 \text{ psi. } < 350,000 \text{ psi.}$ $\therefore \text{O.K.}$ $\sigma_{H_p} = 71,000 \text{ psi. } \therefore \text{O.K.}$	$T = -423^{\circ}\text{F}, P_{\text{BURST}} = 7100 \text{ psi.}$ $\sigma_L = (74,800)\left(\frac{7100}{5340}\right) = 100,000 \text{ psi. } < 150,000 \text{ psi.}$ $\therefore \text{O.K.}$ $\sigma_{H_p} = \frac{(7100)(.85)}{.085} = 71,000 \text{ psi. } \therefore \text{O.K.}$

RING

$$Q_{NET} = .619 Q_2 - 1.51 Q_3 - 9.57 p - 9.18 F$$

$$H_{NET} = -.194 Q_2 + .619 H_2 - .130 Q_3 - 1.51 H_3 + .223 p + 1.070 F$$

$$Q_2 = .5507 p \pm 2.477 F \quad ; \quad H_2 = -.04274 p \mp .3032 F$$

$$Q_3 = .8132 p \mp .8183 F \quad ; \quad H_3 = .058 p \mp .0357 F$$

$$T_1 = .662 p \pm 2.61 F \quad ; \quad T_3 = 6.22 p \pm 6.16 F$$

$$\begin{aligned} Q_{NET} &= .619 (.5507 p \pm 2.477 F) - (1.51) (.8132 p \mp .8183 F) - 9.57 p \mp 9.18 F \\ &= .341 p \pm 1.537 F - 1.227 p \pm 1.237 F - 9.57 p \mp 9.18 F \end{aligned}$$

$$Q_{NET} = -10.456 p \mp 6.406 F$$

$$\begin{aligned} H_{NET} &= -(1.94) (.5507 p \pm 2.477 F) + .619 (-.04274 p \mp .3032 F) \\ &\quad - .130 (.8132 p \mp .8183 F) - 1.51 (.058 p \mp .0357 F) + .223 p \pm 1.07 F \\ &= -.1062 p \mp .481 F - .0302 p \mp .1875 F - .1057 p \pm .1063 F \\ &\quad - .0876 p \pm .0539 F + .223 p \pm 1.07 F \end{aligned}$$

$$H_{NET} = -.1073 p \pm .5617 F$$

$$T = -423^{\circ}F, \quad P_{OP} = 3200 \text{ psi.}$$

$$Q_{NET} = -(0.456)(3200) \mp (6.406)(94) \\ = -33500 \mp 600 = -34,100 \text{ }^{\circ}/\text{in}$$

$$M_{NET} = -(1.073)(3200) \pm (1.5617)(94) \\ = -347 - 53 = -400 \text{ }^{\circ}\text{-}^{\circ}/\text{in}$$

$$\sigma_{MAX} = \frac{34100}{.403} + \frac{(400)(1.291)(.186)}{.0056} \\ = 84,600 + 17100 = 101,700 \text{ psi.} < 350,000 \text{ psi.} \\ \therefore \text{O.K.}$$

$$T = -423^{\circ}F, \quad P_{BURST} = 7100 \text{ psi.}$$

$$Q_{NET} = -(0.456)(7100) = -74300 \text{ }^{\circ}/\text{in}$$

$$M_{NET} = -(1.073)(7100) = -763 \text{ }^{\circ}\text{-}^{\circ}/\text{in}$$

$$\sigma_{MAX} = \frac{74300}{.403} + \frac{(763)(1.291)(.186)}{.0056} \\ = 185,000 + 33000 = 218,000 \text{ psi.} < 350,000 \text{ psi.} \therefore \text{O.K.}$$

$$T = \text{R.T.}, \quad P_{PROOF} = 3500 \text{ psi.}$$

$$\sigma_{MAX} = \left(\frac{3500}{7100} \right) (218,000) = 107,000 \text{ psi.} < 240,000 \text{ psi.} \\ \therefore \text{O.K.}$$

SPHERE (4)

$$t_{END} = .20 \quad ; \quad \beta = 1.117 \quad ; \quad R_2 = 11.3 \quad , \quad R = 1.95$$

$T = -423^\circ F, P_{OP} = 3200 \text{ psi.}$

$$T_3 = (6.22)(3200) \pm (6.16)(94) = 19900 + 580 = 20,480 \text{ #/"}^2$$

$$Q_3 = (8.132)(3200) \mp (8.188)(94) = 26000 + 77 = 26,777 \text{ #/"}^2$$

$$M_3 = (6.058)(3200) \mp (6.037)(94) = 19600 + 3 = 19,603 \text{ #/"}^2$$

$$\sigma_L = \frac{20,480 + (.985)(26,777)}{.20} + \frac{(6)(19,603)}{(6.2)^2}$$

$$\sigma_L = 116,000 + 28,000 = 144,000 \text{ psi.} < 350,000 \text{ psi.} \quad \therefore \text{O.K.}$$

$$\sigma_H = \frac{(3200)(11.3)}{(2)(.20)} + \frac{(2)(19,603)(1.117)^2(11.3) - (2)(26,777)(1.117)(1.95)}{.20} + (.3)(28,000)$$

$$\sigma_H = 90,000 - 31,000 + 3400 = 62,400 \text{ psi.} \quad \therefore \text{O.K.}$$

$T = -423^\circ F, P_{BURST} = 7100 \text{ psi.}$

$$T_3 = (6.22)(7100) = 44,100 \text{ #/"}^2$$

$$Q_3 = (8.132)(7100) = 5770 \text{ #/"}^2$$

$$M_3 = (6.058)(7100) = 42,812 \text{ #/"}^2$$

$$\bar{\sigma}_L = \frac{44100 + (1.25)(5770)}{1.20} + \frac{(L)(412)}{(1.2)^2}$$

$$\bar{\sigma}_L = 249,000 + 62,000 = 311,000 < 350,000 \text{ psi}, \quad \therefore \text{O.K.}$$

$$\bar{\sigma}_{Hp} = \frac{(7100)(11.3)}{(2)(1118)} = 340,000 \text{ psi}, \quad \therefore \text{O.K.}$$

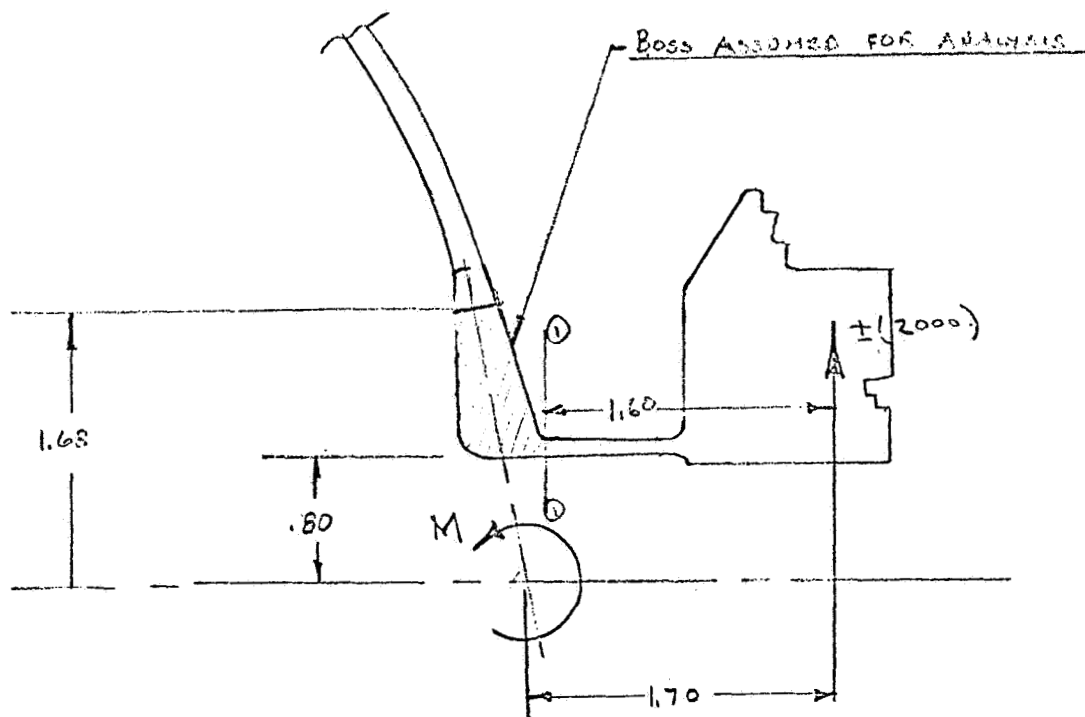
R.T., $P_{PR300} = 3500 \text{ psi}$

$$\bar{\sigma}_L = (311,000) \left(\frac{3500}{7100} \right) = 154,000 \text{ psi} < 240,000 \text{ psi}, \quad \therefore \text{O.K.}$$

$$\bar{\sigma}_{Hp} = (340,000) \left(\frac{3500}{7100} \right) = 167,000 \text{ psi}, \quad \therefore \text{O.K.}$$

B. PRESSURE + LATERAL ACCEL. LOAD

[REF.: WELDING RESEARCH COUNCIL BULLETIN No. 107]



$$M = \pm (1.7)(2000) = 3400 \quad 11-4$$

② Sect. ①-① :

$$M_{DM} = (2000)(1.6) = 3200 \quad \text{H} = \frac{H}{2}$$

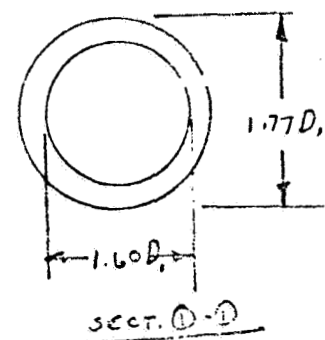
$$I = .05 \left(\overline{1.77^4} - \overline{1.6^4} \right) = .1435 \text{ in.}^4$$

$$f_b = \frac{(3200)(.885)}{.1435} = 17,300 \text{ psi.}$$

$$\overline{L}_P(\text{see pg. 15}) = \underline{182,000}$$

$$\Sigma = 199,300 \text{ psi.}$$

$< 240,000$ psi. \therefore O.K.



$$M = 3400 \text{ }^{11-4}$$

$$r_m = 1.24$$

$$T = .118$$

$$t = .83$$

$$r_o = 1.68$$

$$\gamma = \frac{1.24}{.83} = 1.4$$

$$R_m = 11.3$$

$$C = \frac{.118}{.96} = .123$$

$$U = \frac{1.68}{\sqrt{(11.3)(.118)}} = 1.46$$

$$M_c = .039 M = (.039)(3400) = 132.5 \text{ }^{11-4}$$

$$N_c = \frac{.028 M}{(.118)(1.15)} = (.206)(3400) = 700 \text{ }^{\#}/11$$

$$\bar{\sigma} = \frac{700}{.118} + \frac{(6)(132.5)}{(.118)^2} = 6000 + 57000 = 63,000 \text{ psi.}$$

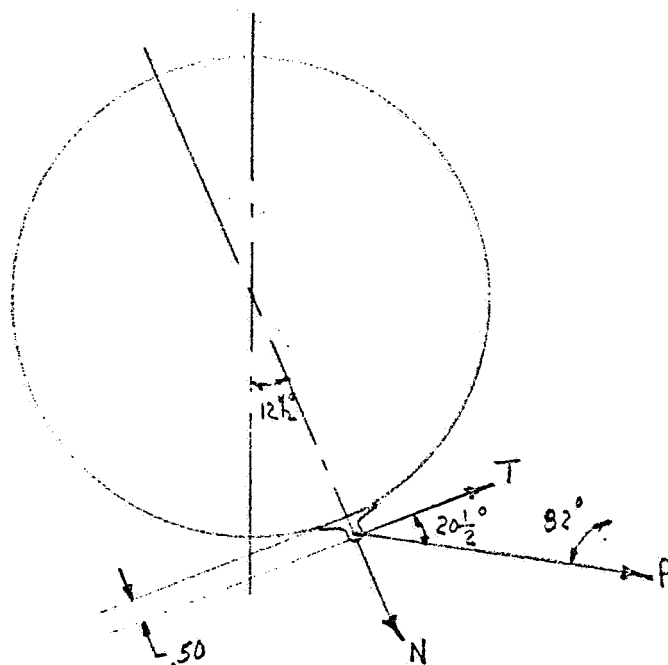
$$\sigma_p [\text{SEE PG. 19}] \cong (144,000)\left(\frac{.2}{.118}\right) = 244,000 \text{ psi.}$$

$$\Sigma = 307,000 \text{ psi.}$$

$$< 350,000 \text{ psi.}$$

O.K.

STRAP SUPPORT BOSS



$$P_{MAX.} = 1350^{\#} [PG, 2]$$

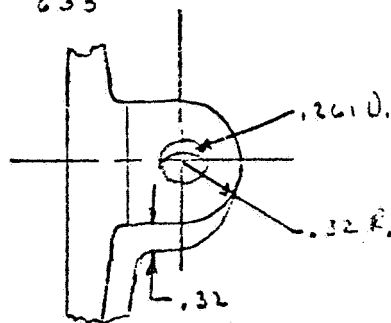
$$T = P \cos 20\frac{1}{2}^\circ = (1350)(.937) = 1265^{\#}$$

$$N = P \sin 20\frac{1}{2}^\circ = (1350)(.350) = 472^{\#}$$

$$\text{MOMENT ON SHELL} = (1265)(.5) = 633 \text{ in-in}$$

$$f_{br} = \frac{1350}{(2.61)(.32)} = 16,200 \text{ psi. O.K.}$$

$$f_s = \frac{1350}{(2)(.19)(.32)} = 11,100 \text{ psi. O.K.}$$



STRESS IN SHELL DUE TO N & MOM.

[REF. - WELDING RESEARCH
COUNCIL BULLETIN 107]

$$r_o = .32 ; R_m = 11.4 ; T = .118$$

$$U = \frac{.32}{\sqrt{(11.4)(.118)}} = .27$$

FROM FIG. SR-1 :

$$\frac{\sigma T^2}{\rho} \approx 1.1 \quad \& \quad \frac{\sigma T^2 \sqrt{R_m T}}{M} = 3.4$$

$$\therefore \sigma = \frac{(470)(1.1)}{(.118)^2} + \frac{(3.4)(633)}{(.118)^2 \sqrt{(11.4)(.118)}}$$

$$= 38,000 + 133,000 = 171,000 \text{ psi.}$$

$$\sigma_{\text{OPER. @ } -423^\circ\text{F}} = \frac{(3200)(11.4)}{(2)(.118)} = 154,000 \text{ psi.}$$

$$\sigma_{\text{TOT}} = 325,000 \text{ psi.} < 350,000 \text{ psi.}$$

\therefore O.K.

APPENDIX C

SPECIFICATION FOR VACUUM MELTED LOW
SILICON CHROME-NICKEL STAINLESS STEEL
SUITABLE FOR ARDEFORM
(AES 256)

AES	
NO.	256
DATE ISSUED:	1/21/66
<u>REVISION</u>	<u>DATE REVISED</u>
A	2/8/66
B	3/15/68

SPECIFICATION FOR VACUUM MELTED LOW
SILICON CHROME-NICKEL STAINLESS STEEL
SUITABLE FOR ARDEFORM

APPROVALS

Prepared by: *RH*
 Met. Eng. *RH-a*
 Design Eng. *SLM*
 Quality Cont. *CB*
 Chief Eng. *Cal*

ARDE, INC.
 Paramus, N. J.

ENGINEERING SPECIFICATION AES 252

1/21/66

AES 256

SPECIFICATION FOR VACUUM MELTED LOW SILICON
CHROME-NICKEL STAINLESS STEEL SUITABLE FOR ARDEFORM

1.0 SCOPE

- 1.1 This specification covers soft sheet, plate and sheet bar material intended for the fabrication of fusion welded pressure vessels by the ARDEFORM process.
- 1.2 This specification is effective upon issue and shall be applicable when specified on Engineering drawings.
- 1.3 This specification is applicable to all ARDE facilities and to all ARDE subcontractors and suppliers.

2.0 APPLICABLE DOCUMENTS

- ASTM Specification E 112 - Estimating the Average Grain Size of Metals
- ASTM Specification E 45 - Determining the Inclusion Content of Steel
- AES 257 - Material Evaluation Specification

3.0 REQUIREMENTS

- 3.1 The steel shall be made by the vacuum induction melting process.
- 3.2 The steel shall be melted using high purity charging materials, low in oxygen, silicon, phosphorous and sulphur.

3.3 The steel shall conform to the requirements as to chemical composition prescribed in Table I.

TABLE I
CHEMICAL COMPOSITION

Carbon, per cent	0.025 to .045
Manganese, per cent	0.10 max.
Silicon, per cent	0.10 max.
Chromium, per cent	18.30 to 18.70
Nickel, per cent	7.10 to 7.50
Molybdenum, per cent	0.15 to 0.35
Nitrogen, per cent*	0.02 to 0.04
Phosphorous and Sulfur, total per cent	0.015 max.
Oxygen, PPM**	60 max.
Hydrogen, ppm***	2 max.
Iron	Balance

* The Nitrogen shall be determined by the Kjeldahl method.

** The Oxygen shall be determined by vacuum fusion gas analysis of a ladle sample or ingot drillings.

*** The Hydrogen shall be determined by vacuum fusion gas analysis of a sample taken from the heat after conversion to slab or sheet bar.

3.4 A ladle analysis of each melt of steel shall be made by the manufacturer, as outlined in 4.1, to determine the percentage of the elements specified in Table I.

- 3.5 The condition of the sheet, plate and sheet bar procurable under this specification shall be fully solution annealed and pickled. The sheet, plate and sheet bar shall be so heat treated as to provide the austenitic grain size as specified in Section 3.6. The material shall be free of intergranular carbides when tested in accordance with 4.3. Hardness shall be RB 90 max.
- 3.6 The grain structure shall be equiaxed and the average grain size of the material shall be in accordance with Table II below. The grain size shall be determined in accordance with the Comparison Procedure specified in ASTM - Spec. E 112.

TABLE IIASTM GRAIN SIZE NUMBER

<u>Material Thickness, in.</u>	<u>Average Grain Size</u>	<u>Maximum Individual Grain Size</u>
Up to .065	6	4
.065 to .125	5	3
.125 to .550	4	3
Above .550	3	2

- 3.7 The inclusion content of the product shall be determined by Method A in ASTM E-45 and shall not exceed the requirements specified in Table III.

TABLE IIIASTM E-45 METHOD A

Type A		B		C		D	
Thin	Heavy	Thin	Heavy	Thin	Heavy	Thin	Heavy
1	0	1	0	1	0	1	1*

* The max. diameter of heavy globular oxides shall be 25 microns and there shall be no more than one, in any given field, having a diameter greater than 16 microns.

- 3.7.1 This requirement shall be met for each sheet or plate thickness purchased.
- 3.7.2 The material shall be free from injurious sub-surface defects and inclusions. The purchaser will subject one sheet from each lot of sheets to ultrasonic inspection to determine if local large inclusions are present. Ultrasonic inspection shall be conducted using 1/8" diameter focusing beam transducer. The oscilloscope gain shall be set to 85% saturation for a standard 3/64" diameter flat bottom hole. All indications above background shall be reported. The permissible size of single defects thus determined shall be no larger than 10% of the sheet thickness, and a maximum of .015 whichever is smaller. Said defects when confirmed by metallographic examination shall be the basis for rejection of the entire lot.
- 3.8 Both surfaces of the material shall be free from scale, severe mechanical gouges and scratches, deep pitting and discoloration. The material shall have a workmanlike appearance. Sheet stock surface shall correspond to a 2D finish. The surface finish of plate and sheet bar shall correspond to a No. 1 finish.

- 3.9 Samples of material otherwise purchasable under this specification shall be submitted to the purchaser in the form of two sheets of 36 x 96 x .060 thick for evaluation by the purchaser for fabricability and weldability. The samples shall be supplied from a portion of an ingot or a slab produced from the melt to be evaluated. Material samples shall be evaluated in accordance with ARDE Material Evaluation Specification AES - 257. If samples do not meet the requirements of the ARDE Material Evaluation Specification, the entire heat shall be subject to rejection. Samples shall be evaluated by the purchaser.
- 3.10 Permissible variations in thickness shall be as specified in Table IV.

TABLE IVPERMISSIBLE VARIATIONS IN THICKNESS OF SHEET AND PLATE

<u>Specified Thickness, in.</u>	<u>Permissible Variations in Thickness, Plus or Minus, in.</u>
0.016 to 0.026	0.002
0.027 to 0.040	0.002
0.041 to 0.058	0.003
0.059 to 0.072	0.003
0.073 to 0.083	0.004
0.084 to 0.098	0.004
0.099 to 0.114	0.005
0.115 to 0.130	0.005
0.131 to 0.145	0.006
0.146 to 0.176	0.007
0.177 to 0.250	0.010

On items over 0.250, thickness shall be no more than 0.010 under the specified dimension and no more than 0.020 over the specified dimension. Sheet bar dimension shall be not less than specified dimension and not more than 10% over the specified dimension.

- 3.11 Permissible variation in width and length is specified in Table V. Sheet, plate and sheet bar 0.131 in. and over in thickness regardless of size may have permissible variations of plus or minus 1/4 in. in width and in length, respectively.

TABLE V
PERMISSIBLE VARIATIONS IN WIDTH AND LENGTH

<u>Specified Width, in.</u>	<u>Permissible Variations in Width, in.</u>	
	<u>Plus</u>	<u>Minus</u>
Up to 42	1/8	0
42 and over	1/4	0

	<u>Permissible Variations in Length, in.</u>	
	<u>Plus</u>	<u>Minus</u>
Up to 120	1/8	0
120 and over	1/4	0

4.0 QUALITY ASSURANCE PROVISIONS

4.1 Analysis

- 4.1.1 Ingot Analysis - The analysis shall be made from drillings taken not less than 1/4 in. beneath the surface of a test ingot made during the pouring of the melt. The chemical composition thus determined, except for the Hydrogen content, shall be reported to the purchaser and shall conform to the requirements specified in Table I. Hydrogen content shall be determined as specified in the notes at the bottom of Table I.
- 4.1.2 Final Check Analysis - Vendor shall provide check analysis of material with each shipment.
- 4.1.3 A check analysis of the material evaluation sheets will be made by the purchaser. The chemical composition thus determined shall conform to the requirements specified in Table I.
- 4.2 Metallographic specimens shall be prepared for each sheet thickness supplied. Said specimens shall present a section of the complete thickness of the sheet or plate. More than one specimen may be used to present a section of the complete thickness of sheet bar.
- 4.2.1 A solution for electrolytic etching shall be prepared by adding 100 grams of reagent-grade oxalic acid crystals ($\text{H}_2\text{O}_2\text{O}_4 \cdot 2\text{H}_2\text{O}$) to 900 ml of water.
- 4.2.2 Etching conditions. Polished specimens shall be etched at one amp/cm² for 30 seconds.

4.2.3 Evaluation of etched structure. The etched surface shall be examined on a metallurgical microscope at 250X. No intergranular pitting shall be observed.

4.3 All records shall be maintained in the ARDE Quality Control Department.

5.0 PREPARATION FOR DELIVERY

5.1 Sheet, plate and sheet bar shall be boxed in containers sufficiently rigid to prevent scratching, bending, or any type of surface damage. Pressure sensitive paper shall be applied to both sides of the sheet and plate. Paper protection for sheet bar is not required.

5.2 Sheet, plate and sheet bar shall have continuous marking printed in the direction of final rolling. The marking shall include grade of steel, heat number and supplier's name.

5.3 The vendor shall furnish with each shipment, three (3) copies of a report containing the chemical composition, room temperature tensile properties, and hardness. This report shall include the Purchase Order Number, Heat Number, Material Specification Number, Size and Quantity of the shipment.

APPENDIX D

PROCEDURE FOR LEAK DETECTION
BY MASS SPECTROMETRY

(AES 454)

AES
NO.

454

DATE ISSUED February 15, 1967

REV	DESCRIPTION	DATE	APPROVAL

PROCEDURE FOR LEAK DETECTION

BY

MASS SPECTROMETRY

	APPD.	DATE	ARDE', INC. PARAMUS, N.J. ENGINEERING SPECIFICATION AES 454
PREPARED BY	ms	2/22/67	
MET. ENG.	RHa	2/22/67	
DESIGN ENG	RAZ	2/22/67	
QUALITY CONTROL	EB	2/27/67	
CHIEF ENG	A.O.	2/28/67	
			SHEET 1 OF 6.

1.0 SCOPE

- 1.1 This specification establishes methods and classes of testing sensitivities for leak detection by passage of "Tracer" fluid from one side of a presumed leak to the other, and the subsequent detection of the fluid on the latter side.
- 1.2 This specification is effective upon issue and shall be applicable when specified on engineering drawings.

2.0 DEFINITIONS

- 2.1 Standard or Calibrated Leak - A self-contained tracer gas supply of at least 90 per cent purity at atmospheric pressure containing a porous glass or quartz element which allows diffusion of the tracer gas at a known rate.
- 2.2 Smallest Leak Detectable - The value of the standard leak in atmospheric cc/sec divided by the leak detector scale reading.
- 2.3 Input Sensitivity - Smallest leak detectable with standard leak attached to the leak detector with vacuum hose three inches in length.
- 2.4 Testing Sensitivity - Smallest leak detectable with standard leak attached to the system under test at the most remote accessible location from the Leak Detector, unless otherwise specified by ARDE. This testing sensitivity shall be quoted in standard cc/second.
- 2.5 Tracer Gas - Type of gas that can be detected by the Mass Spectrometer in use.

3.0 MATERIALS

- 3.1 Helium - 90% purity (minimum)

- 3.2 Argon - 90% purity (minimum)
- 3.3 Neon - 90% purity (minimum)
- 3.4 Polyethylene bags

4.0 EQUIPMENT

- 4.1 Mass Spectrometer

5.0 REQUIREMENTS

- 5.1 The tracer gas to be used for all testing within the scope of this specification shall be helium, argon or neon of at least 90 percent purity.
- 5.2 Testing sensitivity will be measured before and immediately after test and logged on the quality control report. If the test duration is greater than one hour, the test sensitivity shall be rechecked and logged at least every hour during the test.
- 5.3 The test duration shall be twice the time required to detect the testing sensitivity or five minutes, whichever is greater.
- 5.4 Leak tightness requirements shall be defined as being Class AA, Class A, or Class B. A test item shall be considered acceptable if no leak is detectable with a Mass Spectrometer having the testing sensitivity listed in Table I.

TABLE I
TESTING SENSITIVITIES (ATMOSPHERIC CC/SEC)
FOR THE THREE CLASSES OF LEAK TIGHTNESS

<u>Tracer Gas Used</u>	<u>Class AA</u>	<u>Class A</u>	<u>Class B</u>
Helium	1×10^{-9}	5×10^{-8}	1×10^{-6}
Neon	5×10^{-10}	2×10^{-8}	5×10^{-7}
Argon	3×10^{-10}	1.5×10^{-8}	3×10^{-7}

5.5 Where two classes of leak are called out on the same assembly, the areas with the most stringent requirements shall be tested independently.

5.6 Before testing, the test item shall be cleaned free of any foreign materials such as grease, paint, chips, etc., which might tend to mask leakage.

6.0 PROCEDURE

6.1 Unless otherwise authorized by the ARDE Quality Assurance Department, the following leak testing procedures shall be used. Vendors having different standard leak testing procedures are invited to submit them for approval.

6.2 Method I - Vacuum Testing Technique.

6.2.1 Before testing, the system under test shall be completely enclosed in a polyethylene bag and the bag shall be fully inflated with the tracer gas. For large system, portions of the system may be checked separately. In this case, each portion of system so checked shall be considered a separate test, and the test sequence shall be indicated on a worked print showing location checked.

6.2.2 The system under test shall be evacuated.

6.2.3 Inlet valves to the leak detector shall be fully opened during test.

6.2.4 All auxiliary pumping systems must be shut off before test.

6.3 Method II Pressure Testing

6.3.1 Before testing, the system under test shall be completely enclosed in a polyethylene bag. The tracer gas is introduced within the test object under pressure greater than atmosphere. A "sniffer" probe is connected to the leak detector using a flexible hose. The sniffer is sealed within the polyethylene bag. If a leak exists, the outflowing tracer gas enters the system via the sniffer.

- 6.3.2 Inlet valves to the leak detector shall be fully opened during test.
- 6.3.3 All auxiliary pumping systems must be shut off before test.

6.4 Method III Pressure Vacuum Testing

- 6.4.1 Before testing, the unit under test shall be placed inside a vacuum chamber which is connected to the leak detector. Tracer gas is introduced to the unit by an internal pressure greater than atmosphere. If a leak exists, tracer gas will flow out of the unit under test into the vacuum chamber, and then into the system.
- 6.4.2 Inlet valves to the leak detector shall be fully opened during test.
- 6.4.3 All auxiliary pumping systems must be shut off before test.

7.0 REPORTS

- 7.1 A certified quality control report shall be made out by the vendor or ARDE N.D.T. Department and submitted to ARDE Quality Assurance Department. This report shall contain the following information:

- a) Symbol or name of vendor.
- b) Symbol or name of the laboratory performing the testing.
- c) Part number.
- d) Purchase order number.
- e) Date of test.
- f) Marked blueprint or sketch showing location of standard leak and leak detector in relation to test item.
- g) Testing sensitivities as defined in 4.2.5 listed in chronological order.

8.0 REJECTIONS

8.1 Delivered items not meeting the requirements of this specification for the class specified shall be subject to rejection.

APPENDIX E

OGDEN LAB TEST REPORT

APPENDIX E

OGDEN TECHNOLOGY LABORATORIES, INC.
Subsidiary of OGDEN CORPORATION

30 November 1967

Arde, Inc.
520 Winters Avenue
Paramus, New Jersey 07652

Reference: Your Purchase Order Number: 10350
Ogden Job Number: W-8836-1
Test Units: E3590A Vessel Assemblies, Serial
Numbers 3 and 4
Government Contract Number: NAS 8-20713

REPORT OF TEST

TEST PROCEDURE


Each vessel, in turn, was subjected to two (2) pressure cycles. A cycle consisting of 0 to 2,100 psig and return to 0 psig. During the second cycle at 2,100 psig, the external leakage was measured after a two (2) minute period.

TEST RESULTS

The units displayed no apparent evidence of damage as a result of this test.

<u>Leakage Test</u>	<u>Serial Numbers</u>	<u>cc/second</u>
	3	2.9×10^{-7}
	4	1.7×10^{-7}
<hr/>		
Limit: 1×10^{-6} maximum		

for: OGDEN TECHNOLOGY LABORATORIES, INC.
WOODSIDE DIVISION



Floyd Genauer
Quality Assurance Manager

OGDEN TECHNOLOGY LABORATORIES, INC.

Subsidiary of OGDEN CORPORATION

58-17 37th AVE., WOODSIDE, NEW YORK 11377

TEL: 212-478-2010
TWX: 510-227-7062

2 January 1968

Arde, Inc.
580 Winters Avenue
Paramus, New Jersey 07652

Reference: Your Purchase Order Number: 10550
Ogden Job Number: W-8836-2
Test Units: E3590A Vessel Assemblies, Serial
Numbers 6, 7, 8 and 9
Government Contract Number: NAS 8-20713

REPORT OF TESTTEST PROCEDURE

Each vessel, in turn, was subjected to two (2) pressure cycles. A cycle consisting of 0 to 2,100 psig, and return to 0 psig. During the second cycle at 2,100 psig, the external leakage was measured after two (2) minute period.

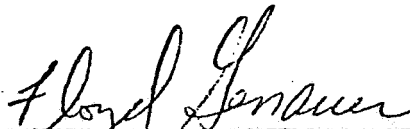
TEST RESULTS

The units displayed no apparent evidence of damage as a result of this test.

<u>Leakage Test</u>	<u>Serial Numbers</u>	<u>cc/second</u>
	6	1.72 x 10 ⁻⁷
	7	3.60 x 10 ⁻⁷
	8	2.40 x 10 ⁻⁷
	9	1.30 x 10 ⁻⁷

Limit: 1 x 10⁻⁶ maximum

for: OGDEN TECHNOLOGY LABORATORIES, INC.
WOODSIDE DIVISION


Floyd Genauer
Quality Assurance Manager

APPENDIX F

MECHANICAL PROPERTIES - HEAT 50793

APPENDIX F
MECHANICAL PROPERTIES - HEAT 50793

The mechanical property data for Heat 50793 is contained herein rather than in Section IV of the report as the report was essentially completed at the time the decision was rendered to fabricate two (2) additional vessels utilizing this heat of material.

A. Experimental Data

Inasmuch as the material achieves its strength through deformation at -320°F , specimens must first be prestrained at this temperature. The usual procedure is to first obtain a true stress vs. true strain curve at -320°F for the material in the annealed condition. This establishes the maximum amount of cold work which can be applied to the specimen in uniaxial tension. Such a curve marked σ_T , is shown for heat 50793 in Figure F-1. The nominal stresses vs. engineering strain for this same heat at -320°F is plotted in Figure F-2. The material may be prestrained any amount up to the maximum shown in Figure F-2 and tensile properties which result will, of course, depend on the amount of prestrain. The effect of varying the prestress -320°F and subsequently aging the prestressed specimens at 800°F is shown in Figures F-3, F-4 and F-5.

HEAT 50793
UNIAXIAL SPECIMEN (ANNEALED)
LOW SILICON STAINLESS STEEL

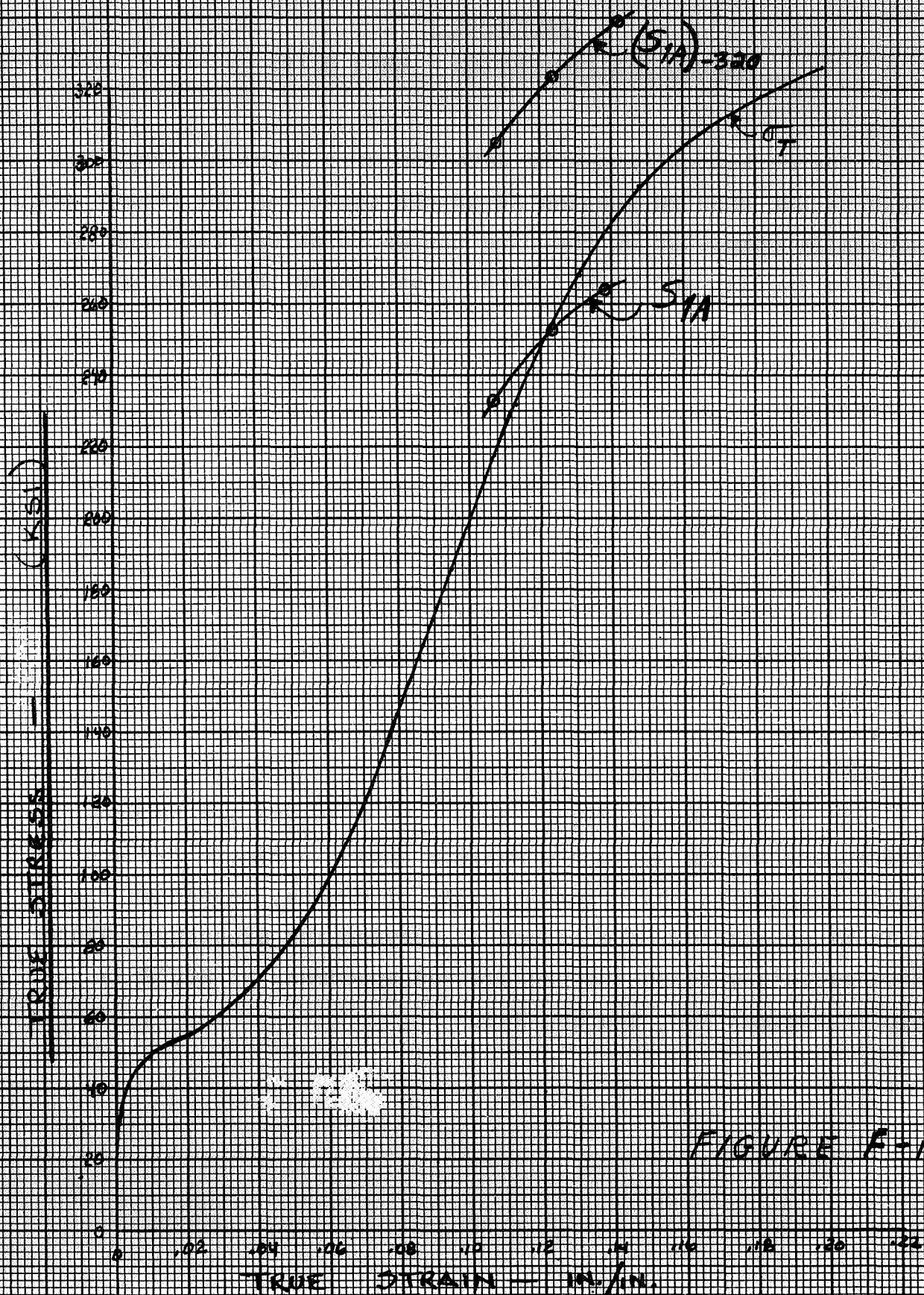


FIGURE F-1

Heat 50793

Uniaxial Specimen

(Annealed)

Low Silicon Stainless Steel

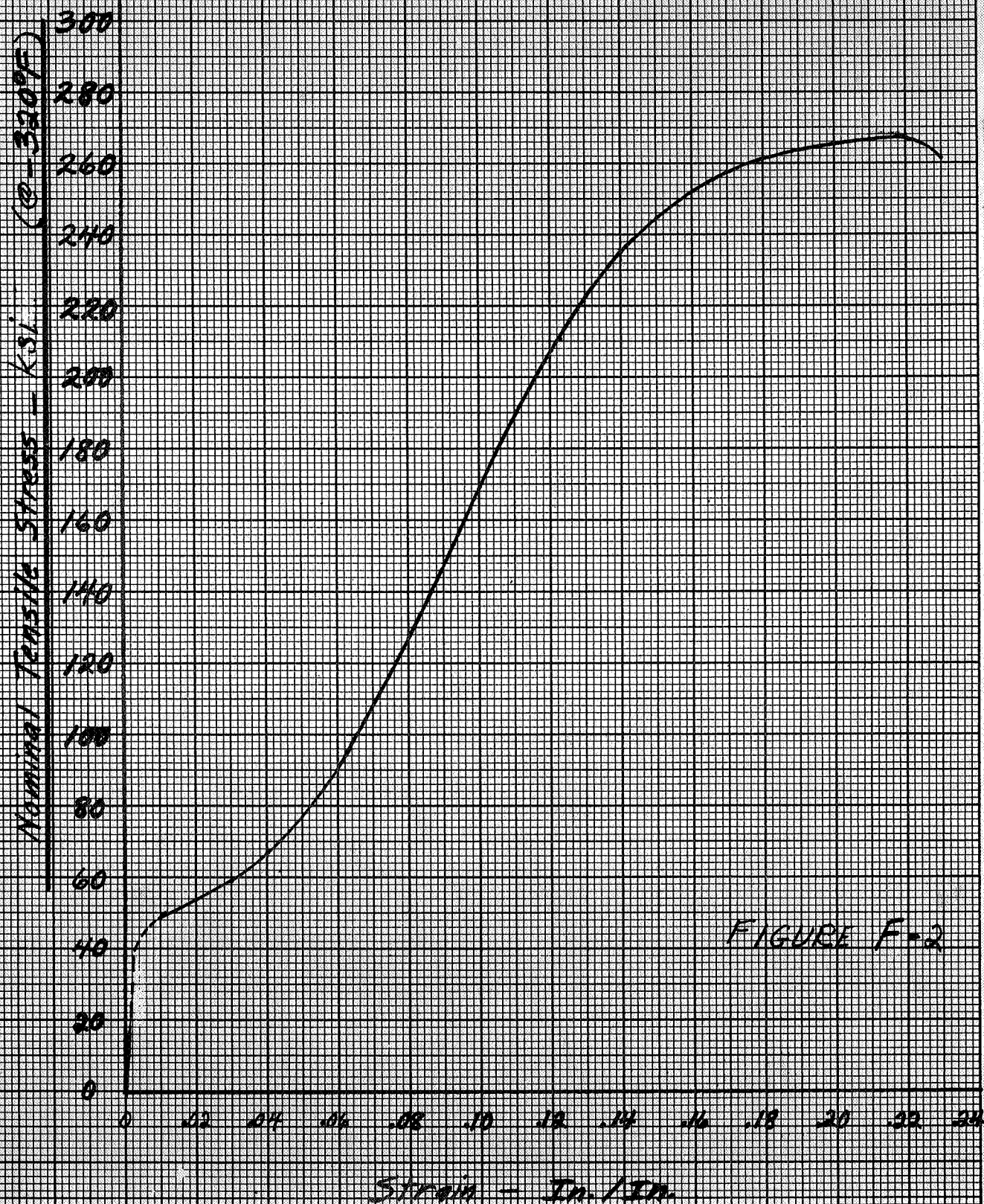


FIGURE F-2

Room Temp. Response Data

HEAT 50793 - AGED

□ Nom. UTE STRENGTH

○ YIELD STRENGTH

NOTE: DATA FROM 2062"
TENSILE COUPONS

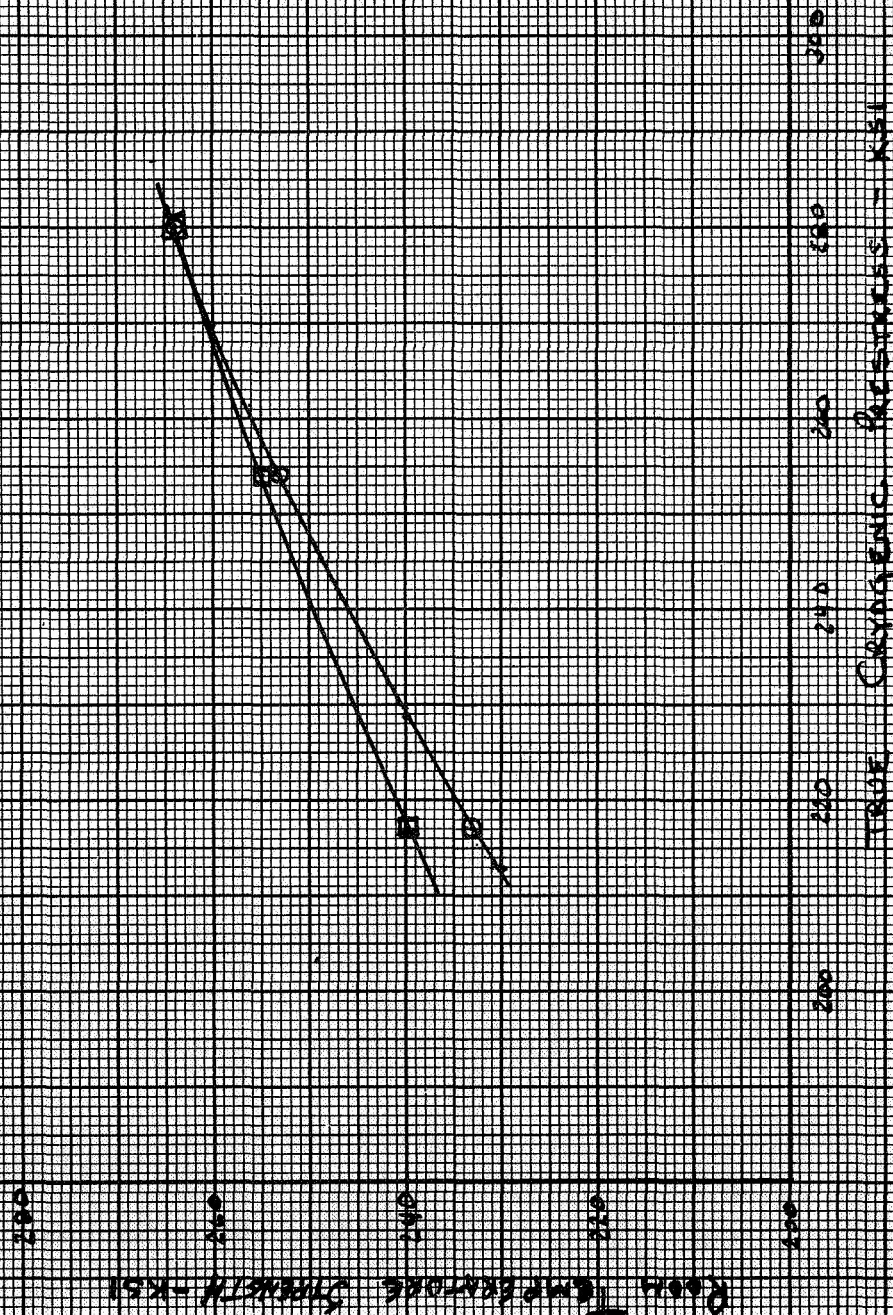


FIGURE F-3

-320°F Response Data

HEAT 50793 - AGED

○ YIELD STRENGTH

□ Nom. ULS STRENGTH

NOTE: DATA FROM .063" TENSILE COUPONS

15% - ALUMINUM - 3.022-

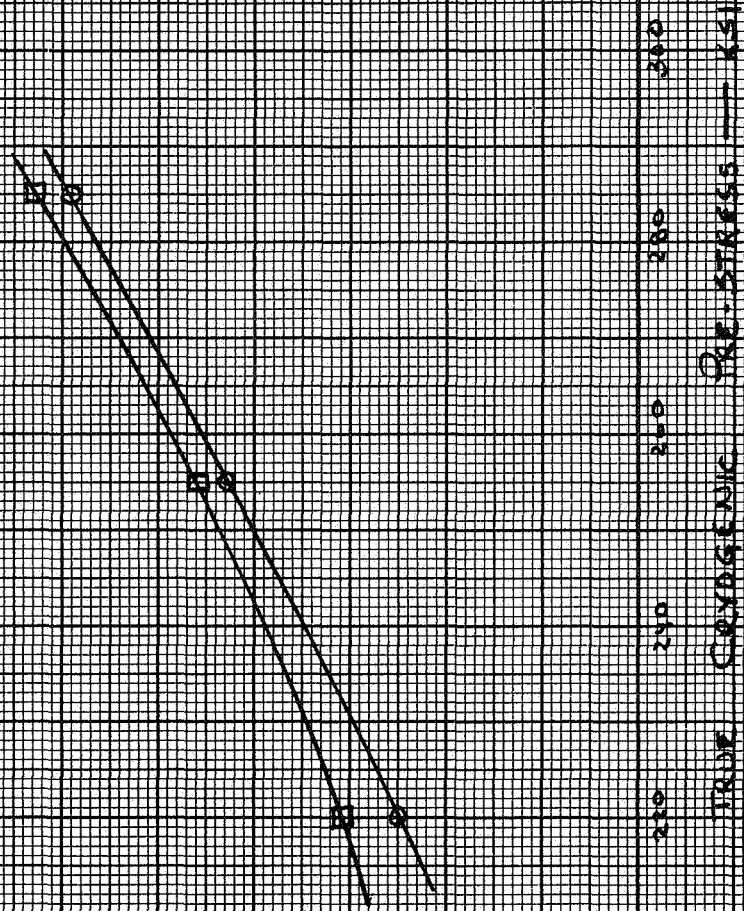


FIGURE F-4

Strength @ -423 F of Low Silicon Stainless
Steel Prestrained @ -320 F
Aged, 20 hours @ 790 F
HT 50793

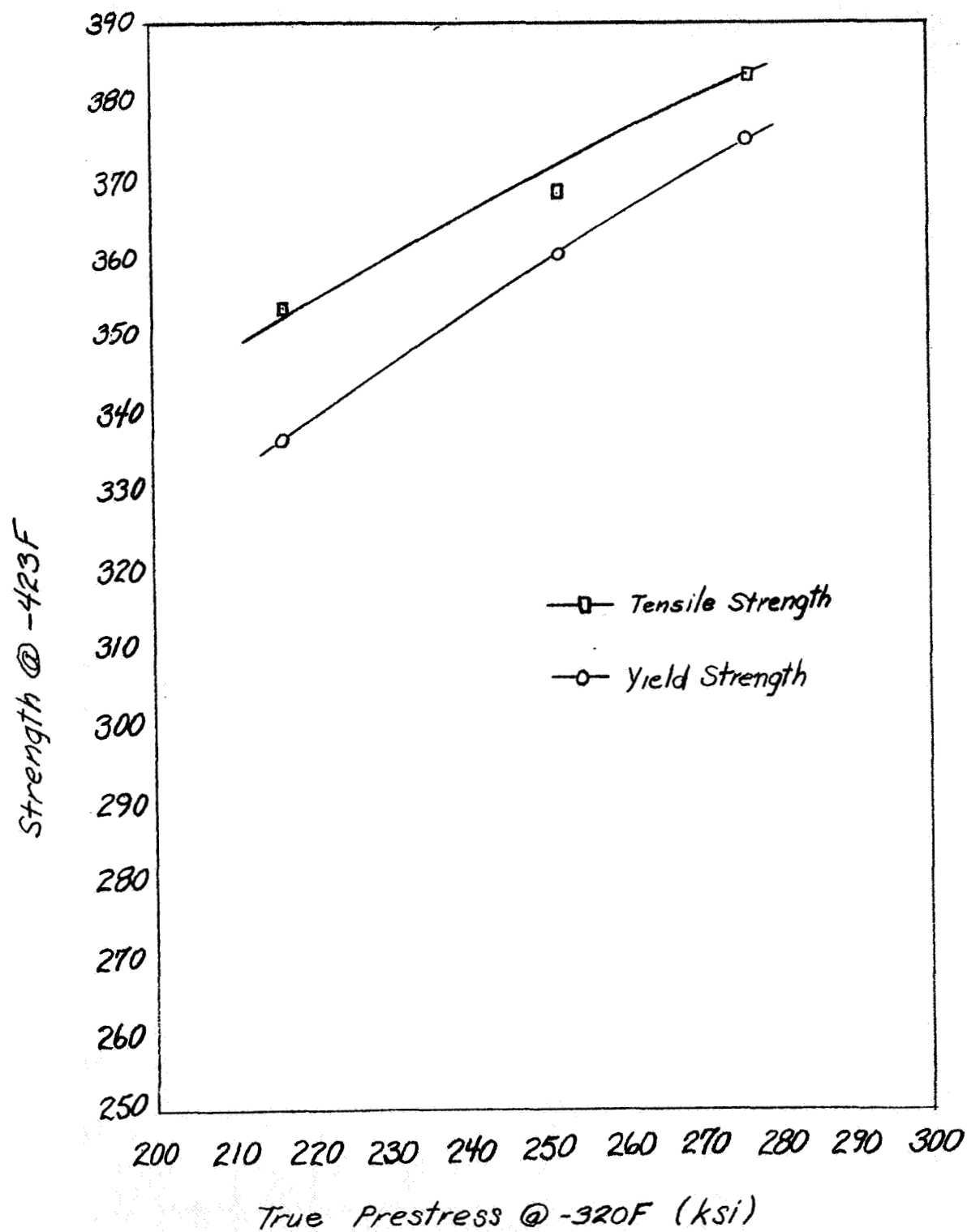


Fig F-5

Figure IV-3 shows the yield and ultimate tensile strength of cryogenically stretched and aged specimens from heat 50793 at room temperature. Figures IV-4 and IV-5 show these properties at -320F and -423F, respectively. The yield strength at -320F and at room temperature is also plotted in Figure F-1 on the same coordinates as the -320F true stress vs. true strain curve for annealed material from heat 50793. The curve, marked S_{1A} in Figure F-1 represents the room temperature yield strength for the prestrained material while that marked $(S_{1A})_{-320F}$ represents the -320F yield strength for prestrained material. The increase in strength due to aging at 800F for 20 hours may be seen by comparing the data for aged material shown in Figures F-3 and F-4 with similar curves for unaged specimens shown in Figures F-6 and F-7.

Several prestressed and aged specimens from heat 50793 were surface cracked and tested at room temperature and -320F. In many cases general yielding occurred before failure and, of course, a K_{1c} value is not valid under these conditions. Therefore, a nominal K_{1c} was calculated for each specimen by using the initial crack dimensions and the failure load. The sheet specimen thickness was only .060. This type of specimen is used at Arde primarily for screening purposes. The nominal K_{1c} values calculated for each specimen was plotted in Figure F-8 as a function of cryogenic prestress.

Additional properties of other heats of low silicon stainless steel are also shown in this section. Figure F-9 shows the yield strength of 5 heats of low silicon stainless steel as a function of test temperature. The data points at room temperature

-320°F Response Data
HEAT 50793 - UNAGED

Normal Data from 1062
 tensile coupons

○ YIELD STRENGTH
 □ NOM. UTS STRENGTH

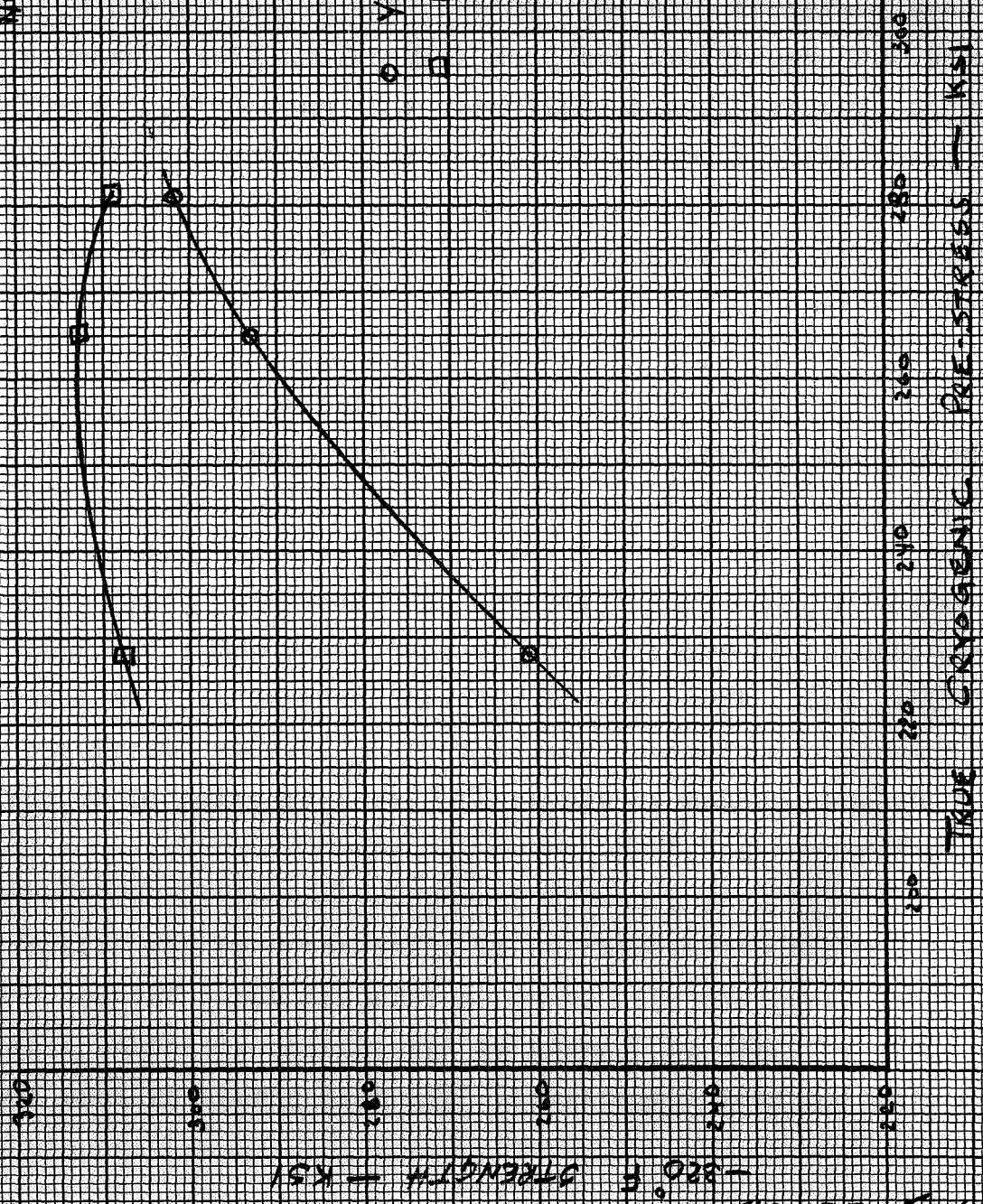


FIGURE F-6

ROOM TEMPERATURE RESPONSE DATA

HEAT 50793 - UNAGED

NOTE: DATA FROM 10603 TENSILE COUPONS

□ NOM. ULT. STRENGTH
○ YIELD STRENGTH

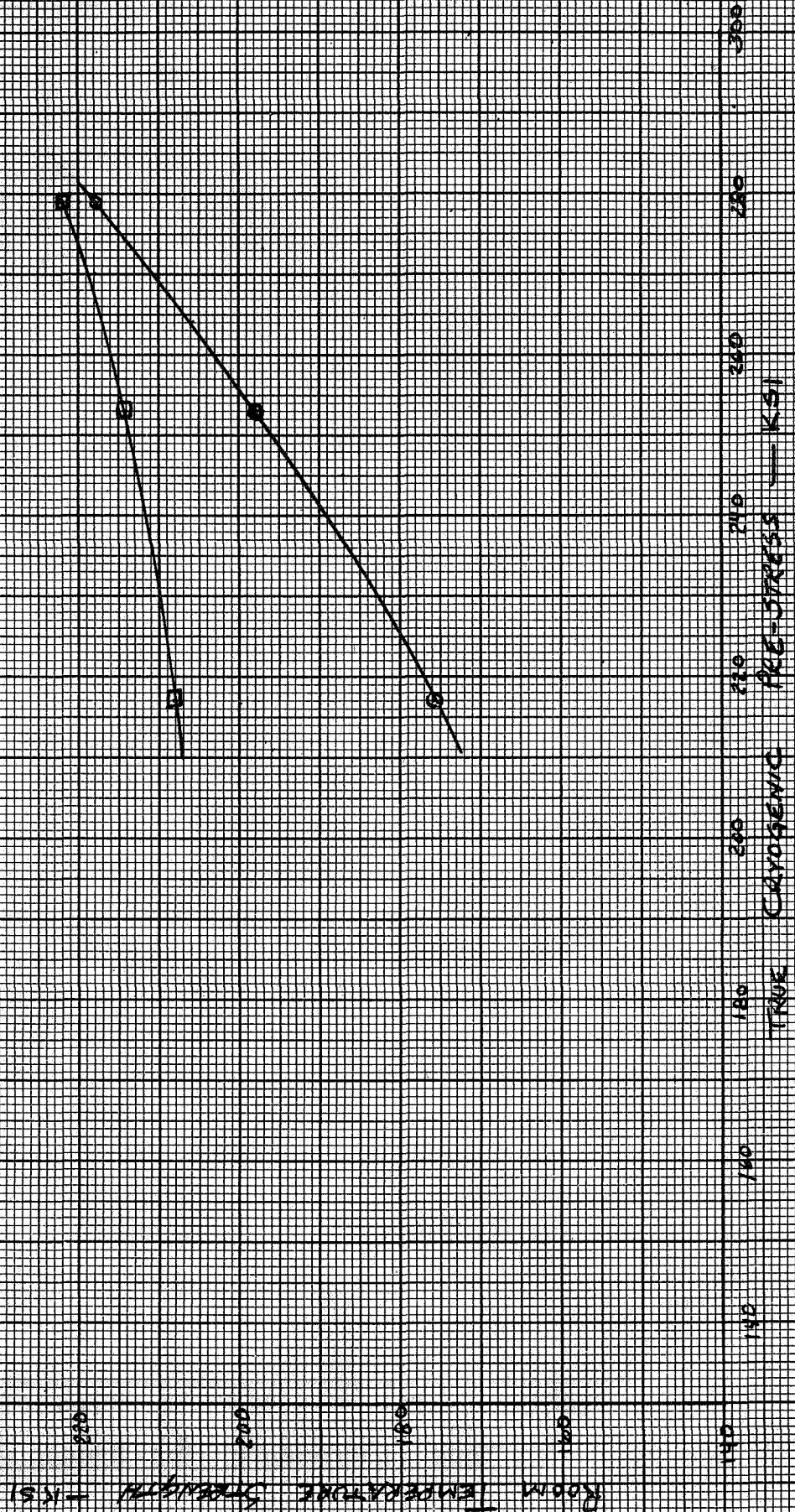


FIGURE F-7

NOMINAL K_{IC} VS TRUE CRYOGENIC PRE-STRESS

HEAT 50793

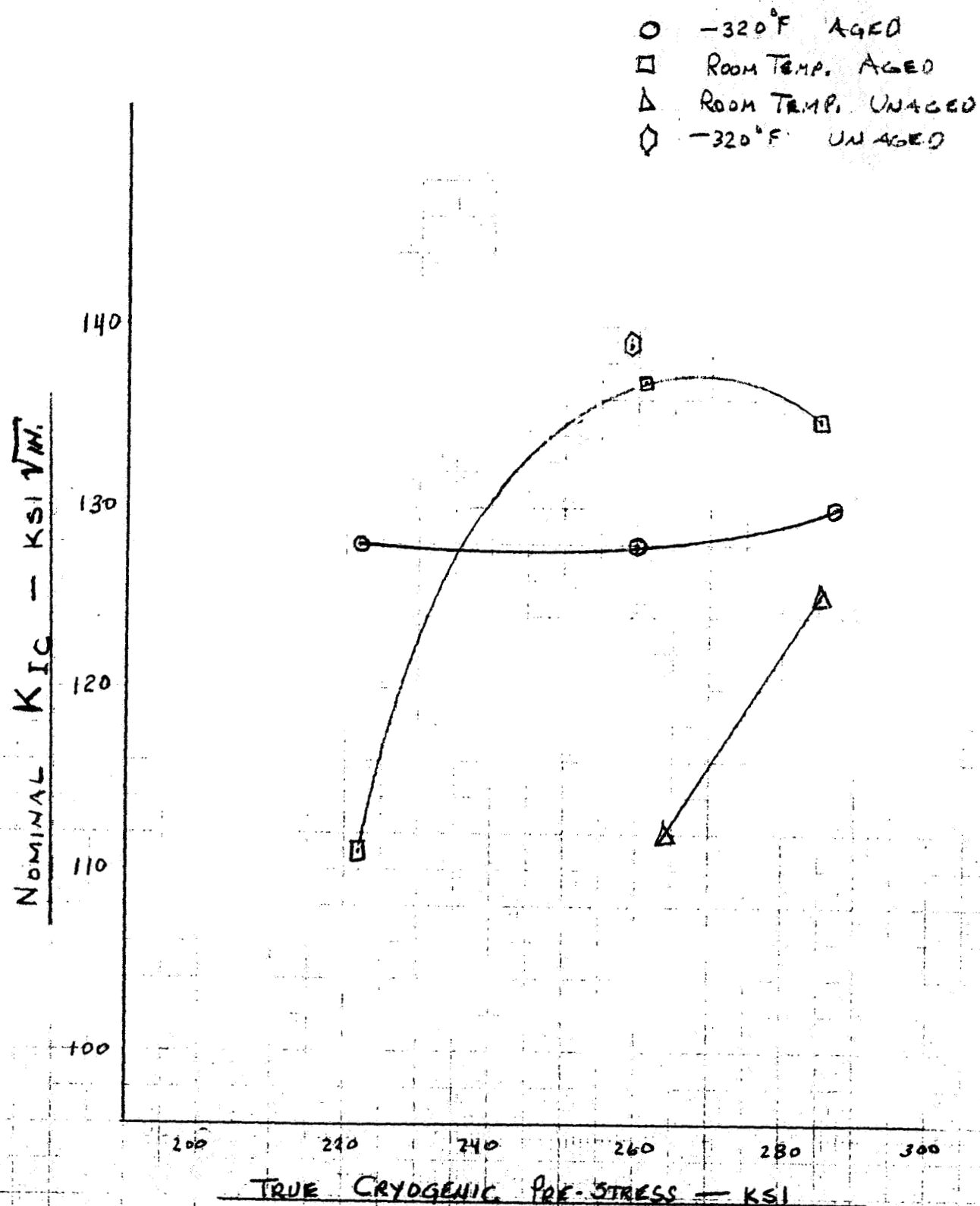


FIGURE F-8

Yield Strength Low Silicon Stainless Steel

5 Heats

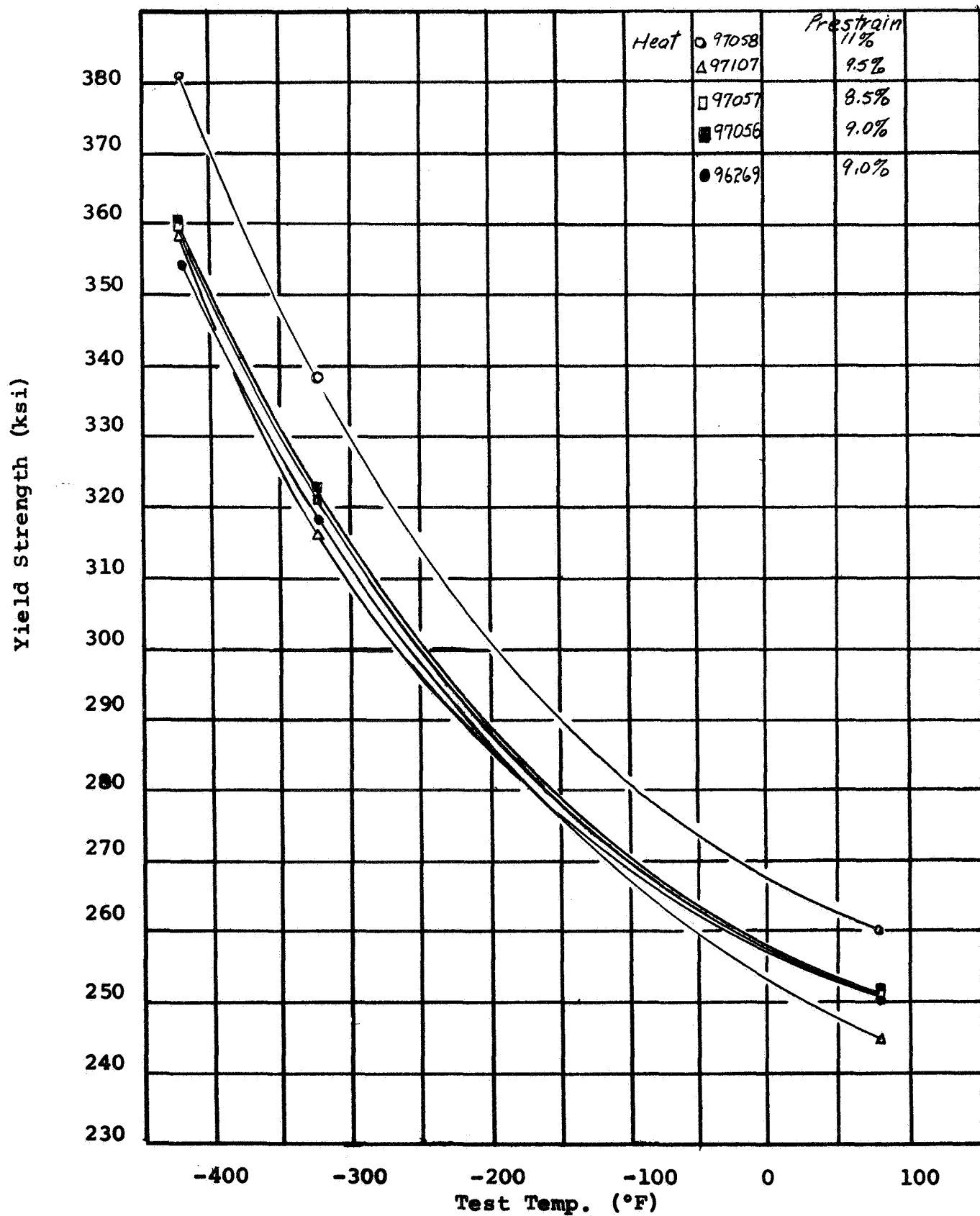


FIGURE F-9